社団法人

日本造船研究協会報告

第 1 号

昭和 29 年 8 月

日聖丸実船試験成績と模型試験成績との比較研究

..... 第1研究部会

Investigation into the Sea-Going Qualities of the Single-Screw Cargo Ship "Nissei Maru" by Actual and Model Ship Experiments ..... The 1st Research Committee

---

The Report
of the
Shipbuilding Research Association
of Japan,
Tokyo, JAPAN
No. 1
August 1954

第1研究部会委員名簿

委員長	菅　四郎	
幹事	土田　陽	元良誠三
委員	青山貞一郎	伊藤達郎
	乾　崇夫	岡田正次郎
	蒲田利喜蔵	木下昌雄
	志波久光	中村彰一
	谷口　中	原田秀雄
	山縣昌夫	

Membership of the 1 st Research Committee

Chairman	Shiro KAN	
Secretaries	Kiyoshi TSUCHIDA	Seizo MOTORA
Members	Teiichiro AOYAMA	Tatsuo ITO
	Takao INUI	Shojiro OKADA
	Rikizo KAMATA	Masao KINOSHITA
	Hisamitsu SHIBA	Shoichi NAKAMURA
	Kaname TANIGUCHI	Hideo HARADA
	Masao YAMAGATA	

Preface

Need for an expensive measurement program on the actual performance of a sea-going vessel had long been felt by all concerned with the research of ship forms in this country.

Thanks to the full co-operation from every field of shipbuilding and shipping circles, such program was realized on a single-screw cargo ship, "Nissei Maru", during 1951 and 1952. Numerous tank tests and wind tunnel tests on the models of this ship were also carried out.

This Report is intended to give a comprehensive account of the results obtained both by the full scale and model experiments.

July, 1954

CONTENTS

PART I. ACTUAL SHIP EXPERIMENTS

Chapter 1

Introduction

In view of the great importance of securing correct and factual knowledge regarding the sea-performance data of an actual ship, as the foundation of methods to investigate the sea-going qualities of vessels, the Experiment Tank Committee of Japan had been planning for several years to carry out systematic actual ship experiments on the sea-worthiness of vessels. Actual preparations were finally completed in 1951, and the experiments were conducted on a cargo ship, S.S. "Nissei Maru", with the support of many Japanese organizations in the field of marine transportation and shipbuilding.

The experiments occupied a period of 129 days, from 26th December, 1951, to 3rd May, 1952 on the ship's maiden voyage from Yokohama to Vancouver, Honolulu, Singapore, Bombay, Mormugao, Shingapore and back to Yokohama, a distance of 21,700 nautical miles.

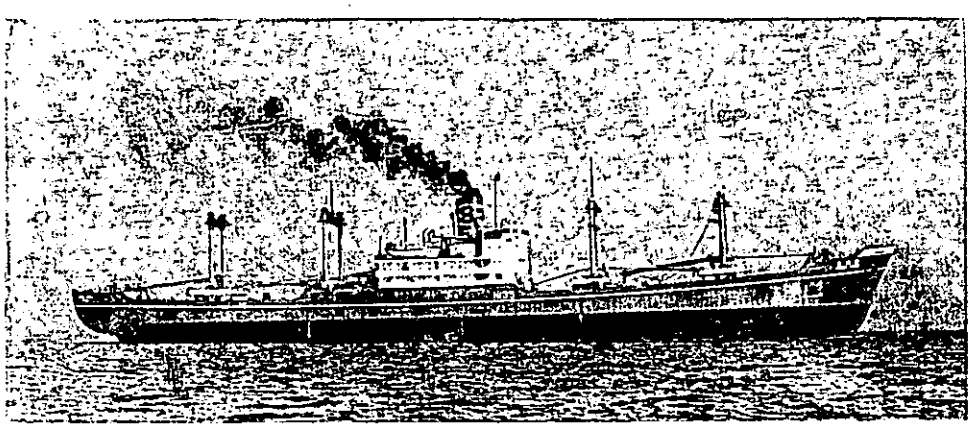

Single-Screw Cargo Steamer "NISSEI MARU"

Ten members of the Committee*1 boarded the vessel, and the ship's speed, revolutions per minute of the propeller, the torque of the intermediate shaft (SHP), the helm angle, the yawing angle, the pitching angle, the rolling angle, the heaving of the ship and the stresses of the hull in several positions, as well as the wind and sea conditions, were measured or observed by them simultaneously. The total measurements recorded amounted to 159, and much interesting and instructive data and experience were obtained.

Chapter 2

Outline of the Vessel and Speed Trial Results

S. S. "Nissei Maru" is a steel single-screw cargo ship completed in December 1951, at the Tsurumi Shipyard of the Nippon Steel Tube Co. Ltd., her particulars are as follows;

Length bet. perpendiculars		128.00 m
Breadth moulded		17.50 m
Depth moulded		10.40 m
Draught	at full load condition	8.25 m
Displacement	,, ,, ,, ,,	13,870 tons

*1. Members who boarded the vessel

Name	Position	
Shiro Kan	Ship propulsion Division, Transportation Technical Research Institute.	Director of the Division.
Tatsuo Ito	Do.	Technical official.
Yasubumi Yamanouchi	Ship Performance Division, Transportation Technical Research Institute.	Do.
Kenji Hata	Technical Research Section, Ship Bureau, Transportation Ministry.	Do.
Takao Inui	Faculty of Technology, University of Tokyo.	Assistant professor.
Seizo Motora	Do.	Do.
Kiyokatsu Hanita	Design Department, Tsurumi Shipyard, Nippon Steel Tube Co. Ltd.	Deputy Chief of the Department.
Masao Kinoshita	Technical Research Laboratory, Hitachi Shipbuilding & Engineering Co. Ltd.	Chief of the 2nd Research Room.
Shojiro Okada	Do.	Researcher.
Kaname Taniguchi	Technical Department, Mitsubishi Shipbuilding & Engineering Co. Ltd.	Chief of the Experimental Tank.

Outline of the Vessel and Speed Trial Results

Block coefficient	at full load condition	.720
Midship coefficient	,, ,, ,, ,,	.987
Longitudinal position of centre of buoyancy		.42 m fore from midship
Designed service speed		13.4 kn
D. W.		9,914 tons
G. T.		6,926 tons
Main engine :	Cross-compound impulse turbine with double reduction gearing.	1 set
	Max. contineous output (105 RPM)	4,000 SHP
	Normal service output (99 RPM)	3,400 SHP
Propeller :	Four blades built-up propeller of manganese bronze.	
	Diameter	5.25 m
Rudder :	Balanced-reaction type.	

The body plan and the fore and aft form of the ship are shown in Fig. 1, the propeller in Fig. 2, and the general arrangement in Fig. 4. The butts of the outside plankings are all-welded and the seams riveted in the bottom, being welded and riveted alternately on both sides, and all the plankings are riveted to the frames.

The results of the official speed trial in light condition, carried out on 19th December, 1951, off Hommoku, are shown in Fig. 3. The Beaufort wind scale was zero, and the sea condition smooth during the trial trip.

As the measuring instruments, specially prepared for the actual ship experiments, were not then properly adjusted, the SHP shown in Fig. 3, was measured by a Hopkinson torsionmeter attached to the first intermediate shaft, and the speed shown in Fig. 3 is the mean ground speed between the mile posts, corrected against the current effect.

Curves for SHP and RPM, corresponding to the trial condition, which were obtained by a self-propulsion test on 6 m paraffin model, are also shown in Fig. 3, by way of comparison (see Part II, Chapter 7).

Chapter 3

Items Measured and Measuring Instruments Employed

1. Outline of the items measured and of the measuring instruments, and their arrangement

Items measured and kinds of instruments are shown in Table 1. For measuring the ship's speed, SHP, and sea condition, two or three different methods were employed concurrently, so as to obtain the most accurate data, because these features were considered to be of more importance than the others. Fig. 4 shows the arrangement of the instruments in the ship.

In order to clarify the sea-going qualities of ships on waves, it was thought desirable to measure those items at the same instant, so that all data obtained would be comparable as to time. For this reason, measurements of these items were conducted as far as possible in the same position, except for a few, where the apparatus could not be moved from its proper position. The crew's spare room at the front of the bridge, port side, was rearranged as the No. 1 measuring room, and a Shiba log, Hitachi torsionmeter and its revolution recorder, rudder angle recorder, and wire strain gauge, were arranged therein; the pilot's cabin on the navigation bridge was also rearranged as the No. 2 measuring room, in which the wind direction and wind speed recorder, heaving recorder, and a Sperry recorder, were installed.

A Togino torsionmeter and a Hopkinson torsionmeter were installed at the aft and fore ends of the shaft tunnel respectively, and an air-gyro recorder on the starboard side of the 2nd deck in the engine room. A stereo-camera was installed at the fore end of the navigation bridge (direction foreward), and another on the starboard side of the navigation bridge (direction to starboard side) having regard to their field of vision. The filming by a 16 mm cine-camera and a 35 mm ordinary camera, and the sketching of the seas and measuring of the wave period were also done at the said positions.

The control centre was on the navigation bridge, being connected

to the No. 1 measuring room, shaft tunnel (Togino torsionmeter), and the engine room (air-gyro recorder), with temporary telephone lines, to facilitate to communicate with each other. A switch was also arranged at the control centre, to make it possible to record a sign every measuring apparatus simultaneously, indicating the beginning and ending of the measurements or time of wave encounter.

Table 1. Items measured and Instruments used

Items measured		Instruments used
Speed of Ship	Through Water	Shiba Log Sal Log Walker Log
	Over Ground	Sextant, Loran
Speed of Revolution of Propeller Shaft		Electric Tachometer Hitachi Revolution Recorder Togino Revolution Recorder
Torque		Hopkinson-Thring Torsionmeter Hitachi Torsionmeter Togino Torsionmeter
Sea and Wave		Stereo Camera, 2 Sets (Forward and Side) 16mm Cine Camera 35mm Camera (Ordinary & Colour Film)
Wind	Direction and Speed	Koshin Vane
	Speed	Robinson Cup
Oscillation	Rolling	Sperry Recorder Air-Gyro Recorder
	Pitching	
	Yawing	
	Heaving	Heaving Meter
Helm Angle		Electric Helm Angle Recorder
Stress of Hull		Wire Strain Gauge Mechanical Strain Gauge (Giken Type and Leuner Type)

Though the wires used for these instruments, temporary telephones, and signal lines, amounted to a considerable number, the places where

they penetrated the bulkheads were all attached by ordinary bulkhead pieces as required by the Shipping Law.

Some recorders (oscillographs and others) in the No. 1 measuring room were suspended by rubber tape to avoid any effects of the ship's oscillation and vibration; instruments in the No. 2 measuring room were fixed to the ship's hull by rubber tape.

2. Measurement of the speed of the ship

A Shiba log*[2] was employed in measuring the ship's speed as the main instrument, and a Sal-log and a Walker log attached to the ship as her own equipments, were used for emergency or auxiliary purposes.

The Shiba log is a speedometer based on the principle that the frequency of Kármán vortex developing behind an obstacle moving through water, is proportional to the speed of the obstacle between a certain range of Reynolds' numbers. This log was used as a type of towing-log in these experiments, and a cabtyre cable (10 mm in dia.), reinforced with piano-wire so as to withstand the tension imposed on it, was used as the towing cable of the speedometer. The distance from the stern to the speedometer was kept at about 120 meters.

The mechanism of this speedometer is shown in Fig. 5. Kármán vortices are created by a regular triangular prism (50 mm on the side and 60 mm in height), a vibrator is attached behind the prism to detect the frequency of the vortex, and the detected frequency is recorded electrically in the ship. The speedometer is maintained in position in the water almost horizontal with edge-plates attached to both ends of the prism and a vertical plate, its depth under the water surface being kept at about 3–4 m by adjusting its weight. An example of the record obtained is shown in Fig. 6.

3. Measurement of the SHP (torque of the intermediate shaft and RPM of the propeller)

For measuring the SHP, three instruments were used concurrently

*2. H. Shiba, "On a New Speedometer" Technical Report of the Ship Research Laboratory, Vol. 7, 1951.

for different purposes, i.e. a Hopkinson torsionmeter was employed for the purpose of obtaining the measured value immediately after every measurement, and an Hitachi torsionmeter*3 was used to ascertain the variation of the torque in the waves by continuous records, and a Togino torsionmeter to get a standard value.

The Hopkinson torsionmeter was attached to the first intermediate shaft, others to the end shaft. The Hitachi torsionmeter is an instrument for electro-magnetically measuring the torque of an intermediate shaft, converting the relative translation of two rings attached to the shaft into the torsion of a magneto-striction tube in the pick-up. This instrument is shown in Fig. 7, together with its arrangement in "Nissei Maru", a picture of the recording part, and an example of the record, in Fig. 8, Fig. 9 and Fig. 10, respectively.

The Togino torsionmater*4 is also suitable for measuring the torque of a shaft, detecting the relative translation of two rings fixed to the shaft, by an optical lever, and recording it on a film, i.e. a lamp with an optical slit and a camera are attached to one ring and a convex mirror to another ring, so as to reflect the ray and imprint the image on a film in the camera, provided the translation of the image is proportional to the torsional strain of the shaft.

---

*3. a) H. Kinoshita & H. Araki, "On a New Torsionmeter and the Speed Trial Results obtained by It" Read at a meeting of the Society of Naval Architects of Japan, 1949.

b) M. Kinoshita & S. Okada, "Results of Measurements on SHP and Tortional Vibration of a Diesel Engine" Read at a meeting of the Society of Naval Architects of Japan, 1952.

c) M. Kinoshita, "A New Torsionmeter of the Magneto-striction Type and a Shaft Horsepower Meter" Abstract Notes and Data concerning the Subjects at the 6th International Conference of Ship's Tank Superintendents, Experimental Tank Committee of Japan, 1951.

*4. a) S. Togino, "On the Togino Torsionmeter" Journal of the Society of Naval Architects of Japan, Vol. 54, 1934.

b) S. Togino, "Optical Torsionmeter" Congress Int. des Direct de Bassins, Paris, 1935.

c) S. Togino, "The Latest Type of Togino Optical Torsionmeter" Abstract Notes and Data concerning the Subjects at the 6th International Conference of S.T.S., Exp. T.C. of Japan, 1951.

d) T. Ito, "A Togino Torsionmeter used for the Experiments on Nissei Maru". Tech. Rep. of the Trans. Tech. Res. Inst. Vol. 3, No. 1, 1953.

As a considerable time was needed for the experiments on the "Nissei Maru", the devices were arranged to make it possible to renew the film and the lamp while the shaft was turning, i.e., another ring was attached to the shaft on which the camera and lamp were attached, which could be stopped at anytime by taking out the cluch. The instrument is shown in Fig. 11, its arrangement in Fig. 12, and an example of the record in Fig. 13.

4. Measurement of the waves

The method of measuring the wave scale was regarded as being most difficult, and no completely satisfactory plan materialized even after a good deal of discussion. Finally it was decided to direct efforts to obtain as much data as possible not only by instruments but by actual observations, i.e., two sets of stereo-cameras—one facing forward and the other starboard—were used as the main instruments, the filming being done by 16 mm cine-camera and a 35 mm camera, the wave period being measured by a stop-watch, and observations being conducted by some of the members as additional measures.

Fig. 14 and Fig. 15 shows the arrangement of the stereo-camera, Fig. 16 an example of the record, and Fig. 17 an example of the contour lines of waves analized from the record in Fig. 16.

The mean values of the wave height, wave length, absolute period and angle of encounter with the ship, were observed and sketched during a period of three minutes in every periodical measurement. Observations were conducted regarding the degree of influence of waves upon the ship's performance, which would be represented by an average of wave scales in relation to the time of observation. The wave period was obtained in such a way that a distinct foam on the crest of the wave was chosen, and the time during which the foam descended and ascended again to the next crest was measured repeatedly, and their average value recorded. In sketching the wave patterns, the length of the crest lines were also recorded as correctly as ever possible.

5. Measurement of the wind

A Koshinvane*5 was employed as the main instrument, attached to the portal of the fore mast, its indicator and recorder were installed in the No. 2 measuring room. This recording was carried out not only during every periodical measurement, but throughout the whole time the ship was being navigated. An outside view of the Koshinvane is shown in Fig. 18, the arrangement in Fig. 19 and an example of the record in Fig. 20.

As to measuring the wind speed, Robinson cups were attached to the opposite side of the same portal to which the Koshinvane was fixed. Though the cups had been tested in a wind tunnel up to 35 m/s wind speed, they were all broken by their rotating shafts in a short time, due to the gyro-action caused by the violent rolling of the ship during the voyage.

6. Measurement of the ship's oscillation

Rolling, pitching, and yawing were recorded by an air-gyro recorder, and rolling and pitching by a Sperry recorder as an auxiliary.

A heaving-meter, the main part of which is an altimeter utilizing the atmospheric pressure difference proportional to the altitude, was tried for measuring the heaving of the ship, but the results were not adoptable.

The air-gyro recorder is an instrument reconditioned for this purpose from the servo-mechanism of an aircraft automatic pilot, and is suitable for recording the ship's oscillations around her three main momentum axis. The principle of its mechanism are shown graphically in Fig. 21, outside view in Fig. 22, and an example of the record in Fig. 23.

The main part of this air-gyro recorder consists of two air-turbine gyroscopes (18,000 r.p.m.), one of which is a free-gyro with its axis fixed to the space, from which the yawing is detected; the other is a

*5. M. Sanuki, "Studies on Biplane Wind Vanes, Ventilator Tube and Cup Anemometers" Meteorology & Geophysics, Vol. I, No. 1-4, 1950, and Vol. II, No. 3-4, 1951.

kind of artificial horizon having a restoring apparatus so as to keep its axis vertical, rolling and piching being detected from it. Rolling is recorded as the rate 1.6 mm/1°, and piching and yawing 2.2 mm/1°.

This instrument has the merit that its records are not affected by the position (height above C.G. of the ship); its sensibility is about 1/4°, but there is a tendency for small steps to show on its recorded diagram at maximum and minimum points.

7. Measurement of the helm angle

An electric resistance coil was attached along to the bow of a wooden quadrant fixed to the rudder head, and a wire brush to the hull, so as to make contact with the coil when the rudder was moved, thus the change in the helm angle was converted into a change of the electric current proportional to the helm angle, and the current was recorded automatically. An example of the record obtained is shown in Fig. 10.

8. Measurement of stresses on hull structure

As a preliminary step to future systematic researches on the hull stresses of actual ships, measurements of strain were taken at several points of hull structure simultaneously with other measurements as described before.

Electric resistance wire strain gauges were used as the principal means of measurement, while strain meters of a mechanical type were employed to support those measurements. Fig. 24 shows the positions where the strain meters were attached and, at a certain number of points, both the direct reading mechanical type and wire strain gauges were used, in order to compare the values of their recordings.

A strain recording unit having a resistance wire strain gauge of 20 mm gauge length, and a recording apparatus, consisting of initial balance attachments, a Brush Universal Analyzer and a pen writing oscillograph were used, a general view of the wire strain gauge and the recording apparatus being shown in Fig. 25 and Fig. 26, and a typical oscillogram in Fig. 27.

The Giken type direct-reading mechanical strain meters of 400 mm gauge length were secured in place by means of studs welded to the surfaces where measurements were to be made (refer to photograph Fig. 25), and the strain was measured every two seconds during one to two minutes by a dial gauge having an 0.01 mm graduation.

The Leuner strain meter of 700 mm gauge length were secured in position by steel pieces welded to the surface at the point of measurement, and pencil recordings of the strain were taken automatically. The records obtained from this strain meter, however, were considered unreliable because of the excessive friction of the mechanical parts and, therefore, it was decided not to use them.

9. Miscellaneous

The values of the sea-water temperature, sea-water density, atomospheric temperature, atomospheric pressure, fuel and fresh water consumption were obtained from the ship's Log-book.

Chapter 4

Course of the Ship, Weather, Sea and Ship's Condition

1. Preliminary researches on the climate and sea conditions

Preliminary researches on the climate and sea conditions in the North Pacific Ocean in winter have been in progress since 1950 by the Experiment Tank Committee of Japan, to secure fundamental data necessary to the design of efficient ocean going ships. The data obtained included much valuable advice and information for designing measuring instruments and planning the experiments. Such data are absolutely necessary in making it possible to generalize the results of the experiments without limiting them to a particular season of the year or to a particular course taken by the vessel on the experiments. Though the results of the said researches are both important and interesting, they will not be described in this paper on account of limited space.

2. The course of "Nissei Maru" and the weather and sea conditions

"Nissei Maru" left Yokohama on her maiden voyage at 15.20 on December 26th, 1951, in a light condition, arriving at Vancouver at 13.30 on January 8th, 1952, encountering considerable spells of bad weather, though the voyage was on the average favourable, with the wind and waves being generally fair.

Fully loaded with wheat, she sailed for India via Yokohama at 17.30 on January 16th, 1952, following a south-west course along the boundary line in Load Line Rules, turning dead west at point 34°-55'N, 149°-0'W, at 5.20 on January 22nd, when she encountered heavy storms every day, and terrific wind with waves growing in height. The voyage was so strenuous that the vessel exhausted her fuel reserve and was obliged to abandon the intention of proceeding direct to Yokohama and to touch at Honolulu for bunker supplies.

The ship turned toward Honolulu at 34°-29'N, 170°-25'W, at 1.30 on January 28th, arriving at Honolulu at 9.15 on January 31st.

For economic reasons, the schedule of the ship was changed, and she headed direct for India, instead of proceeding to Yokohama as was originally intended, three of the members of the Experimental Tank Committee disembarking at Honolulu and proceeding back to Japan by air, as they could not absent themselves too long from their duties.

After leaving Honolulu at 8.05 on February 1st, the vessel touched at Singapore, staying one night for bunkering (where one of the Members of the Committee had to be disembarked owing to illness), and arrived at Bombay at 12.30, February 29th.

Having discharged all her cargo of wheat at Bombay, the vessel sailed from there at 8.10 on March 4th in a light condition, arriving at Port Mormugao, Portugese India, at 5.10 on March 5th, where she remained forty days for cargo, one of the Committee members disembarking there, and five remaining on board.

The "Nissei Maru" sailed from Mormugao for home at 17.40, April 15th fully loaded with ore, but the speedy journey home which the members desired and expected could not be realized due to the progres-

Table 2. Loading Conditions at Departure and Arrival

Item			Yokohama Departure	Vancouver Arrival	Vancouver Departure	Honolulu Arrival	Honolulu Departure	Singapore Arrival	Singapore Departure
Date (Time)			1951·12·26 (1520)	1952·1·8 (1330)	1952·1·16 (1730)	1952·1·31 (0915)	1952·2·1 (0730)	1952·2·20 (1435)	1952·2·21 (0625)
Specific Gravity of Sea Water			1.024	1.023	1.021	1.024	1.025	1.025	1.025
Draught (stem)		m	2.62	2.26	7.90	7.73	8.10	7.74	8.18
〃	(F.P.)	〃	2.48	2.12	7.87	7.72	8.10	7.74	8.18
〃	(A.P.)	〃	6.19	5.30	8.64	8.11	8.38	7.94	8.52
〃	(midship)	〃	—	3.76	8.26	7.90	8.23	7.81	8.34
〃	(mean)	〃	4.34	3.74	8.26	7.90	8.23	7.82	8.34
Trim (aft.)		〃	3.71	3.18	0.77	0.39	0.28	0.20	0.34
Displacement		t	6,593	5,591	13,817	13,156	13,808	13,005	14,020
Loading	Fuel Oil	〃	664	316	733	282	794	205	949
	Feed Water	〃	191	86	170	87	100	46	53
	Cargo	〃	—	—	8,633	8,633	8,633	8,633	8,633
	Others	〃	1,872	1,323	415	288	415	255	519

Item			Bombay Arrival	Bombay Departure	Mormugao Arrival	Mormugao Departure	Singapore Arrival	Singapore Departure	Yokohama Arrival
Date (Time)			1952·2·28 (2045)	1952·3·4 (0810)	1952·3·5 (0510)	1952·4·15	1952·4·23	1952·4·24	1952·5·3
Specific Gravity of Sea Water			1.025	1.025	1.024	1.0235	1.024	1.025	1.020
Draught (stem)		m	8.18	2.70	2.68	8.17	7.97	8.29	8.19
〃	(F.P.)	〃	8.18	2.62	2.60	8.17	7.97	8.29	8.19
〃	(A.P.)	〃	8.20	4.75	4.70	8.26	8.12	8.45	8.15
〃	(midship)	〃	8.16	3.70	3.67	8.18	8.02	8.34	8.13
〃	(mean)	〃	8.17	3.70	3.67	8.19	8.03	8.35	8.14
Trim (aft.)		〃	0.02	2.13	2.10	0.09	0.15	0.16	−0.04
Displacement		t	13,666	5,534	5,479	13,685	13,397	14,035	13,552
Loading	Fuel Oil	〃	707	690	669	495	240	718	399
	Feed Water	〃	41	181	177	72	32	80	28
	Cargo	〃	8,633	—	—	9,144	9,144	9,144	9,144
	Others	〃	419	797	767	108	115	227	115

Table 3. Loading Conditions at Sea

Item		Yokohama to Vancouver		Vancouver to Honolulu		
Experiment No.		1~22	23~51	52~70	71~88	89~96
Date		1951·12·26~ 1952·1·1	1952·1·2~ 1952·1·8	1952·1·17~ 1952·1·21	1952·1·22~ 1952·1·27	1952·1·28~ 1952·1·31
Condition No.		I	II	III	IV	V
Displacement	t	6,440	6,130	13,700	13,450	13,250
Draught (F.P.)	m	2.52	2.39	7.72	7.63	7.65
〃 (A.P.)	〃	5.97	5.74	8.61	8.45	8.23
〃 (mean)	〃	4.25	4.07	8.17	8.04	7.94
Trim (aft.)	〃	3.45	3.35	0.89	0.82	0.58
KG*	〃	6.35	6.50	6.52	6.55	6.64
⊗G (aft.)	〃	4.79	4.83	0.59	0.47	0.16
GM*	〃	1.69	1.69	0.94	0.89	0.78
Wetted Surface Area (Naked)	m²	2,351	2,305	3,413	3,377	3,350
Wetted Surface Area (With App.)	〃	2,402	2,356	3,464	3,428	3,401

* Free surface effects are considered

Item		Honolulu to Singapore	Singapore to Bombay	Bombay to Mormugao	Mormugao to Singapore	Singapore to Yokohama
Experiment No.		97~113	114~125	126~131	132~139	140~154
Date		1952·2·1~ 1952·2·20	1952·2·21~ 1952·2·28	1952·3·4~ 1952·3·5	1952·4·16~ 1952·4·23	1952·4·24~ 1952·5·3
Condition No.		VI	VII	VIII	IX	X
Displacement	t	13,410	13,840	5,510	13,540	13,850
Draught (A.P.)	m	7.74	8.17	2.63	8.04	8.23
〃 (A.P.)	〃	8.29	8.32	4.75	8.16	8.29
〃 (mean)	〃	8.02	8.25	3.69	8.10	8.26
Trim (aft.)	〃	0.55	0.15	2.12	0.12	0.06
KG*	〃	6.52	6.44	7.20	6.30	6.34
⊗G (aft.)	〃	0.14	−0.25	2.90	−0.32	−0.35
GM*	〃	0.91	1.04	1.38	1.14	1.15
Wetted Surface Area (Naked)	m²	3,372	3,434	2,198	3,392	3,437
Wetted Surface Area (With App.)	〃	3,423	3,485	2,249	3,443	3,488

* Free surface effects are considered.

sive fouling of the bottom and propeller when the ship was anchored at Mormugao. Touching at Singapore en-route, she reached Yokohama at 15.10, May 3rd. The ship's course and every noon position are shown in Fig. 28.

Statistical analyses were compiled as to weather and sea conditions by measurements and observations during the whole voyage. The frequency diagram of wind and sea scales are shown in Fig. 29, as an example of the analyses.

3. Loading condition

The arrival and departure conditions at every port on the course (draught, displacement, etc.) are shown in Table 2. For the convenience of further analysis, the whole course was devided into 10 parts, and standard conditions for each part were decided as shown in Table 3.

Chapter 5

Measurement Results

1. Kinds and frequency of the experiments

Regular measurements of the ship's sea-performance at fixed times every day, were carried out as well as progressive tests varying the ship's RPM stepwise at proper occasions.

The times of regular measurements were chosen as 9, 12, and 15 o'clock having regard to the light necessary for filming the sea conditions. After leaving Honolulu, regular measurements were made only once a day at noon, as some members of the Committee left the ship at Honolulu, and very few recording papers remained, and the sea conditions were thought comparatively calm.

Progressive tests were conducted 6 times in total as follows, on the bases of different loading and sea conditions.

Exp. No.	Loading cond.	Course	Sea condition.	Wind force.	Remarks
9– 13	Light (I)	Y–V	Slight (North Pacific O.)	3–4	No relative wind
39– 42	Do. (II)	Do.	High (Do.)	6–8	
57– 60	Full (III)	V–H	Moderate (Do.)	4	
115–119	Do. (VII)	S–B	Smooth (Maracca St.)	2–3	
126–131	Light(VIII)	B–M	Do. (Arabian Sea)	3–4	
141–146	Full (X)	S–Y	Do. (Borneo Sea)	1–2	Fouled cond.

On the other hand, as temporary experiments, the effect of steering methods (automatic, hand, and keeping the helm angle at 0°) on the ship's performance in abeam wind were measured, as well as the effect of the length of the towing line of the Shiba log on its readings, but no clear difference was detected.

All the data obtained in each experiment was consolidated in a graph separately against the time base as shown in Figs. 30 and 31, as examples. The observed values of the sea and weather conditions are also recorded in the diagram.

Tables 4–6 show the mean values of all the measured items throughout 3 minutes. For the figures showing the ship's speed against the water shown in Tables 4–6, those values obtained by the Shiba log (some examples of record are shown in Fig. 32) were adopted in principle, except for a few cases when this log was thought unreliable, and in such cases the most reliable values obtained by other instruments were employed.

For the torsion of the intermediate shaft and SHP, the values obtained by the Hitachi torsionmeter were adopted in principle, with which a continuous record throughout 3 minutes could be secured, except for Exp. Nos. 21–45, No. 97 and after, for which records were not obtained, and the values by the Togino torsionmeter were employed.

The wave encounter periods were computed from the wave encounter marks for Exp. No. 80–96, and from the observed wave period and ship speed in other cases.

The yawings are shown in the form θ_1/θ_2 for the amplitude and

T_1/T_2 for the period respectively, where θ_1, T_1 mean the amplitude and period of forced yawing by every wave, and θ_2, T_2 that of a zig-zag motion caused by automatic steering (see Fig. 70).

For speed and direction of wind, the values at measured position, say at the portal of the fore mast, are shown, and no corrections for either height from water surface or effect of ship's body were carried out. The results of measurements of the profile of the sea surface by the stereo-cameras have not yet been completely analyzed.

Though the measurements of the hull stresses were continued up to Exp. No. 99, the values for Exp. No. 94 and the following ones are not shown in Tables 4–6, because of the extremely small measured values. Stresses are shown only in their variations, not in absolute values, because dummy gauges as temperature compensaters were not attached at the measuring positions, and there were remarkable variation of strain when the ship stayed in ports, and hence zero-point of the stresses was not certain.

To gain a general idea of the SHP loss in heavy weather on each course, the values of SHP & RPM were plotted against the ship's speed as shown in Figs. 33–38. In these figures, the SHP & RPM curves for smooth water obtained from self-propulsion tests on a 6 m paraffin model are also shown by way of comparison (see Part II. Chap. 7).

Some typical pictures of the surface conditions when measurements were taken are shown in Figs. 39–56.

Chapter 6

Brief Considerations on the Results of Measurements

1. Measurements of waves

When the measurements were taken, attention was concentrated on the irregularity of the ocean waves throughout the whole voyage. The waves observed were far more irregular as to both time and locality than was previously expected, and no wave trains were observed which encountered the ship in regular periods and amplitudes. The

condition of the sea surface around the ship seemed to be very confused, and the size and profile of the waves seemed to be remarkably different as to time and locality.

Therefore, it was thought difficult to secure a standard sea condition affecting the sea-performance of the ship, by measuring the waves in a certain location and at a certain instant, even though they were measured as accurately as possible. Measuring waves by a stereo-camera has a weak point in connection with the said features.

As to the observations of waves, though high accuracy could not be expected, observers made efforts to get an average value considering the irregularities of the waves as to both time and locality. Therefore the observed values do not necessarily agree with those of significant waves after Sverdrup & Munk.*6

On the voyage to Honolulu, the observed waves had short crest lines, several times the wave lengths at the largest, so that it was thought not suitable to compute the period of encounter of the waves from the wave length and the angle of encounter. And, as was considered previously, it was recognized plainly that the slope of a wave was steeper on the lee-side than the weather-side.

The relations between the wave height to the wave length observed are shown in Fig. 57, the straight line showing the wave length to wave height being 1/20 for comparison. It is very interesting to find that the ratio wave height to wave length which has been used as a standard value in calculating the strength of ship's structure, coincides approximately to the average value of the observed values in these experiments.

The relation between the wave length and the wave period is shown in Fig. 58 in which it will be recognized that the majority of the observed periods are larger than those of the trochoidal wave, the reason for which will of course lie partly in the low accuracy of observation (observed wave heights agree comparatively with those analysed from

*6. H. U. Sverdrup & W. H. Munk, "Wind, Sea and Swell. Theory of Relation for Forecasting" March, 1947. H. O. Pub. No. 601,

stereo-camera, but the observed lengths differ considerably from those of a stereo-camera), but will lie mainly in the fact that the wave periods were measured on comparatively distinct and large waves, the wave lengths being measured as the average value as to time and space.

2. Comparison of measured values of the torque by various kinds of torsionmeters

In this experiment, a Hopkinson torsionmeter was attached to the first intermediate shaft, and a Togino and a Hitachi torsionmeter to the end shaft.

Recordings were made as follows; with the Hopkinson torsionmeter, the average values throughout three minutes were measured in every experiment, with the Hitachi torsionmeter, continuous records throughout three minutes in each experiment were taken, and with the Togino torsionmeter, semi continuous recordings during several decades of seconds at the begining and ending of every experiment.

The Togino torsionmeter is an optical instrument having an optical system different from that of the Hopkinson torsionmeter. It can record the variation of torque during one rotation of the shaft continuously, eliminating the effects of the bending of the shaft by a couple of meters attached symmetrically to the shaft against the shaft centre. Differences between the records obtained by those two meters were about 10% at max. instanteneously, 5% at max. in average values out of several decades of seconds, and 1.9% in total average. These differences will decrease when the average values over a long period of time are taken.

A Togino torsionmeter was used as standard because of its high accuracy as stated above. Its records compare fairly well with those of Hitachi torsionmeter in average values (0.5% larger than the Togino torsionmeter in average at the same instant) and in mode of variation; those of a Hopkinson torsionmeter also coincide more than was expected,

except in heavy weather when there were large fluctuations in the torque.

3. Variation of the torque of the intermediate shaft in rough seas

The percentage of difference between maxima and minima values of the torque recorded by the Hitachi torsionmeter against the average values are shown in Figs. 59 and 60.

On the voyage from Yokohama to Vancouver, though ship was in a light load condition and the wind and seas were generally fair, sometimes excessive variations of 100–150% (215% at Exp. No. 40) occurred when the sea reached a "High sea" condition, and consequently the propeller was regarded to be racing.

On the other hand, from Vancouver to Honolulu, though the ship was fully loaded and the voyage was very strenuous as stated before, the variations were not so excessive considering the rough sea conditions, being 50–70% at the largest, the majority of them remaining in a range of 10–50%.

4. Increase of the average value of the torque of the intermediate shaft in rough seas

The average values of the torque of the intermediate shaft are plotted against the ship's speed in Figs. 61–64. In these figures, a curve showing the torque in calm water Q_0 obtained from self-propulsion tests on a 6 m paraffin model (2% of the propeller torque added as the loss due to stern tube friction), and a group of curves showing certain magnified values of Q_0, are also shown by way of comparison.

The average values of the torque in Condition I and Condition II, where the wind and wave were generally fair, are not so large compared to Q_0, and remain 1.4 times of Q_0 on the ship's speed base, and 1.1 times of Q_0 on the RPM base except Exp. Nos. 1～7. At Exp. Nos. 1～7, the wind and sea were almost head on and the average values of the torque reached about 1.8 times on the ship's speed base and 1.4 times on the RPM base. In some cases, the average torque was smaller than Q_0, it being considered that these phenomena were due to the

effects of a fair wind and the propeller racing.

On the other hand, in Conditions III–V fully loaded, no sign of racing was found, the increase of torque being most pronounced in Condition IV when the ship was labouring against strong wind and waves just ahead of the bow, amounting to 5 times in speed base and 1.8 times in RPM base at the maximum. In Condition V, with the advantage of a fair wind and waves, the increases in the torque were comparatively small even in high wind and wave scales. In Conditions III–V, encountering wind and waves in an almost constant direction, the relation between the rate of increase of the torque and sea condition was clearly recognized.

5. Increase of SHP and RPM in rough seas

In Figs. 33–38, the SHP and RPM are plotted against the ship's speed, from which it will be easily seen that there are similar inclinations between the degree of increase of the SHP and those of the torque, i.e., in Conditions I and II, the rate of increase of SHP and RPM with the sea condition are not clear, while in Conditions III–V, they are very distinct.

Anyhow, the results of the periodical measurements in Conditions I–V, as well as those of the progressive tests in Conditions I–III, are thought to introduce interesting and instructive data in connection with the effects of rough seas on a ship's performance, and the Authors are considering to develope their analysis with model experiments in waves as well as wind tunnel experiments.

6. SHP and RPM in a calm sea

The results of the experiment (Exp. No. 52) conducted in the Juan de Fuca Strait just after leaving Vancouver, fairly agree with the results of the tank experiments in smooth water.

During the voyage from Honolulu to Singapore (Condition VI), in calm seas, the results of periodical measurements during a period of 20 days, fairly coincide with those of the tank experiment, and the

plotted points grouped around one point on the graph.

7. Average ship's speed, SHP, etc. on each course

The average ship's speed over ground obtained by the observed positions and time of advance, as well as the average speed through water obtained by the distance run measured by a Sal-log and time of advance, are shown in Table 7. The difference between the two kinds of speeds has usually been reported as the tidal current, though it contains errors in measuring speed, surface flow, etc. In Table 7, it will be found that the values of the tidal current obtained in such a way agree with those shown in the pilot chart, at least in their direction; its speed was also found to be in reasonable order in average, therefore it can be said that the distance run measured by a Sal-log installed in the ship was fairly correct.

The average value of the ship's speed, RPM and SHP measured at periodical measurements on each course are shown in Table 8, and the SHP and RPM necessary to attain to the said average speed in calm sea as well as the ship's speed attainable by the above mentioned average SHP in calm sea, were computed from tank experiment results, and from these values, the rate of increase of SHP and RPM, the rate of decrease of ship's speed in each course were computed, as shown in Table 8.

Table 7. Average Ship's Speed and Tidel Current on Each Course.

Course	Time of Advance	Over Ground		Through Water		Tidal Current
		True Distance Run	Average Speed	Distance Rum by Log	Average Speed	
	hour	n. mile	kn	n. mile	kn	kn
Yokohama→ Vancouver	322.43	4329.3	13.42	4176.7	12.95	.47
Vancouver→ Honolulu	352.9	356.7	10.11	3615	10.24	− .13
Vancouver→ 35°N 150°W	116.11	1296	11.16	1320.9	11.38	− .22
35°N 150°W → 34°-29′N 170°-25′W	159.0	1256	7.90	1301.1	8.18	− .28
34°-29′N 170°-25′W → Honolulu	778	1015	13.05	993	12.76	+ .29
Honolulu → Singapore	443.2	5950	13.43	5646	12.74	+ .69
Singapore → Bombay	183.2	2454	13.40	2326	12.70	+ .70
Mormugao → Singapore	187.3	2226	11.88			
Singapore → Yokohama	222.5	2931	13.17	2839	12.76	+ .41

Table 8. The Rate of increase of the SHP and Loss of the Speed on Each Course

Course	Measured Values			In Still Water		$\frac{SHP_{mean}}{SPH_0}$	V_0	$\frac{V_{mean}}{V_0}$
	V_{mean}	SHP_{mean}	RPM_{mean}	SHP_0	RPM_0			
Yokohama–Vancouver	13.04	2,475	91.68	1,870	84.0	1.323	14.15	.921
Vancouver–Honolulu	10.53	3,311	90.30	1,360	73.0	2.435	13.69	.770
Vancouver–(35°N 150°W)	11.24	3,200	91.84	1,680	78.5	1.905	13.51	.832
(35°N 150°W)–(34°-29′N 170°-25′W)	8.61	3,196	85.62	780	59.9	4.100	13.54	.636
(34°-29′N 170°-25′W)–Honolulu	13.43	3,794	97.74	3,070	96.2	1.235	14.23	.944
Honolulu–Singapore	13.36	3,403	96.38	3,030	95.2	1.123	13.69	.976
Singapore–Bombay	13.01	3,486	95.43	2,800	93.0	1.245	13.81	.942
Mormugao–Singapore	12.17	3,415	93.29	2,180	85.5	1.567	13.75	.885
Singapore–Yokohama	12.67	3,730	96.95	2,560	89.9	1.458	14.06	.901

8. Oscillations of the ship

As was stated before, actual ocean waves are very irregular, and accordingly oscillations of a ship are also very irregular in their period as well as amplitude. Therefore, the results of the measurements were expressed in their average values for convenience sake, though it is difficult to express them as regular oscillation.

After Exp. No. 80, the times at which the crests of waves passed through the ship's bow were recorded as the encounter marks, and from these, the variation and average values of the period of encounter throughout a period of three minutes can be obtained. An example of the frequency distribution of periods of oscillations of the ship are shown in Fig. 65. Therefore, the periods of encounter T_e shown in Tables 4–5, are average values out of the distributed periods as stated above, and when encounter marks could not be obtained, T_e was computed from the following formula.

$$T_e=\lambda/(v\cos\alpha-v_{wave})$$

where v is the ship's speed measured and λ is the wave length derived from the observed period regarding an ocean wave as a trochoidal wave (observed wave lengths were not adopted as they were thought to be observed shorter than actual). In addition, the period of yawing was adopted as period of encounter, when computed periods were thought

to be not suitable, because the period of yawing must coincide with the period of encounter.

As to the ship's natural period of oscillations, the following values were adopted; period of rolling $T_r=2\pi\frac{k}{\sqrt{g\cdot GM}}$

period of pitching $T_p=2\pi\frac{k'}{\sqrt{g\cdot GM'}}$

where k and k' are the radii of gyration around the ship's longitudinal and transverse axis, containing the virtual masses, for which the following values were chosen,

full load condition: $k=5.78$ m$=$B/3.03, $k'=42.7$ m$=$L/3

light load condition: $k=7.81$ m$=$B/2.24, $k'=55.7$ m$=$L/2.3

from the above values, the periods were computed as in the following table;

Condition No.	Rolling		Pitching	
	GM (m)	T_r (sec.)	GM' (m)	T_p (sec.)
I—II	1.69	12.2	230	7.28
III	0.94	12.0	149	7.02
IV	0.89	12.3		
V	0.77	13.25		

The frequency diagrams of the periods of encounter and periods of oscillations during the voyage from Yokohama to Vancouver, and Vancouver to Honolulu, are shown in Fig. 66, in which one frequency represents an average value out of one measurement, the frequency of periods of encounter not being counted in such cases, for which a record of oscillations could not be obtained.

From Fig. 66, it will be recognized that the distribution of pitching periods fairly coincides with those of the periods of encounter, and therefore as to pitching, the free oscillations diminish because of the large damping force, and forced oscillations will only remain even in such irregular waves. On the contrary, the distribution curve of the rolling periods has a hump around the rolling natural period, independent

of the period of encounter, showing that rolling in the natural period will only occur in such irregular waves. The above mentioned relations will be recognized from Fig. 67 too, in which, the period of oscillations is plotted against the period of encounter.

In Fig. 67, the plotted points for pitching coincide with a 45° line, showing that they are forced oscillations; on the other hand, those for rolling gather around a horizontal line corresponding to the natural rolling period, showing that they are free oscillations. As the ocean waves were extremely irregular, ideal synchronous oscillations did not occur, i.e., supposing the ship encounters a wave train having a period near to the ship's natural period, after 2–3 waves have passed, and the ship rolls to a considerable large angle, another wave train having a different period of phase will come, and the ship will be prevented from a further increase of rolling angle.

The frequency diagram of sea conditions in each course is shown in Fig. 68, as well as that of the angle of oscillation by way of comparison. The angle of oscillations is plotted against the sea scales in Fig. 69, in which it will be recognized that the rolling angles are independent of the sea condition, and reach to a considerable amplitude when the ship synchronizes with the waves, even in comparatively smooth seas.

As the period of encounter is distributed in a considerable range around their average value as shown in Fig. 65, there are occasions that a large angle of roll will occur when the average periods of encounter differ considerably from the ship's natural period, but it may be possible to reduce the rolling angle by changing the ship's course slightly and avoiding the synchronism. For instance, at 17.00, 19th, January, a large rolling angle of 25° (to one side) occurred by an abeam wave of 11 sec. in period, but the excessive rolling was reduced to almost zero by changing the ship's course 58° to lee-ward from the original course.

On the contrary, the pitching angle seems to have a certain relation to the sea conditions as shown in Fig. 69, and its amplitude is an increasing function of the sea condition.

As shown in Fig. 70, the yawing measured consists of a forced yawing by every wave and a zig-zag motion of the ship caused by automatic steering, the period of the former coinciding with the period of encounter of the waves, the latter being as long as 60–160 sec. When the ship encountered fair waves, the period of encounter was long, and therefore the amplitudes of the forced yawing were large, and those of the zig-zag motion small; and when the vessel encountered head waves, the results were vice-versa.

Records of the helm angle are also given in Fig. 70, in which it will be noticed that the helm angle was taken proportional but reverse to the ship's heading angle. The helm angles were 5°–10° in average, except in Exp. Nos. 62, 63, 74, 76, in which they reached to excessive angles as much as over 20° to one side (zig-zag motions also reached to large amplitude), and the loss of SHP can not be overlooked.

9. Fouling on the ship's bottom

"Nissei Maru" was docked on 30th November, 1951, and painted with one coating of anti-corrosive paint, and two coatings of anti-fouling paint respectively. Leaving the dock on 2nd December, she stayed in Tokyo Bay for 24 days during which preliminary trial on the 16th, official trial on the 19th, and owner's trial on the 25th were conducted respectively. Therefore, although she remained for a comparatively long period before her departure, her bottom was not fouled, and was in an ideal condition when she left Yokohama, having regard to the season of the year.

She anchored at the following ports;

Vancouver	for 8 days	Bombay	for 4.5 days
Honolulu	,, 1.5 ,,	Mormugao	,, 41.5 ,,
Singapore	,, 1 ,,	Singapore	,, 0.5 ,,

Therefore, it can be assumed that no great fouling to affect the ship's sea-performance occured on the voyage up to Mormugao.

During 41 days anchorage at Mormugao (depth of water 6–9 m, water temperature 30°C average), the ship's bottom and propeller were

thought to be fouled to a considerable degree, the effect of which on the ship's performance appearing clearly on the voyage from Mormugao to Yokohama.

The difference between the performance data of the above-mentioned voyage and that from Honolulu to Bombay, mainly attributable to the effect of fouling, and comparing the data measured in progressive tests in the Malacca Strait when voyaging to India, and that in the Borneo Sea on the vessel's return voyage, the effect of the fouling will easily be demonstrated, regarding the ship's displacement, sea and weather conditions almost equal in both measurements. From this comparison, it will be seen that a speed loss of 0.8 knots in the average resulting from the fouling.

Five days after her arrival at Yokohama, the bottom condition of the vessel was examined by the members of the Committee when she was in dock. As it was found that she might have slightly touched ground after her arrival at Yokohama, a thorough examination could not be conducted on the flat part of the bottom. But examples of pictures of the fouled condition are shown in Figs, 71–74.

As the vessel was in a light condition during the greater part of her stay at Mormugao, no fouling occurred above the light draught, only a slight roughing of the paint surface being noticed; below the light draught as far as the bilge keel, barnacles of 5 mm diameter had adhered to the outside plankings almost all over the whole area. On the flat part of the bottom, barnacles of the same size were thinly attached mixed with barnacles of 1 cm diameter and serpulas. The fouling of the flat part of the bottom was less than was expected, but it was thought that some of the grown substances might be torn off when the ship touched ground, and it was observed that the paint surface was chafed at many points.

As regards the bilge keel, though the upperside was not fouled, the lower side was densely covered with barnacles of 1 cm diameter over almost the whole area; the side and bottom of the sole-piece were dense with fully grown barnacles 1–1.5 cm in diameter.

As the pictures and sketches reveal, the fouling of the propeller was considerable, while the attached matter on the blades was almost torn off by the rotation of the propeller except near the root, but even in this cleared-up condition, it was considered that its effect on the propulsive efficiency of the ship could not be overlooked.

The barnacles which developed on the bottom and propeller had all died, only their shells remaining when the investigation was conducted, and there was no noticeable difference in the condition of fouling on each side of the ship.

10. Stress measurement of hull structure

It was not possible to compute the longitudinal stresses of the hull structure at sea and to make a comparison between the stresses measured and calculated, as the wave profile and water pressure distribution on the vessel were not investigated at that time. However, it is possible to make some brief discussions regarding the measured stresses of hull structure at sea.

(1) The records obtained by a Giken-type strain meter, which were taken from readings on a dial gauge every two seconds, almost coincided with the records taken by a wire strain gauge measured at the same position and at the same time. Therefore, the data obtained by the two strain gauges are considered to be reliable.

(2) Although the points of measurement were few and were relatively concentrated toward midship, the values of the mean range of the stress fluctuation for each location were obtained as shown in Fig. 75, taking the mean range of stress at location 1 as standard unit (1.00). The measured locations 3, 5 and 4, 7 were selected on the outer and inner surface of the steel plating respectively, where dotted lines indicate measurements on the outer surface.

(3) The maximum range of stress fluctuation throughout the voyage was recorded to be 6.1 kg/mm^2 at location 9 in Experiment No. 56.

(4) Stress measurements at location 7 were taken throughout the

the entire voyages and the data obtained were plotted on a graph for each course, so as to find the relation between range of stress, mean and maximum, and wave length (length along ship centre line) or wave height, but because the actual waves were so irregular, it was not possible to clarify their relationship. However, during the course of the voyage between Vancouver and Honolulu, there was a tendency for the range of stress to increase with the increase of wave length, but no tendency was observed to indicate that the range of stress becomes highest when the ship's length and wave length coincide with each other.

(5) It is difficult to explain accurately the relation between amplitude of pitching and range of stress (at location 7) for the same reason above stated, but the mean period of pitching and that of the range of stress were approximately the same with a slightly shorter period for the latter.

Upon comparison of the records between amplitude of pitching and change of stress, it was found that the stress changed to the compression side when the bow moved upward and the phases coincided with each other. The tendency was recognized in which the range of stress, mean and maximum, increased in accordance with the increase of the pitching angle, mean and maximum, respectively.

(6) It has been generally accepted that a dynamic stress develops on the hull structure from a shock to the fore bottom part, the phenomena of which were experienced often during the voyage. In Fig. 76, a typical record of slamming phenomena obtained by the strain gauge is illustrated, and the maximum range of dynamic stress will be recognized as approximately 20% of the case without slamming phenomena.

(7) The frequencies of the vibratory stress on the hull structure measured on the voyage from Yokohama to Vancouver was 115 to 120 cycle per minute and about 88 cycle per minute from Vancouver to Honolulu. These observed frequencies are estimated to be nearly equal to the fundamental frequencies of vertical flexual vibration of the ship's

hull when actually loaded, in ballast and fully loaded condition at sea. Therefore, the dynamic stress can be recognized to originate from dynamic force, acting to the forward bottom part, which induces a vertical bending vibration of the hull. A maximum range of dynamic stress of 1.0 kg/mm^2 was recorded, but the figure cannot be recognized as the maximum value on ship's hull because of the limited number of measured positions.

Table 3. Yokohama—Vancouver

Cond. No.	Exp. No.	Date	Time	*1 Weather	Temp. Air °C	Temp. Sea Water °C	Course deg.	Wind: Beaufort Scale	Wind: Relative Direction Range deg.	Wind: Relative Direction Mean deg.	Wind: Relative speed Range m/s	Wind: Relative speed Mean m/s	Wind: Absolute Direc. deg.	Wind: Absolute Speed m/s	Wave: *2 Sea	Wave: Length m	Wave: Height m	Wave: Direct. deg.	Wave: Observed Period sec.	Ship Speed kn	Torque: Mean t−m	Torque: Fluctuation Max. t−m	Torque: Fluctuation Min. t−m	Torque: Fluctuation Amp. %
		1951																						
	1	12.26	20.02	o	15				S 7~ 22	S 13	13 ~19	16									17.23	22.34	13.20	53
	2	27	9.25				52	NW 7	P 70~110	P 85	10.5~20.5	16	309	16.4						10.98	19.93	28.57	15.07	68
	3	〃	12.05	bc	12.0	16.5	52	NW/W7	P 70~100	P 85	9.5~21.5	16	306	16.5	R					11.27	18.71	24.10	14.54	56
	4	〃	15.00				50	NW/W5	P 50~ 85	P 70	5.5~14	10	304	10.0	〃	70	2.5	P 70	11	11.27	19.28	26.34	13.43	66
	5	28	9.00				〃	NW 6	P 50~ 70	P 65	12 ~17	14.5	320	13.0	R.R	45	1.5	P 80	7	11.56	20.60	25.45	17.14	39
	6	〃	12.00	o	5.6	12.0	〃	NW/W6	P 60~ 80	P 70	8.5~11.5	10	301	10.0	SI	40	2	0	9	12.74	19.27	24.10	12.78	59
	7	〃	15.00				55	NW 3	P 45~ 65	P 55	5 ~ 9	7.5	308	6.4	〃	50	1.5	P 10	9	12.51	19.49	25.93	13 01	66
	8	29	9.10				〃	WSW 4	P 95~180	P 140	0 ~ 2	1	242	8.0	〃	40	1.5	P 10	8	13.54	20.09	24.25	16 37	39
	9	〃	12.05	c	3.3	4.5	〃	W/N 4	P 30~100	P 70	2 ~ 7	5	277	7.3	〃	50	1	P 10	6	13.88	20.44	21.92	17.29	23
	10	〃	12.15				〃	WSW 3	P 35~100	P 70	1 ~ 3	1.5	248	6.1	〃					12.54	17.19	22.64	11.70	64
I	11	〃	12.20				〃	SW/W4	P 95~ S110	P 175	1 ~ 5.5	3	237	8.7	〃					11.12	13.74	26 37	9.87	47
	12	〃	12.40				〃	SW/W4	S115~ P125	S 175	0 ~ 5	3	233	8.1	〃					9.67	9.93	12.16	7.57	46
	13	〃	12.57				〃	SW/W4	(var.)	P 125	0 ~ 4	2	241	8.3	〃	40	1		6	14.80	24 81	27.04	12.50	22
	14	〃	15.00				〃	WNW 5	P 50~ 95	P 75	5 ~11	9	294	10.1	〃	30	0.8		5	14.37	23.68	24.90	19.51	23
	15	30	9.04				64	W/N 5	P 75~115	P 100	6 ~ 9.5	7.5	284	11.6	Mod	15	1	P 120	4	14.30	23 00	26.09	16.79	40
	16	〃	12.02	bc	0.6	5.5	62	W/N 6	P 60~120	P 105	5.5~13	9	284	13.0	〃	20	1	P 120	4.5	14.08	23.65	26.78	17.60	39
	17	〃	15.00				〃	W/N 6	P 95~155	P 115	5 ~11	8	276	13.0	R.R	30	1	P 120	5	14.11	24.04	27 00	18.59	35
	18	31	9.00				〃	W 5	P105~160	P 130	2.5~ 8	6.5	267	12 0	Mod	30	1.5	P 140	4.5	13.47	18.56	22.19	14 92	39
	19	〃	12.00	b	1.7	3.5	〃	W 7	P110~160	P 135	6 ~12.5	10	269	15.8	SI	40	2	P 150	4	13.7	18.93	22.76	13.27	50
	20	〃	15.20				78	W 5	P85~ S175	P 155	2 ~ 7	5	269	11.6	〃	40	2	P 165	5	13.5	19.56	21.65	15 28	32
		1952																						
	21	1. 1	12.00	bc	3.3	4.0	80	W/S 5	P85~ S175	S 160	1.5~ 8	4.5	253	11.5	〃	40	1.8	P 160	5	13.24	19.53	23.24	14.51	45
	22	〃	15.00				〃	SW/W5	S 90~150	S 130	3 ~ 8.5	6	237	11.9	〃	40	2	P 170	5	13.39	18.03	22 95	11.23	66
	23	2	9.10				85	S/E 7	S 30~ 95	S 70	10.5~24.5	17.5	174	16.4	R	10	1.5	S 90	4	12.76	19.33	21.82	16.21	29
	24	〃	12.00	d	5.6	4.5	90	S/W 7	S 50~100	S 77	8 ~26	17	193	17.3	〃	30	1.5	S 90	5	13.01	19.84	23.72	14.38	45
	25	〃					〃	S/W 7	S 20~105	S 80	9 ~24	16	193	16.2	〃	〃	〃	〃	〃	12.75	18.84	22.05	13.82	43
	26	〃					〃	S S W 7	S 25~105	S 85	5.5~23	15	198	15.8	〃	〃	〃	〃	〃	12.00	17.68	23.70	10.75	73
	27	〃					〃	S S W 7	S 5~130	S 85	6 ~24	15	199	15.8	〃	〃	〃	〃	〃	12.66	19.60	21.70	17 03	24
	28	〃	12.35				〃	S/W 7	S 50~110	S 80	7 ~23.5	15	194	15.2	〃	〃	〃	〃	〃	12.21	19.09	23.50	11.02	66
	29	〃	15.00				〃	S/W 7	S 10~115	S 80	7 ~21	15	195	15.3	H	40	2.5	S 90	6	12.93	18.60	24.32	11.52	69
	30	2	9.00				〃	SW 5	S 65~130	S 95	4 ~11	7	228	10.4	R.R	30	1.5	S 130	5	13.85	19.51	24.18	11.77	64
	31	〃	12.00	d	7.2	6.0	〃	SW 6	S 70~140	S 110	3.5~15	10	228	14.2	〃	40	1.5	S 115	6	13.66	20.47	25.19	13.48	57
	32	〃	15.00				〃	NW/W5	P 75~140	P 105	3 ~ 7.5	5	300	9.7	Mod	50	1.5	S 105	6	13.23	18.51	23.30	13.00	57
	33	3	9.00				〃	W 7	P150~ S135	180	4.5~14	10	270	17.4	〃	40~70	2	S 175	4~14	14 30	20 20	21.72	17.36	22
	34	〃	12.00	o	3.3	5.0	94	NW 7	P 90~145	P 120	7 ~17	13	314	17.7	〃	30	1	P 150	6	13 9	20.28	25.37	14.40	54
	35	〃	15.00				〃	NW/W8	P 80~170	P 140	5.5~19	14	301	19.6	R.R	50	3	P 150	7	13.1	16.36	23.62	7.87	95
	36	4	9.00				〃	NW/W9	P115~175	P 145	8 ~26	19	300	24.8	H	50	2	P 155	7	13 0	17.50	22.86	11.10	67
II	37	〃	12.00	c	3.5	5.0	87	WNW 7	P100~175	P 145	4 ~15	12	289	18.4	〃	60	2	P 165	7	11.90	16 27	25.35	7 73	108
	38	〃	14.00				〃	WNW 8	P105~175	P 140	4 ~17.5	13	292	19.1	〃					13.88				
	39	〃	15.00				〃	NW 7	P 90~140	P 115	6 ~22	13	312	16.7	〃	40	2.5	P 155	6 5	12 2	18.70	27.58	9.72	96
	40	〃					〃	NW 6	P 95~160	P 115	5 ~15	10	310	13.3	〃					10.9	14.22	29.43	−1.24	215
	41	〃					〃	NW/W7	P110~165	P 135	7 ~19	13	300	16.8	〃					9.49	12.06	19.70	2.62	142
	42	〃	15.35				〃	NW 8	P100~155	P 130	9.5~26.5	18	309	20.7	〃					7.04	8.09	14 81	2.50	152
	43	5	9.00				〃	NW 6	P 90~130	P 110	5 ~16	11	313	14.3	R.R	40	1.5	P 155	6	12.2	17.43	23.86	12.00	68
	44	〃	12.00	o	5.0	5.5	85	WNW 6	P110~155	P 130	5 ~12	9	295	13.6	〃	40	1.5	P 160	7	11.65	17.50	24 68	7 82	91
	45	〃	15.00				92	NW/W5	P 85~130	P 110	2.5~ 9	6	306	10.1	Mod	80	1.5	P 160	11	12.5	17.40	24 82	10 78	81
	46	6	12.00	o	5.6	6.5	〃	W/S 6	S120~175	S 150	3 ~ 9.5	6.5	257	13.2	〃	40	1.2	S 170	7	13.90	19.51	22 76	13.66	47
	47	〃	15.00				〃	NW/W6	P100~160	P 130	3 ~13	9	300	14.7	SI	60	1 5	S 160	8	13 90	18 35	24 25	9.26	82
	48	7	9.10				〃	NW/W4	P 45~110	P 80	2.5~ 5	4	304	7.6	Sm	40	1		7	13 75	19 99	22 19	17.75	22
	49	〃	12.00	bc	7.8	6.5	〃	W 4	P 85~170	P 135	0 ~ 2.5	1.5	275	8.2	SI					13 8	19.35	23 03	15.53	37
	50	〃	15.00				87	WNW 3	P 5~ 65	P 30	2 ~ 5	3	287	4.5	Sm	50	0.7		7	13.3	17.97	25 05	11.40	76
	51	8	9.00							S 70		11		10.7	〃					13.1	17.02	17.60	16.48	7

Table 3. Yokohama—Vancouver

Remarks; * 1 b=blue sky, bc=blue sky with cloud, c=cloudy, o=overcast cloudy, d=drizzling rain, r=rain
* 2 C=Calm, V. Sm=Very Smooth, Sm=Smooth, Sl=Slight, Mod=Moderate, R.R=Rather Rough
R=Rough, H=High

RPM	SHP	Oscillation									Stress												Helm Angle		Remarks	Exp. No.
		Period of Enc. sec.	Pitching			Rolling			Yawing			Position No.	Stress Max. kg/cm²	Stress Mean kg/cm²	Mean Half Period sec.	Position No.	Stress Max. kg/cm²	Stress Mean kg/cm²	Mean Half Period sec.	Position No.	Stress Max. kg/cm²	Stress Mean kg/cm²	Mean Half Period sec.	Port Max. deg.	Stab. Max. deg.		
			Max. deg.	Mean deg.	Period sec.	Max. deg.	Mean deg.	Period sec.	Max. deg.	Mean deg.	Period sec.																
72.3	1739	—	2.0	1.0		2.0	.5		/1.0																Yokohama Dep.	1
85.4	2378	—	4.5	2.7		3.0	2.0																			2
87.0	2274	8.6	4.0	2.0	7.5	5.0	2.1	12	/3	/1.6	8.6	2	153.5	71.0	4.0	6	114.0	49.0	4.0	7	146.0	82.0	4.0			3
88.1	2371	9.8	5.0	2.5	9.0	7.5	4.0	11.2	/3	/1.7	9.5	2	153.5	54.3	3.6	6	114.0	44.5	3.6	7	210.0	79.0	3.6			4
90.1	2692	7.5	6.5	3.0	8.2	4.3	1.5	11.2	1/3		7.5	2	153.5	75.8	4.2	6	114.0	58.7	4.2	7	186.0	90.0	4.0			5
90.6	2437	9.0	4.8	1.8	8.2	2.1	1.1	12	1.5/2		8.2	2	115.0	58.3	3.2	6	114.0	37.1	3.2	7	146.0	61.3	3.2			6
90.1	2453	6.2	4.1	2.2	7.5	2.2	.9	12.8	1/1.5		7.5	2	122.8	44.1	3.0	6	92.0	31.2	3.0	7	156.0	57.1	3.0			7
94.7	2656	7.6	3.5	2.5	7.8	3.1	1.4	13.8	/1		10.0	2	102.3	37.8	3.0	6	78.0	32.1	3.0	7	84.0	42.0	3.0			8
95.7	2729	8.1	2.4	1.3	6.9	2.5	.8	11.2	/1.5	/1.2	8.6	2	78.4	38.4	3.9	5	59.0	33.3	3.9	7	62.0	41.0	3.9			9
86.5	2077	7.8	3.3	1.9	9.0	2.3	1.3	13.8	/2.1	/1.5	12	2	76.7	39.5	4.0	5	117.0	48.0	4.0	7	77.5	41.0	4.0			10
77.1	1478	7.5	2.3	1.5	9.0	3.6	2.1	10.0	/1.7	〃	8.5	2	76.7	43.2	3.7	5	79.5	36.6	3.7	7	84.0	37.0	3.7			Progressive test 11
65.4	907	7.3							1/2.0	〃																12
101.9	3592	3.3							〃	〃		2	76.7	30.0	3.6	5	73.5	32.8	3.6	7	58.0	32.6	3.6			13
101.8	3366	2.6							/1.7	/1.2		2	76.7	31.0	3.4	5	96.0	24.0	3.4	7	85.0	41.0	3.4			14
102.3	3285	9.9							/4.5	/2.2		2	76.7	42.1	4.3	5	73.5	29.0	4.1	7	136.0	41.7	4.1			15
102.3	3379	9.5							/4.0	/2.5		2	115.0	30.7	4.7	5	84.0	29.0	4.7	7	156.0	54.0	4.4			16
102.6	3445	9.4							/5.5	/2.2		1	113.5	67.6	6.0	5	96.0	47.0	6.0	7	105.0	48.7	6.0	7.5	4.35	17
92.3	2379	18.9							/5.0	/2.2		1	113.5	74.4	6.4	5	96.0	57.6	6.4	7	146.0	82.5	6.4	14.0	6.2	18
91.9	2439	25.7							/7.8	/2.4		1	151.5	63.5	5.5	5	123.0	57.3	5.5	7	122.0	59.5	5.5	8.9	6.4	19
90.1	2461	35.7				5.5			/9.8	/2.5		1	151.5	58.6	5.0	5	112.0	49.5	5.0	7	116.0	48.5	5.0	7.8	5.6	20
91.9	2506	27.9			15~18	5.5		10~12	/3.5	/2.0		1	151.5	51.6	6.1	5	123.0	54.0	6.1	7	116.0	48.0	6.1			21
92.4	2326	38.4				9.5			/4.0	/2.0		3	151.5	80.0	6.5	5	157.0	72.7	6.5	7	175.0	84.5	6.5			22
89.5	2416	4				11.5		8	/6.0	/2.2		3	151.5	68.0	4.5	5	110.0	36.7	4.8	7	140.0	73.5	4.5			23
91.7	2540	5							/4.2	/2.1		3	227.0	106.0	4.4	5	110.0	29.0	5.5	7	157.5	91.0	5.0			24
88.4	2326	—																								25
86.7	2141	—																							Aut. Steering	26
88.8	2431	—																							Hand 〃	27
88.2	2351	—																							Rudder 0°	28
91.2	2369	6				16.1			/6.0	/2.8		3	227.0	83.5	4.2	5	24.0	14.7	8.0	7	209.0	74.0	4.4			29
93.8	2556	12.1				10.3	13.7		/4.0	/2.0		3	200.0	61.5	4.0	5	159.0	53.0	4.0	7	122.0	40.5	4.0			30
94.8	2710	8.7				13.7			/3.4	/2.6		4	115.0	32.8	4.0	5	96.0	37.7	4.0	7	116.0	40.0	4.0			31
89.0	2301	7.4				8.9			/3.6	/2.1		4	230.0	81.2	5.4	5	216.0	79.0	5.4	7	232.0	77.5	5.4			32
93.9	2649	—				5.5			/4.0	/2.0		4	153.0	47.2	5.7	5	147.0	53.0	5.7	7	156.0	62.4	5.7			33
94.3	2671	23.3			18	3.4			/4.8	/2.3		4	193.0	96.0	7.1	5	192.0	96.0	7.1	7	186.0	101.0	7.1			34
89.3	2040	17.7			12	6.8			/4.8	/2.5		4	153.0	99.0	7.0	5	192.0	91.0	7.0	7	166.0	113.0	7.0			35
89.3	2058	16.7				8.2			/5.0	/2.3		4	322.0	172.0	9.0	6	138.0	71.0	9.0	7	231.0	130.0	9.0			36
89.8	2040	19.0			17	10.7		13	/4.2	/3.0		4	250.0	147.0	7.0	6	114.0	64.5	7.0	7	166.0	107.0	7.0			37
		—			17	9.7		11	/3.8	/2.7															Log Test	38
96.5	2521	15.9										8	286.0	117.0	6.7	6	138.0	63.7	6.7	7	254.0	105.0	6.7			39
85.6	1760	—										8	287.0	115.0	7.0	6	143.0	53.0	7.0	7	228.0	98.0	7.0			40
76.9	1295	—																							Prog. Test	41
65.5	740	—										8	250.0	100.0	5.7	6	88.0	39.6	5.7	7	175.0	82.0	5.7			42
91.0	2215	16.6				12.8		14	/5.3	/2.6		8	191.0	89.0	5.6	6	66.0	38.4	5.6	7	146.0	84.0	5.6			43
95.9	2343	14.4	0		17	4.8	3.1	12	/5.8	/2.2		10	204.6	80.5	5.4	6	88.0	36.0	5.4	7	146.0	66.0	5.4			44
92.0	2225	16.3	0			4.8		12	/4.3	/2.5		10	204.6	66.2	5.0	6	102.0	35.0	5.0	7	156.0	55.5	5.0			45
92.8	2527	19.7	0		17	5.2	2.2	14				10	136.0	59.2	5.0	6	61.5	26.5	5.0	7	116.0	43.0	5.0			46
93.7	2460	17.9	0		19	5.0	2.8	13				9	115.0	67.0	6.6	11	102.0	51.0	6.6	7	42.0	28.9	6.6	3.9	8.8	47
92.3	2576	17.9	2.0		17	5.0	2.8	13				9	384.0	153.5	7.0	11	332.0	129.5	7.0	7	210.0	90.0	7.0	11.6	10.9	48
92.3	2494	—	1.0			4.1	2.8					9	153.5	46.0	5.0	11	76.7	30.7	5.0	7	144.0	38.6	5.0	2.0	6.5	49
90.5	2270	18.3	2.0		20	4.8	2.1					9	136.5	73.0	5.7	11	153.0	70.7	5.7	7	89.0	50.7	5.7	1.0	6.0	50
												9	272.8	146.0	7.3	11	265.0	167.0	7.3	7	156.0	120.0	7.3	4.9	9.4	
84.9	2017	—																							Vancouver Arriv.	51

30-2

Table 4. Vancouver—Honolulu

Cond. No.	Exp. No.	Date	Time	*1 Weather	Temp. Air °C	Temp. Sea Water °C	Course deg.	Wind: Beaufort Scale	Wind: Relative Direction Mean deg.	Wind: Relative Direction Range deg.	Wind: Relative Speed Range m/s	Wind: Relative Speed Mean m/s	Wind: Absolute Direc. deg.	Wind: Absolute Speed m/s	*2 Sea	Wave: Length m	Wave: Height m	Wave: Direc. deg.	Wave: Observed Period sec.	Ship Speed kn	Torque: Mean $t-m$	Torque: Fluctuation Max. $t-m$	Torque: Fluctuation Min. $t-m$	Torque: Fluctuation Amp. %
		1952																						
	52	1.16	19.00	o	0	4.0		3	P 30~ 40	P 35	9 ~11	10		6.2	Sm					12.6	19.89	20.35	19.51	4
	53	17	9.07				234	S S W 4	P 15~ 30	P 25	13 ~19	17.5	199	7.0	Mod	6	1		5.2	12.3	23.52	24.02	22.45	7
	54	〃	12.00	o	5.6	6.5	〃	S S W 6	P 15~ 30	P 25	15.5~22	19	199	13 6	〃	10	2	P 10	5	11.85	24.59	25.59	23.87	7
	55	〃	15.00				〃	S S W 7	P 10~ 25	P 20	14 ~23	20.5	206	15.1	R.R	54	2	P 5	5	11.56	24.75	25.93	23.41	10
	56	18	9.00				〃	NW/W5	S 35~ 60	S 45	11 ~15	13.5	302	10.0	Mod	45	1.5	S 20	6.5	11.16	24.90	27.08	22.34	19
	57	〃	12.00	o	7.8	8.0	232	W 4	S 10~ 35	S 25	10 ~14	12	275	6.9	〃	50	2.5	S 45	9	11.65	25.64	28.31	21.65	26
	58	〃	12.10				〃	W 4	S 15~ 30	S 25	9 ~12.5	10.5	276	6.9	〃					10.55	20.62	24.24	18.82	26
III	59	〃	12.20				〃	W 4	S 10~ 35	S 25	8 ~13	10	276	6.3	〃					8.8	18.21	18.82	15.53	18
	60	〃	12.30				〃	W N W 4	S 20~ 45	S 35	8 ~13	11	287	8.1	〃					7.9	14.46	15.91	13.12	19
	61	〃	15.00				〃	W/S 4	S 0~ 25	S 15	10.5~15	13	262	7.4	〃	30	1.5	S 10	8	11.85	24.29	26.02	22.67	14
	62	19	9.00				〃	W N W 8	S 35~ 70	S 50	17 ~25	22	294	19.1	H	45	3	S 45	8	9.95	25.34	28.31	23.26	20
	63	〃	12.00	b c	6.7	8.5	245	NW/W7	S 20~ 75	S 45	10.5~25	20	301	17.1	〃	60	4	S 35	9	8.65	26.45	28.31	23.41	19
	64	〃	15.00				〃	W N W 7	S 25~ 50	S 35	14 ~24	19.5	292	15.9	〃	90	5	S 50	10	9.25	27.18	29.70	22.94	25
	65	20	9.00				230	NW/W3	S 20~ 45	S 30	8 ~12	10	299	5.4	SI	90	2	S 25	9.5	13.1	25.05	25.55	23.52	8
	66	〃	12.00	o	10.0	9.5	232	W 2	S 0~ 22	S 10	7 ~10.5	9	269	2.6	〃	60~100	1.5	S 90	6~ 9	13.2	25.90	27.08	24.79	9
	67	〃	15.00				〃	S S E 2	P 5~ 30	P 20	6 ~10	8	162	2.6	〃	60~ 80	1.2	S 80	8~10	13.0	24.88	25.90	23.26	11
	68	21	9.00				〃	S E 7	P 50~100	P 75	12 ~20	17	139	16.4	R	45	2	P 30	6.5	10.3	24.21	26.39	21.02	22
	69	〃	12.00	d	15.5	14.5	〃	S/E 6	P 40~ 60	P 50	12 ~17	15	164	12.4	〃	55	3	P 40	6.5	9.6	24.52	29.38	20.92	34
	70	〃	15.00				〃	S 5	P 25~ 50	P 37	12 ~17	14.5	178	10.8	〃	70	3	P 40	8	9.86	28.31	32.70	22.34	37
	71	22	9.00				270	W/N 5	S 0~ 15	S 5	13 ~19	16.5	279	10.8	R.R	100	3	0	9.5	10.93	25.70	29.64	21.65	31
	72	〃	12.00	b c	12.8	14.5	〃	W N W 5	S 0~ 20	S 10	11 ~20	17	287	11.4	R	120	5	S 10	10	11.07	25.75	36.83	19.97	66
	73	〃	15.00				〃	W/N 5	S 0~ 15	S 10	12 ~19	16.5	282	11.4	R.R	130~200	6	S 10	10	10.15	25.04	29.64	21.08	34
	74	23	9.00				〃	W/N 7	S 0~ 20	S 12	14 ~23	19.5	286	15.2	H	100	5	S 5	10	8.73	27.86	31.32	23.75	27
	75	〃	12.02	b c	11.5	14.5	265	W 6	P 5~ S 20	S 7	11 ~22	17	275	13.3	〃	110	5	S 10	9.5	7.41	24.15	27.44	17.90	40
	76	〃	15.00				〃	W/N 8	S 5~ 25	S 17	16 ~26	22	286	19.0	〃	100~140	5.5	S 10	7~10	6.17	28.23	32.59	24.63	28
	77	24	9.00				250	W 7	S 10~ 35	S 20	16 ~27	21	276	18.1	〃	150	6	S 20	12	6.10	26.02	31.79	20.20	45
IV	78	〃	12.00	b	13.3	15.5	〃	W 7	S 5~ 20	S 15	16 ~21	19	268	15.5	〃	100	6	S 15	10	7.23	24.72	28.61	20.77	32
	79	〃	15.00				270	W N W 5	S 5~ 25	S 20	11 ~19	15	296	10.8	〃	120	5	S 10	10	8.73	25.37	30.03	19.78	40
	80	25	9.00				〃	W S W 7	P 10~ 30	P 20	13 ~22.5	18	246	14.7	〃	140	6	S 5	10	6.84	26.97	36.80	15.76	41
	81	〃	12.00	o	11.1	15.0	〃	W/S 6	P 0~ 10	P 5	13 ~21	17.5	264	13.8	R	140	7	S 5	11	7.06	27.29	34.35	19.93	53
	82	〃	15.00				〃	W/N 6	S 0~ 20	S 10	11.5~19	16	283	13.1	〃	140	5	S 5	10	5.61	21.20	26.39	14.69	55
	83	26	9.00				〃	W N W 7	S 5~ 20	S 15	15 ~22	19	290	15.2	〃	180	6	S 10	11	7.78	29.49	36.18	21.92	48
	84	〃	12.00	b c	12.2	14.5	〃	W/N 6	S 0~ 15	S 5	10 ~21	17.5	277	13.1	R.R	150	6	S 10	11	8.57	27.63	31.98	21.65	37
	85	〃	15.00				〃	W/N 6	P 5~ S 10	S 5	11.5~21.5	18	277	13.6	R	140	5	0	11	8.85	28.03	36.38	21.38	54
	86	27	9.00				〃	W/S 4	P 0~ 20	P 8	11 ~17	13	257	7.9	Mod	100	4	S 5	10	10.10	31.63	36.57	25.55	35
	87	〃	12.00	d	13.9	15.5	〃	S W/W5	P 10~ 25	P 20	10.5~16	15	239	10.1	〃	100	2	0	10	11.57	29.77	33.20	26.24	23
	88	〃	15.05				〃	S W 5	P 20~ 40	P 30	14 ~17.5	16	224	11.1	〃	40	1.5	P 15	6.5	11.99	29.67	32.86	25.55	25
	89	28	9.00				142	W 8	S 90~130	S 110	9 ~23	16	271	19.4	H	70	5	S 160	10	13.24	28.13	32.86	24.90	28
	90	〃	12.00	b c	14.4	15.5	〃	W/N 8	S 85~135	S 120	7 ~20	16	278	20.1	R	100	5	S 160	10	12.72	30.35	33.20	24.79	28
	91	〃	15.00				〃	W/N 6	S 75~135	S 105	4 ~15	10	277	13.8	〃	100	4	S 145	10	13.85	30.01	33.81	24.90	30
V	92	29	9.00				130	W 6	S 80~135	S 110	4 ~13	7.5	274	11.9	SI	35	2	S 155	6.5	13.71	26.09	27.20	22.76	17
	93	〃	12.00	b c	17.5	19.0	〃	W/N 5	S 75~145	S 115	3 ~ 9	6	260	10.9	〃	100	1.5	S 160	10	13.42	26.82	28.96	24.25	18
	94	〃	15.00				〃	NW/W6	S 115~170	S 150	4 ~ 8.5	6	298	12.5	〃	90	2	S 160	8.5	13.55	26.71	30.35	23.78	25
	95	30	9.05				144	W/N 5	S 65~105	S 85	5 ~ 8.5	6.5	278	9.0	〃	140	5	S 165	13	13.61	26.62	29.70	24.15	21
	96	〃	12.00	b	22.8	22.0	〃	W 4	S 50~ 90	S 75	4.5~10	7	271	8.4	Mod	160	1.5	S 160	14	13.32	27.02	29.68	24.17	20

Table 4. Vancouver—Honolulu

RPM	SHP	Oscillation										Stress												Helm Angle		Remarks	Exp. No.
		Period of Enc. sec.	Pitching			Rolling			Yawing			Position No.	Stress		Mean Half Period sec.	Position No.	Stress		Mean Half Period sec.	Position No.	Stress		Mean Half Period sec.	Port Max. deg.	Stab. Max. deg.		
			Max. deg.	Mean deg.	Period sec.	Max. deg.	Mean deg.	Period sec.	Max. deg.	Mean deg.	Period sec.		Max. kg/cm²	Mean kg/cm²			Max. kg/cm²	Mean kg/cm²			Max. kg/cm²	Mean kg/cm²					
91.1	2531																							6.0	8.9	Vancouver Dep.	52
94.4	3102	3.0	1.0	0.5		0			/1.7		/5.4	9	153.5	37.2	2.4	11	102.0	35.4	2.4	7	77.5	20.6	2.4	6.4	3.1		53
93.9	3224	2.8	1.0			1.0			0.9/1.5			9	170.5	61.0	2.4	11	131.5	48.2	2.4	7	77.5	33.5	2.4	4.0	3.6		54
92.9	3211	3.4	1.6	0.8	6.9	1.4	0.7	12.9	0.6/1.0		/4.3	9	272.8	149.5	2.2	11	307.0	158.0	2.2	7	175.0	84.0	2.2	0.3	0.5		55
91.5	3181	4.2	3.5	1.6	7.2	2.6	1.4	12.9	0.8/2.8		8.2/90	9	384.0	158.0	2.8	11	229.0	115.0	2.8	7	186.0	77.0	2.8	13.5	4.6		56
92.4	3308	6.4	7.2	3.3	10.6	11.0	3.9	11.2				9	307.0	147.5	3.0	11	235.0	127.0	3.0	7	200.0	110.0	3.0	10.5	4.3		57
83.6	2407		7.4	1.7	9.0	11.4	3.6	12.9																11.0	5.0	Progressive Test	58
75.5	1919		4.5	1.3	8.2	5.8	3.4	15.0																13.5	4.4		59
67.4	1360		3.2	1.2	7.8	11.1	5.2	13.8																15.8	1.5		60
91.9	3110	5.3	3.0	1.6	6.4	10.8	4.2	12.9	1.0/2.7		8.2/70	8	215.0	91.0	3.1	10	329.0	114.0	3.1	7	155.0	70.0	3.1	9.0	6.1		61
89.4	3163	6.2	4.3	1.8	6.4	6.3	3.6	11.3	1.4/6.4		6.7/80	8	323.0	132.5	2.6	10	357.0	135.5	2.6	7	231.0	106.0	2.6	23.9	13.1		62
87.2	3221	7.1	5.1	2.4	7.2	5.3	2.2	10.0	2.3/6.9		7.2/70	8	287.0	165.0	3.0	10	284.0	149.0	3.0	7	254.0	129.0	3.0	22.8	17.5		63
88.8	3380	7.5	5.3	2.5	7.8	10.0	4.3	11.2	1.0/5.4		7.5/70	8	358.0	114.5	2.8	10	281.0	148.0	2.8	7	336.0	125.0	2.8				64
96.4	3373	8.2	1.8	0.9	7.8	6.8	4.8	12.0	1.1/2.2		8.2/	8	143.0	52.4	4.0	10	61.4	14.7	4.0	7	116.0	44.0	4.0	4.6	2.5		65
96.3	3482	8.2	2.3	1.0	8.6	9.2	5.4	12.9	1.6/2.4		8.2/	8	179.0	75.7	4.2	10				7	105.0	52.5	4.2	4.5	5.6		66
93.6	3251	8.0	2.0	0.8	9.0	6.2	2.4	12.9	1.2/2.5		11.3/120	8	107.5	50.0	3.7	10	153.0	67.5	3.7	7	97.5	42.0	3.7	3.6	5.1		67
89.9	3040	4.5	2.3			2.4	1.1	12.5	0.5/2.0		6.8/120	1	265.0	120.0	3.6	10	279.0	125.5	3.5	7	231.0	113.0	3.6	4.6	13.3		68
89.7	3069	6.0	3.5	1.7	7.5	2.5	1.3	12.8	1.1/2.0		6.2/100	1	265.0	136.0	3.7	10	259.0	155.0	3.7	7	234.0	135.0	3.7	2.0	11.9		69
90.0	3558	6.2	5.4	2.6	8.2	3.0	1.8	12.0	1.4/4.7		7.8/100	1	340.0	156.0	3.6	10	350.0	149.0	3.6	7	312.0	133.0	3.6	10.1	18.7		70
91.7	3290	6.9	3.8	2.6	8.0	2.9	2.0	10.9	1.0/3.5		8.8/100	1	227.0	132.5	4.0	10	229.0	124.0	4.0	7	210.0	115.5	4.0	6.3	8.5		71
91.8	3306	5.1	5.5	2.6	8.6	4.0	2.2	12.9	1.0/1.7		7.9/160	1	303.0	121.0	3.3	10	263.0	114.0	3.3	7	273.0	105.0	3.3	8.1	6.2		72
89.2	3118	7.5	6.1	2.5	8.6	4.6	2.6	13.8	1.6/3.6		7.5/120	1	378.0	135.0	3.0	10	416.0	131.5	3.0	7	336.0	109.0	3.0	10.8	8.4		73
87.1	3389	7.5	4.8	3.1	8.2	6.5	2.8	12.9	1.6/4.9		9.5/ 90	1	303.0	144.0	3.2	10	306.0	131.5	3.2	7	250.0	121.0	3.2	17.5	16.1		74
79.7	2688	7.1	5.1	3.0	9.5	5.1	2.5	12.0	2.1/4.5		10.0/180	1	303.0	151.5	3.4	2	281.0	132.5	3.4	7	294.0	125.0	3.4	7.7	3.0		75
79.6	3136	6.4	7.3	2.0	7.3	7.6	2.9	12.8				1	340.0	182.0	3.4	2	281.0	132.5	3.4	7	294.0	151.0	3.4	13.0	9.8		76
78.8	2861	9.0	6.0	3.0	8.6	10.1	6.1	12.9	2.0/5.4		9.0/160	1	416.0	182.0	3.9	2	384.0	161.0	3.9	7	432.0	177.5	3.9	10.4	6.3		77
77.6	2680	8.1	4.4	2.2	8.6	7.3	3.6	12.9	1.8/5.4			1	303.0	98.5	3.0	2	255.0	74.0	3.0	7	231.0	92.5	3.0	4.6	4.3		78
85.5	3028	7.8	5.2	3.4	8.6	8.3	5.7	12.0	1.8/3.8		10.0/120	1	416.0	160.0	3.5	2	332.0	110.0	3.5	7	399.0	143.0	3.5	6.9	5.9		79
83.8	3154	8.6	9.6	2.8	8.6	4.2	1.7	12.9				1	492.0	182.0	3.6	2	341.0	136.4	3.6	7	420.0	163.0	3.6	10.9	8.0		80
82.1	2441	11.2	7.8	2.9	10.0	3.5	1.5	10.0				1	378.0	151.5	3.5	2	329.0	110.0	3.4	7	373.0	138.0	3.4	4.7	6.4		81
69.0	2042	7.5	8.5	2.4	6.7	5.0	1.8	10.0				1	378.0	166.5	3.6	2	306.9	131.5	3.6	7	336.0	143.0	3.6	18.1	8.5		82
85.1	3503	7.8	7.8	2.2	7.5	7.2	2.1	10.6				1	378.0	166.5	3.4	2	306.9	136.4	3.4	7	312.0	152.0	3.4	24.5	4.7		83
86.2	3326	9.0	5.9	2.3	8.2	7.5	2.2	12.0				1	389.0	162.0	3.4	5	318.0	122.0	3.4	7	294.0	125.0	3.4	17.5	5.2		84
86.1	3372	9.5	5.9	3.0	10.0	7.0	5.9	12.0				1	340.0	136.0	2.8	5	288.0	120.0	2.8	7	336.0	122.0	2.8	12.5	6.2		85
93.4	4124	7.3	5.9	1.8	7.5	3.9	1.2	11.3	/ 4.0			1	303.0	121.0	3.2					7	294.0	109.0	3.1	10.7	8.0		86
96.8	4026	7.5	4.0	2.0	7.8	4.5	1.8	11.2	/10.0			1	303.0	133.5	3.2	5	264.0	109.0	3.2	7	254.0	113.0	3.2	9.0	4.5		87
97.7	4049	8.0	3.5	1.4	6.9	3.0	1.1	12.0	/ 2.5			1	260.0	121.0	3.3	5	205.0	93.5	3.3	7	210.0	92.5	3.3	6.2	5.8		88
98.5	3868	13.8	6.1	2.3	12.9	7.5	3.2	12.0	/ 5.5			1	303.0	108.5	4.0	5	252.0	84.0	4.0	7	250.0	75.5	4.0	16.4	2.5		89
98.6	4177	20.0	5.3	1.6	16.3	5.7	2.4	12.0	/ 7.0			1	378.0	131.5	4.9	5	288.0	96.0	4.9	7	315.0	113.0	4.9	26.3	0.2		90
101.1	4237	13.8	3.7	1.9	15.0	8.0	3.0	12.8	/ 5.5			1	303.0	112.5	4.6	4	212.0	80.0	4.6	7	231.0	88.0	4.6	12.5	4.2		91
97.7	3560	16.3	0.8			7.0	2.4	12.8				1	216.0	78.0	3.9	4	230.0	69.0	3.9	7	166.0	49.5	3.9	7.8	2.3		92
96.2	3662	18.0	5.3	2.2	18.0	4.7	2.0	13.8				1	189.0	60.5	4.3	4	195.0	50.2	4.3	7	186.0	61.0	4.3	8.0	5.0		93
96.4	3595	25.7	1.4			5.0	3.1	13.8																5.9	4.8		94
97.2	3613	22.5	3.0	1.3	20.0	2.9	1.5	12.0																9.8	3.0		95
96.2	3637	19.9	4.1	1.2	18.0	5.0	1.8	12.0																10.3	5.4	Honolulu Arriv.	96

Table 5. Honolulu—Bombay—Yokohama

Cond. No.	Exp. No.	Date	Time	*1 Weather	Temp. Air °C	Temp. Sea Water °C	Course deg.	Wind: Beaufort Scale	Relative Direction: Range deg.	Relative Direction: Mean deg.	Relative Speed: Range m/s	Relative Speed: Mean m/s	Absolute: Direc. deg.	Absolute: Speed m/s
	97	2. 1	12.15	b	19.0	19.5	260	NE 5	S 65~ 110	S 90	3 ~ 7	5	43	8.5
	98	2	12.05	b	22.5	23.5	251	NE/N 3	S 0~ 60	S 30	3 ~ 5	4	37	4.5
	99	3	12.00	b	24.0	24.5	251	NE 5	S 55~ 145	S 105	2 ~ 5	4	43	9.0
	—	4	〃	b	23.5	24.0	251			S 135		4		
	100	6	12.05	c	24.5	24.0	260	SE/S 2	P 0~ 35	P 20	5 ~ 6.5	6	145	2.5
	101	7	〃	b	24.0	25.0	258	ESE 3	P 30~ 60	P 40	2.5~ 4.5	4	115	4.6
	102	8	〃	b	26.0	25.0	257	NE/E 4	S 10~ 170	S 50	1 ~ 3	2	59	6.8
	103	9	〃	b	26.5	25.0	256	E 5	P 110~ 180	P 150	1 ~ 4	2.5	85	9.0
VI	104	10	〃	b	28.5	25.5	258	E 5	P 95~ 145	P 125	1.5~ 4	3	94	9.0
	105	11	〃	b c	28.5	26.5	260	E/N 4	S 20~ 40	S 20	0 ~ 1	1	74	6.0
	106	12	〃	b c	27.5	26.5	258	ENE 5	S 110~ 155	S 130	2 ~ 4.5	3	63	9.2
	107	13	〃	c	26.5	27.5	260	E 5	S 155~ P 115	P 160	1.5~ 4	3	86	9.9
	108	14	〃	b c	26.0	26.0	258	E/N 5	P 170~ S 145	S 175	1.5~ 5.5	3.5	76	10.5
	109	15	〃	b	28.5	27.0	256	ENE 5	S 130~ 170	S 150	1.5~ 4	3	67	9.6
	110	16	〃	c	27.5	26.0	259	NE 3	S 35~ 60	S 50	3 ~ 4	3.5	48	5.4
	111	17	〃	b c	26.5	27.0	254	NE/N 1	S 10~ 10	S 10	5 ~ 6	3.5	34	1.8
	112	18	〃	b	25.5	27.5	222	NE/E 2	P 3~ 15	P 5	4 ~ 5.5	4.5	55	2.5
	113	19	〃	o	22.5	26.0	242	N 4	S 50~ 90	S 65	7 ~ 10	8.5	356	8.4
	114	21	〃	o	25.5	26.0	305	NW/N 1	S 5~ 10	S 5	6.5~ 9	8	331	1.6
	115	22	10.35				304	NNE 2	S 12~ 20	S 15	6.5~ 8.5	8	24	2.4
	116	〃	10.50				〃	NE/N 2	S 18~ 22	S 20	7.5~ 8	7.5	30	2.5
	117	〃	11.05				〃	NE/N 2	S 20~ 30	S 25	7 ~ 8	7.5	31	2.8
	118	〃	11.20				〃	NE/N 2	S 25~ 33	S 30	7 ~ 8	7.5	29	3.7
	119	〃	11.35	b c	29.0	29.0	〃	NE/N 3	S 30~ 48	S 40	6.5~ 7.5	7	36	4.3
VII	120	23	12.05	b c	28.5	27.5	268	NE 4	S 55~ 74	S 65	4 ~ 5.5	5	44	6.5
	121	24	〃	b	27.0	27.5	274	NE/N 3	S 37~ 58	S 50	6 ~ 7	6.5	31	5.3
	122	25	〃	b	26.5	27.0	266	NNE 5	S 50~ 83	S 70	7 ~ 10	9	19	9.2
	123	26	〃	b	27.5	28.5	318	ENE 6	S 58~ 85	S 75	10 ~ 13.5	12	66	12.2
	124	27	〃	b	28.5	28.5	335	SW/S 2	P 23~ 31	P 25	5.5~ 6.5	6	218	2.8
	125	28	〃	b	25.0	25.5	343	WNW 1	P 5~ 20	P 10	6.5~ 7	6.5	287	1.4
	126	3. 4	15.13				164	NW/N 4	S 40~ 65	S 50	2.5~ 3.5	3	324	6.8
	127	〃	15.28				〃	NW/N 4	S 45~ 70	S 55	2.5~ 3	3	326	7.3
VIII	128	〃	15.43				〃	NW 3	S 40~ 80	S 50	3.5~ 4	3.5	318	6.1
	129	〃	15.58				〃	NW 4	S 50~ 80	S 65	3 ~ 4	4	313	6.7
	130	〃	16.13	b	30.0	26.5	〃	NW/N 4	S 60~ 100	S 80	1 ~ 2.5	2	327	6.6
	131	〃	16.28				〃	NW/N 4	S 90~ 110	S 100	0.5~ 2.5	1.5	330	6.3
	132	4.16	12.07	b c	29.0	29.5	157	NW/N 2	P 5~ S 10	S 5	2.5~ 4	3	330	3.0
	133	17	12.00	b	25.5	28.5	137	NW/N 2	S 5~ P 18	P 5	3.5~ 5	4	328	2.0
	134	18	11.55	b	27.5	28.5	90	NNE 1	P 5~ 20	P 15	5.5~ 8	7	20	1.9
IX	135	19	11.57	c	26.5	28.5	〃	NNE 3	P 25~ 38	P 30	8.5~ 10.5	9.5	27	5.9
	136	20	12.05	b c	28.5	29.0	88	N/E 3	P 28~ 38	P 30	7 ~ 9	8	7	4.3
	137	21	〃	b c	28.5	29.0	82	W/N 2	P 3~ 21	P 10	3.5~ 5	4	278	2.7
	138	22	〃	b c	28.5	28.5	124	N/E 1	P 6~ 21	P 15	5.5~ 7.5	6	11	1.7
	139	23	11.55	b c	27.5	29.5	126	N/W 1	P 2~ 17	P 10	5 ~ 6.5	5.5	348	1.3
	140	24	〃	b c	27.0	29.0	63	SE 2	P 10~ 20	P 15	7 ~ 9	7.5	134	2.1
	141	25	10.40				35	SE/S 2	S 15~ 25	S 20	6 ~ 7	6.5	150	2.1
	142	〃	10.55				〃	SE/S 2	S 18~ 22	S 20	5.5~ 7	6.5	148	2.3
	143	〃	11.10				〃	SE/S 2	S 15~ 25	S 20	5.5~ 7	6.5	144	2.3
	144	〃	11.25				〃	SE/S 1	S 5~ 17	S 10	4 ~ 6	5.5	147	1.1
	145	〃	11.40				〃	SE 1	S 12~ 25	S 15	4.5~ 5.5	5	137	1.4
	146	〃	11.55	b	28.5	29.0	〃	S/E 2	S 11~ 26	S 20	5 ~ 6.5	5.5	166	2.3
X	147	26	〃	c	25.5	27.5	45	N/W 3	P 21~ 29	P 25	9 ~ 10.5	10	347	5.0
	148	27	〃	b c	29.0	29.0	〃	E/N 2	S 6~ 15	S 10	8 ~ 10	9	80	3.2
	149	28	〃	b	29.5	29.0	41	SE/S 1	S 10~ 20	S 15	6 ~ 7	6.5	145	1.9
	150	29	〃	b	29.0	28.5	32	W 3	P 32~ 44	P 35	5 ~ 6.5	6	274	4.1
	151	30	〃	r	22.5	25.5	56	N/E 5	P 26~ 37	P 30	12.5~ 15.5	14	7	9.4
	152	5. 1	〃	c	23.5	24.0	54	ESE 4	S 22~ 40	S 25	10.5~ 12.5	11.5	108	6.4
	153	2	〃	b	20.5	21.5	〃	N/E 1	P 2~ 15	P 5	6 ~ 9	7.5	16	1.2
	154	3	〃	b c	20.0	17.5	48	SW/S 6		S 150	4 ~ 8	5.5	214	11.8

30-5

Wave					Ship	Mean			Oscillation						Remarks	Exp. No.
									Pitching			Rolling				
*2 Sea	Length m	Height m	Direc. deg.	Observed Period sec.	Speed kn	Torque $t-m$	RPM	SHP	Max. deg.	Mean deg.	Period sec.	Max. deg.	Mean deg.	Period sec.		
Sl	70~100	1~1.5	P110	12	13.13	24.40	96.0	3271	3.1	1.0	12.8	3.0	1.8	12	Honolulu Dep.	97
Sm	50~ 70	0.5	P150		13.28	25.18	95.0	3341	2.0	0.8	10.9	5.0	2.9	15		98
Sl	50	〃	P135	13	13.18	23.72	96.0	3180	〃	1.3	11.5	6.2	3.7	12.8		99
〃	30~ 40	〃	P 10		13.3	25.35	96.0	3400								—
〃	20	〃	T150	16	13.16	25.22	96.0	3381	1.6	0		3.0	2.0	12.8		100
〃	50	1~1.5	P150	14	13.20	25.13	97.0	3409	0.4	〃		4.1	1.9	15.0		101
Sm	100	2~3	S 60	12.5	13.30	24.79	95.0	3294	3.0	1.2	11.2	6.7	2.9	13.8		102
Mod	100~150	1.5~2	S 70		13.26	25.60	96.5	3460	2.5	0.9	8.6	5.8	2.5	11.3		103
Sl	40	1~1.5	P170	13	13.49	24.82	97.0	3367	0.9	0.2		5.2	2.1	12		104
〃	40	1	P150	15	13.44	25.21	97.0	3489	0.7	0		2.6	1.1	12		105
Sm	30	0.5~1	P150	14	13.36	24.57	96.6	3344	1.5	0.3		3.3	1.8	12.9		106
Sl	30	1	P135	15	13.65	26.54	97.7	3622	1.8	0.5	9.0	2.5	1.3	12		107
〃	40	0.7	P160	13	13.44	25.74	97.3	3497	1.4	0.4	10.6	4.1	2.2	12.9		108
〃	30	1	P140	16	13.44	25.94	96.8	3507	0	0		2.5	1.3	12.9		109
〃	—	0	—	—	13.44	25.68	96.1	3447	〃	〃						110
Sm	—	〃	—	—	13.43	25.25	96.6	3407	〃	〃						111
V. Sm	—	〃	—	—	13.38	25.30	96.7	3417	〃	〃					Singapore Arriv.	112
Sl	5	0.5	P135	10	13.53	25.65	95.5	3421	〃	〃						113
〃	—	0	—	—	13.00	24.86	94.5	3281	〃	〃					Singapore Dep.	114
Sm	—	〃	—	—	13.97	30.31	104.2	4411	〃	〃						115
〃	—	〃	—	—	13.44	28.45	100.1	3977	〃	〃						116
〃	—	〃	—	—	13.19	24.77	96.0	3321	〃	〃					Progressive Test	117
〃	—	〃	—	—	12.00	19.84	85.2	2361	〃	〃						118
〃	—	〃	—	—	10.81	15.91	75.2	1671	〃	〃						119
Sl	10	0.4	P170		13.19	25.92	94.5	3481	0.7	〃		2.0	0.9	9.0		120
〃	60	1	P140	5	13.03	26.51	95.3	3581	0.9	0.2		2.1	0.7	7.8		121
Mod	50	〃	P 40	5	13.05	24.95	95.2	3318	1.4	〃		2.5	0.8	8.2		122
R.R	15	1.5	S135		13.18	25.98	95.4	3462	0.8	0		2.1	0.7	8.2		123
V. Sm	—	0	—	—	13.00	25.86	95.0	3431	0	〃					Bombay Arriv.	124
Sm	10	0.5	P 50	3	12.90	25.86	94.5	3413	〃	〃						125
〃	—	0	—	—	16.08	27.56	108.2	4164	〃	〃					〃 Dep.	126
〃	—	〃	—	—	15.66	26.50	105.0	3885	〃	〃						127
〃	—	〃	—	—	15.02	23.58	100.1	3496	〃	〃					Prog. Test	128
〃	—	〃	—	—	14.26	20.53	95.4	2784	〃	〃						129
〃	—	〃	—	—	12.96	16.03	85.0	1902	〃	〃						130
〃	—	〃	—	—	11.50	12.53	76.0	1380	〃	〃						131
V. Sm	—	〃	—	—	11.98	26.12	92.4	3371	0.5			1.6	0.4	7.5	Morumugao Dep.	132
Sm	10	0.4	P 20	6	11.86	25.18	91.3	3211	0.8							133
Sl	10	0.3	P 20	6	11.98	25.60	92.6	3311	0.9	0.2	8.2	3.0	1.2	9.0		134
〃	20	0.4	S 40	6	11.86	26.30	94.5	3471	〃			2.9	1.1	10.6		135
〃	—	0	S 80	—	12.02	26.70	94.7	3581	1.2	0.4	10.6	3.0	1.6	10.0		136
V. Sm	—	〃	—	—	12.56	26.70	94.7	3581	0	0		0.5				137
〃	—	〃	—	—	12.56	26.72	93.3	3482	〃	〃					Singapore Arriv.	138
C	—	〃	—	—	12.53	26.32	92.8	3412	〃	〃						139
V. Sm	—	〃	—	—	12.77	28.47	97.1	3631	〃	〃					〃 Dep.	140
〃	—	〃	—	—	13.41	31.65	103.1	4567	〃	〃						141
〃	—	〃	—	—	13.17	29.12	101.6	4182	〃	〃						142
〃	—	〃	—	—	12.73	27.42	96.1	3680	〃	〃					Prog. Test	143
〃	—	〃	—	—	11.32	22.15	85.7	2681	〃	〃						144
〃	—	〃	—	—	9.92	16.53	75.8	1750	〃	〃						145
〃	—	〃			12.92	27.88	97.3	3789	〃	〃						146
Sm	20	0.6	S 15	5	12.62	27.87	97.4	3791	〃	〃						147
Sl					12.61	28.19	96.8	3811	0.7	0.3	7.2	1.1	0.7	6.9		148
Sm	15	0.6	P 10	3	13.02	28.28	97.5	3852	0.6			1.0	0.5	6.6		149
Sl	15	1	S 45	5	12.71	27.36	97.1	3710	0.5			1.7	0.9	9.5		150
Mod		0.6	S 15		11.70	27.82	95.5	3710	0.8	0.2	6.7	1.8	0.6	6.9		151
Sl			0		12.67	26.71	97.1	3421	0.5			1.0	0.4	5.8		152
Sm	15	0.6	P 10	3	12.67	26.50	96.7	3575	0.9	0.4	6.9	1.4	0.5	6.9		153
Mod	10	0.5	P150		13.04	26.58	97.8	3429	0.1			1.6	0.6	7.5	Yokohama Arriv.	154

Length bet' Perpendiculars	128.00 m	Designed Full Load Condition,	Draught moulded	8.25 m
Breadth moulded	17.50 m		Displacement (inc. skin)	13,870 tons
Depth moulded	10.40 m		Black Coefficient	.728
			Prismatic Coefficient	.738
			Midship Coefficient	.987
			Long. Position of C. of Buoyancy	.42m forward of Midship

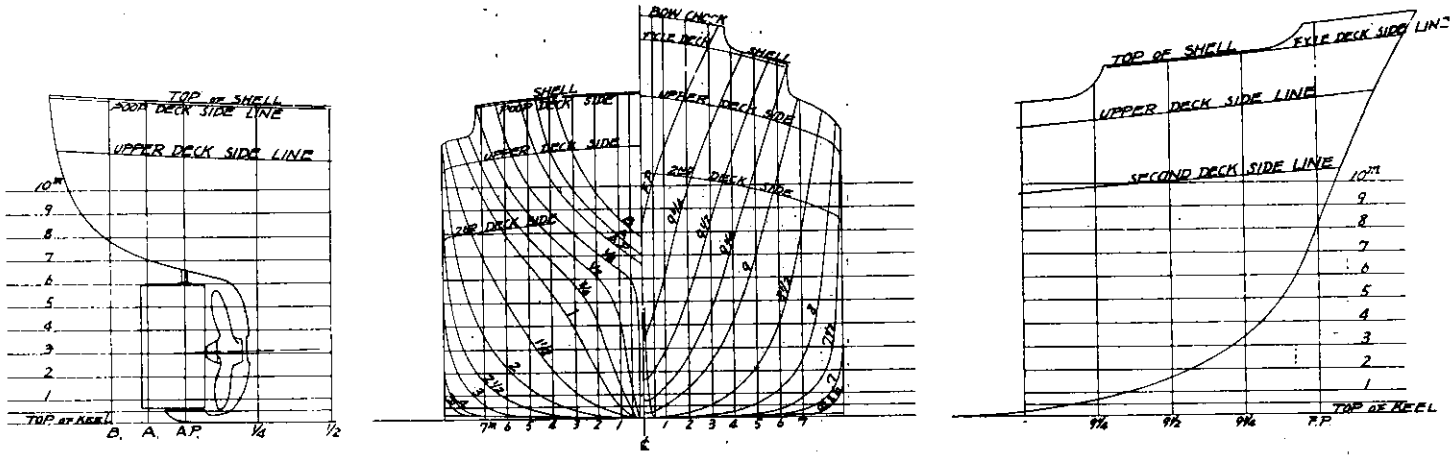

Fig. 1 Body Plan, Stem and Stern Contour of "Nissei Maru"

Diameter	5,250 m
Boss Ratio	.229
Expanded Area Ratio	.402
Max Blade Width Ratio	.236
Blade Thickness Ratio	.0463
Angle of Rake	10°-0°
Direction of Turning	Right Handed
Number of Blades	4
Material	Mn. Bronze

Radius	Pitch	Pitch Ratio
.3R	4.754 m	.904
.4R	4.460 "	.849
.5R	4.250 "	.809
.6R	4.155 "	.791
.7R	4.150 "	.790
.8R	- "	-
.9R	- "	-
1.0R	- "	-

Measured pitch at .07R, 4.13 m

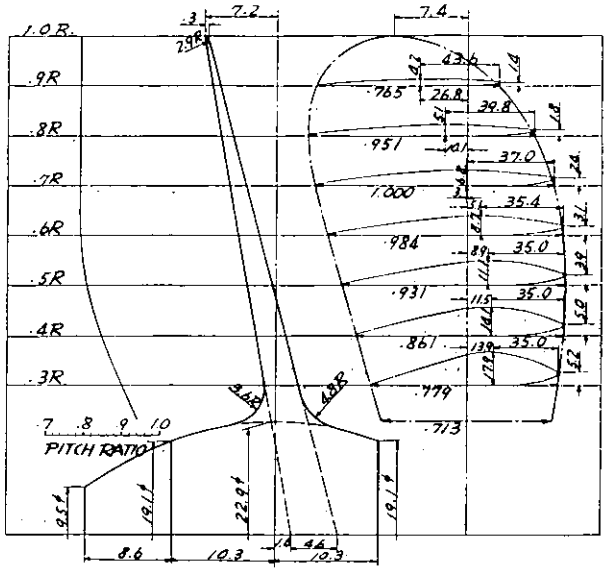

The dimensions of the blade sections are expressed in percentages of the width.
The width of the section in percentages of maximum width.
All other dimensions in percentages of diameter.

Fig. 2. Propeller of "Nissei Maru"

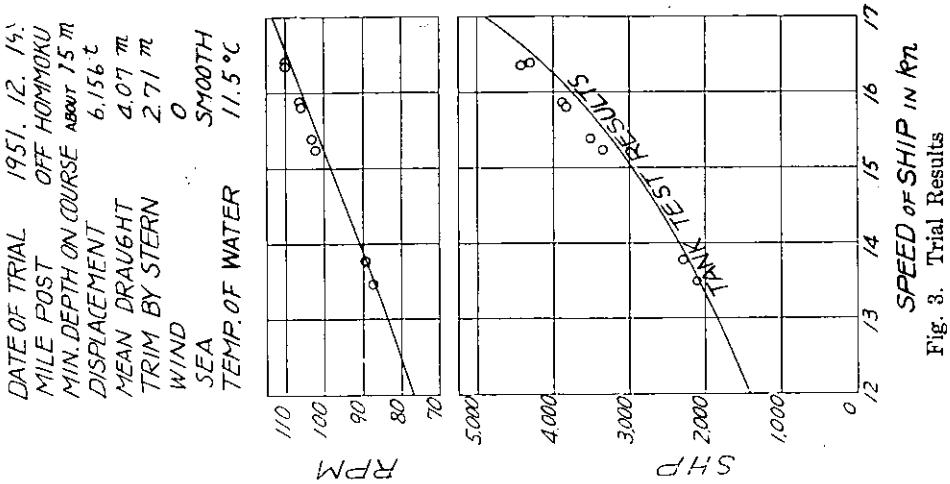

Fig. 3. Trial Results

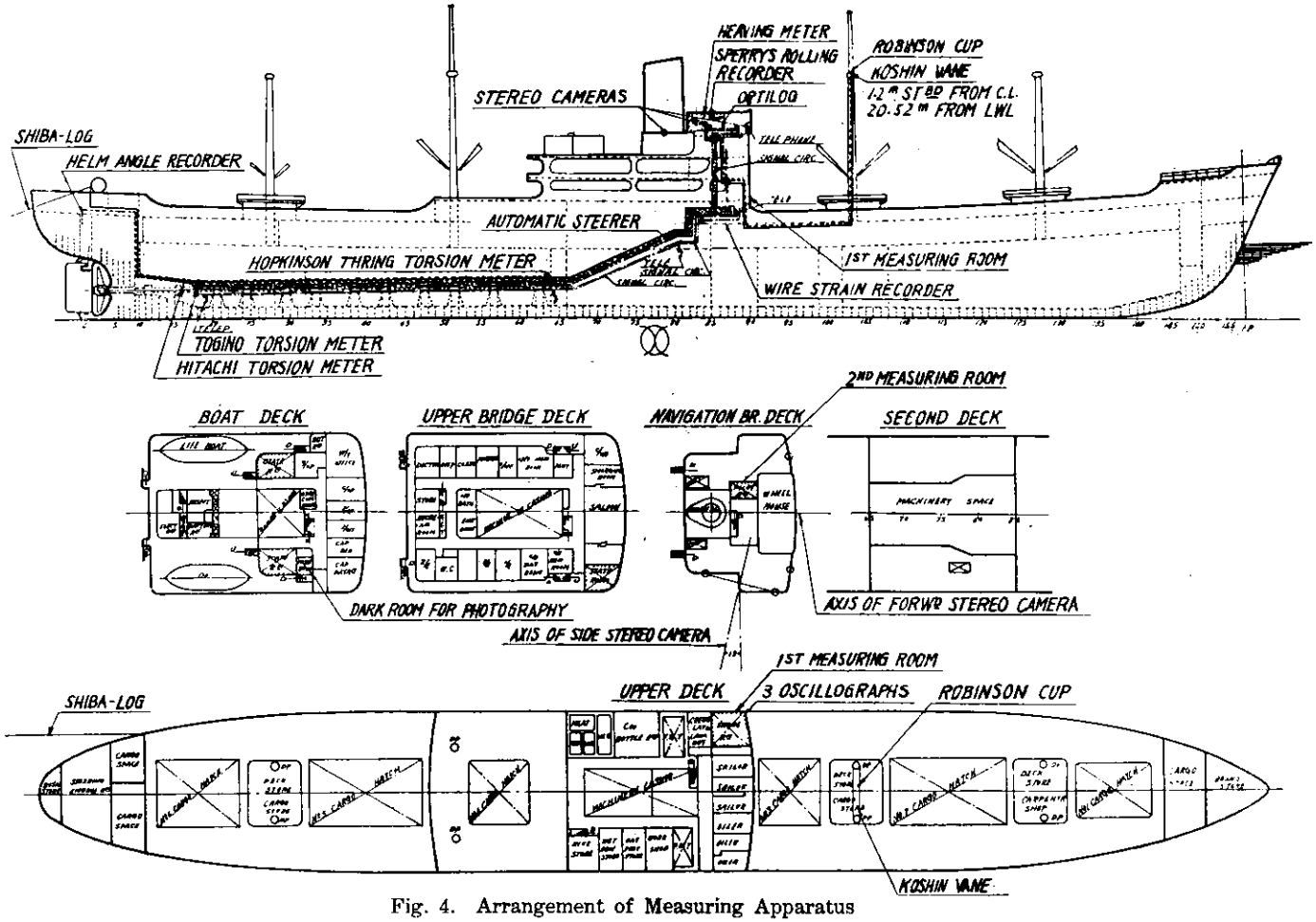

Fig. 4. Arrangement of Measuring Apparatus

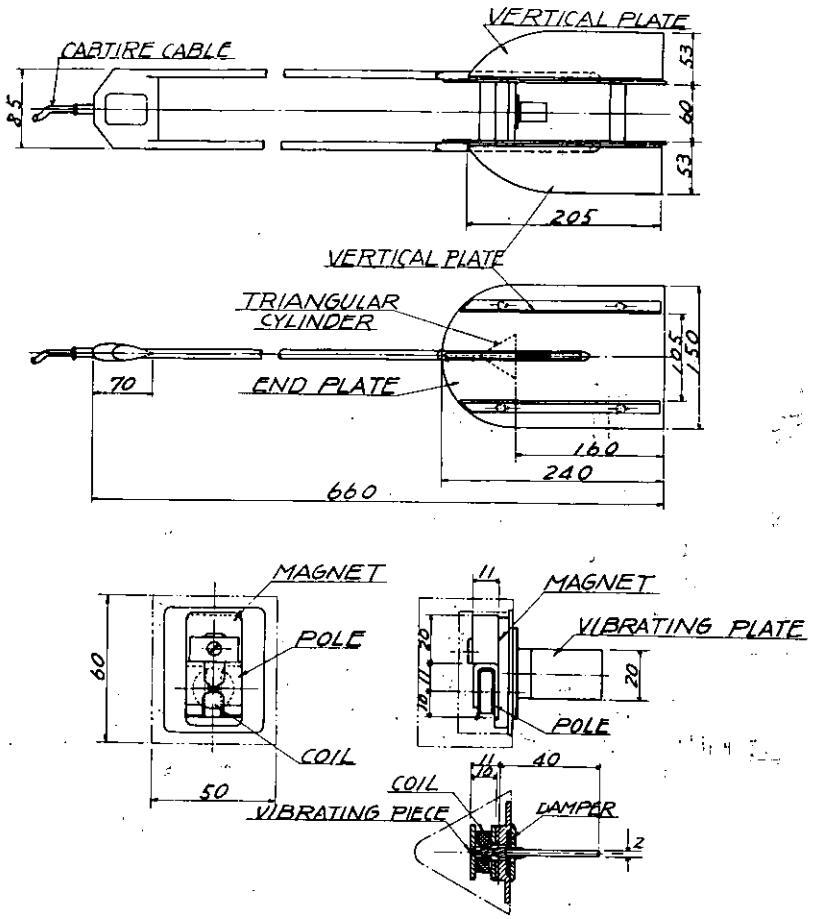

Fig. 5. Details of Shiba Log

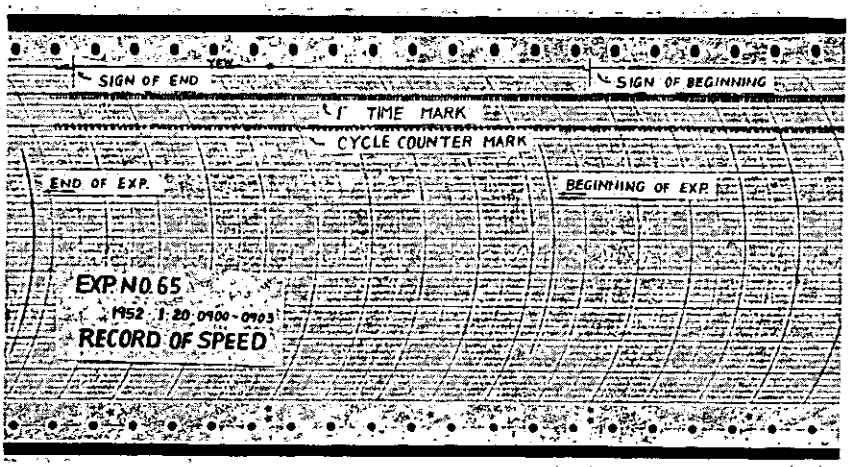

Fig. 6. An Example of Record by Shiba Log.

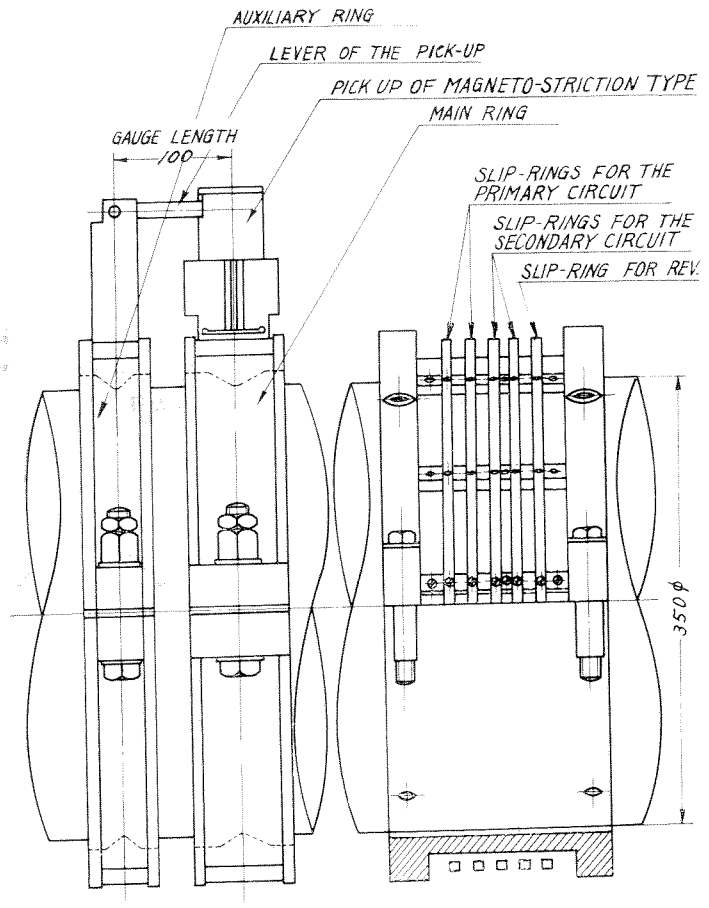

Fig. 7. Arrangement of Hitachi Torsionmeter

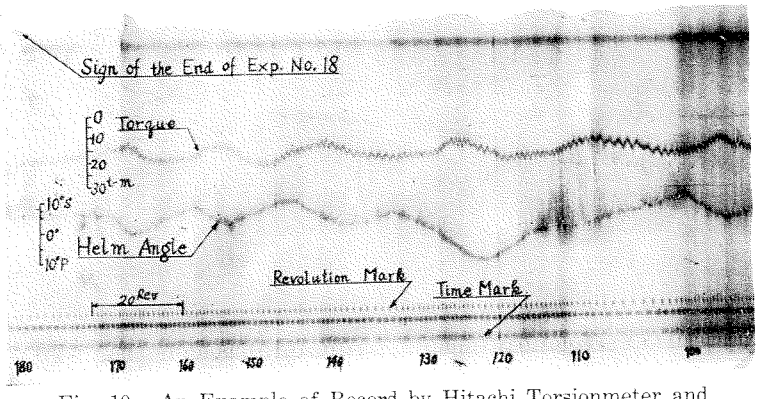

Fig. 10. An Example of Record by Hitachi Torsionmeter and Helm Angle Recorder

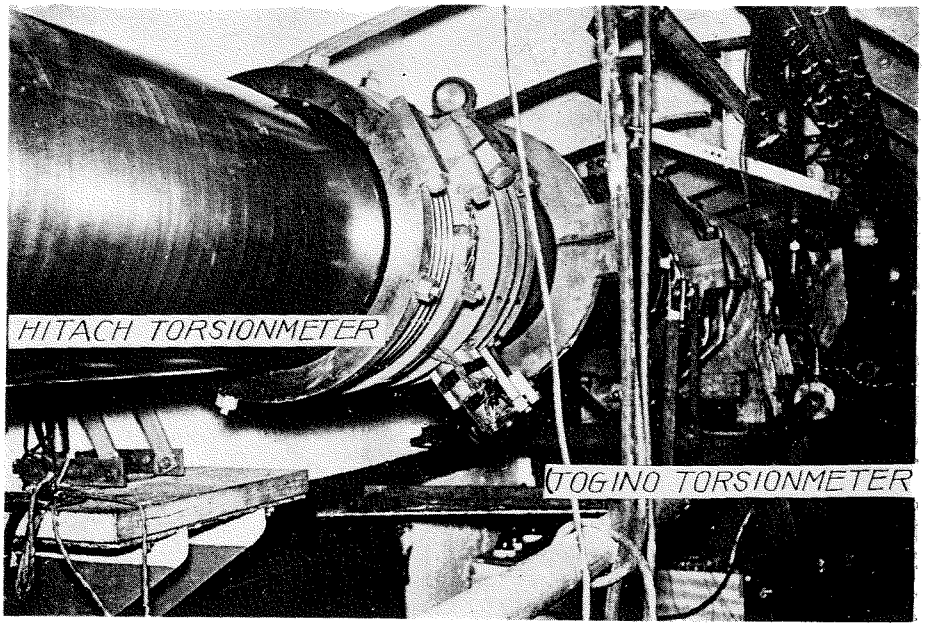

Fig. 8. Hitachi Torsionmeter

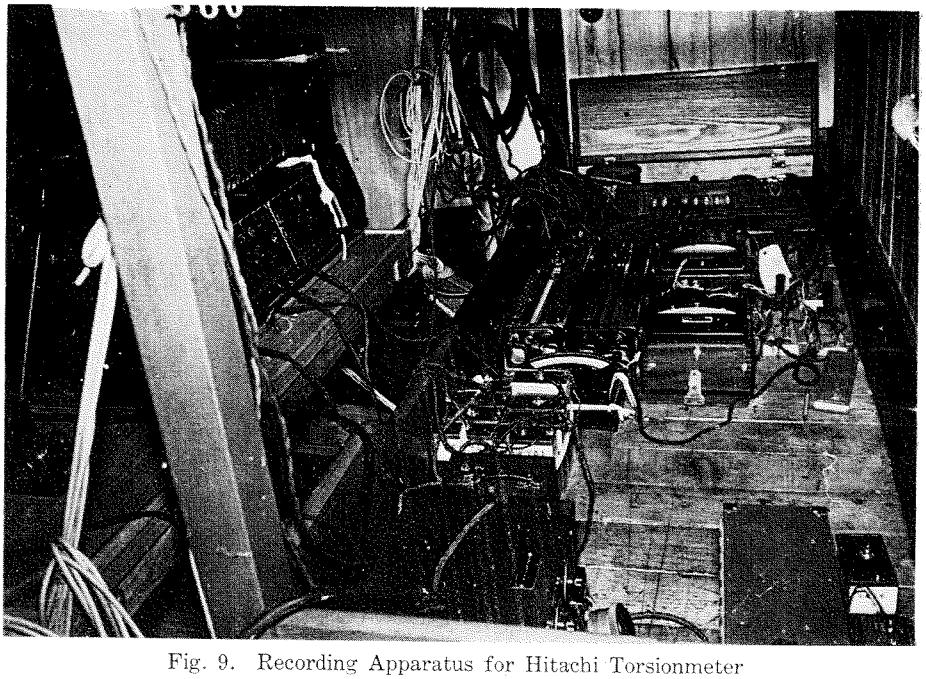

Fig. 9. Recording Apparatus for Hitachi Torsionmeter

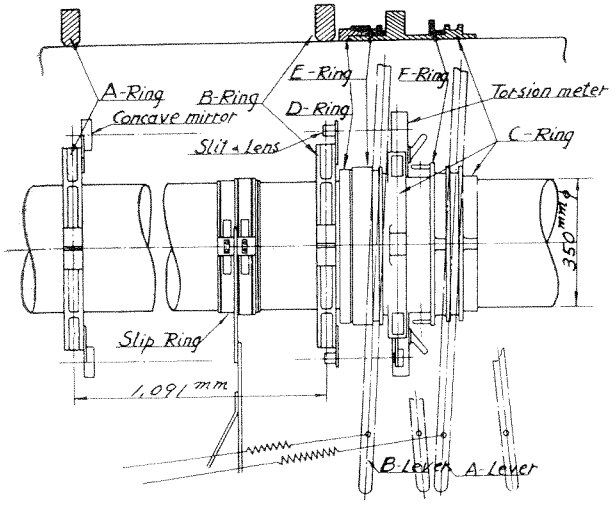

Ring	Attachments	Remarks
A	Concave mirror	Fixed to axis
B	Slit for light source Slit for base line Camera Lense	Do
C	Lamp Camera box A-Lever	Loose to axis & Coupled to D-ring with teeth & groove
D	———	Fixed to axis
E	B-Lever	Axially movable on C-ring
F	C-Lever	Loose to C-ring & feeding film

Fig. 11. Arrangement of Togino Torsionmeter

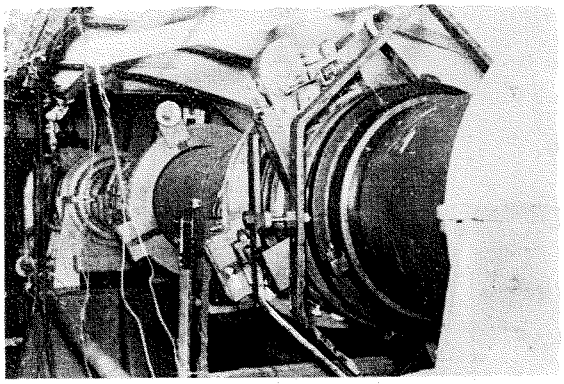

Fig. 12. Togino Torsionmeter

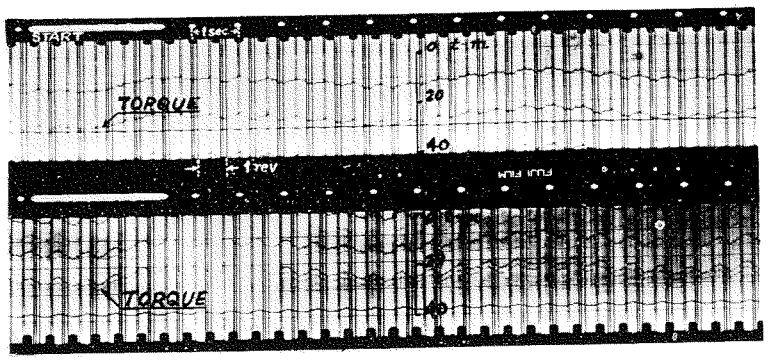

Fig. 13. An Example of Record by Togino Torsionmeter

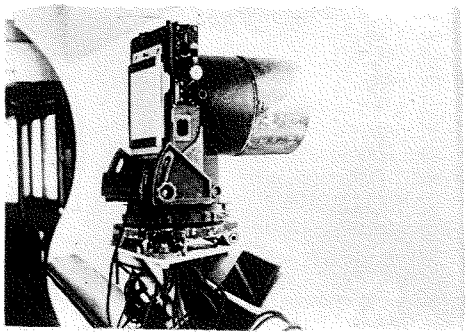

Fig. 14. Forward Stereo-Camera

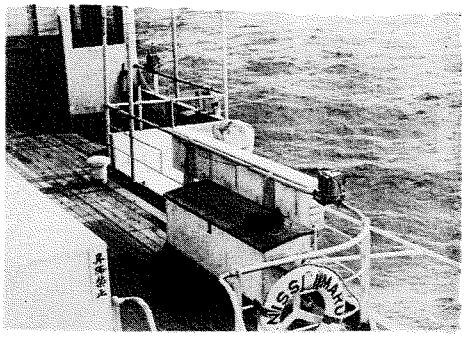

Fig. 15. Side Stereo-Camera

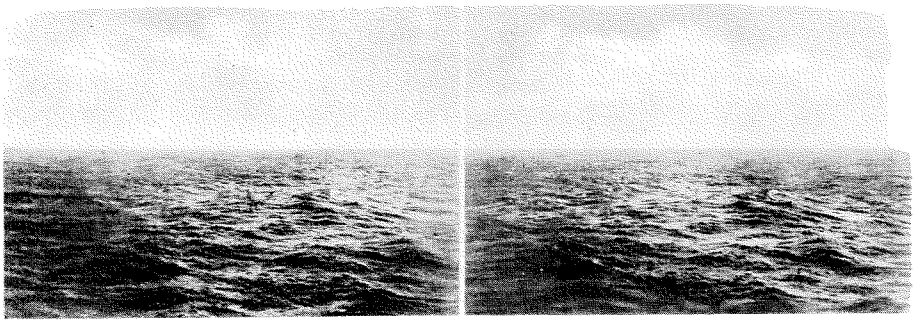

Fig. 16. An Example of Record by Side Stereo-Camera
(Exp. No. 17)

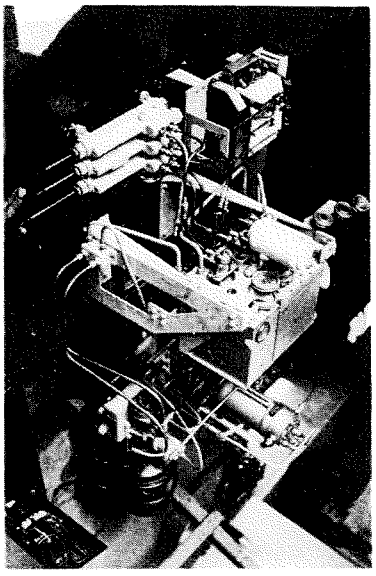

Fig. 22. Air-Gyro Recorder

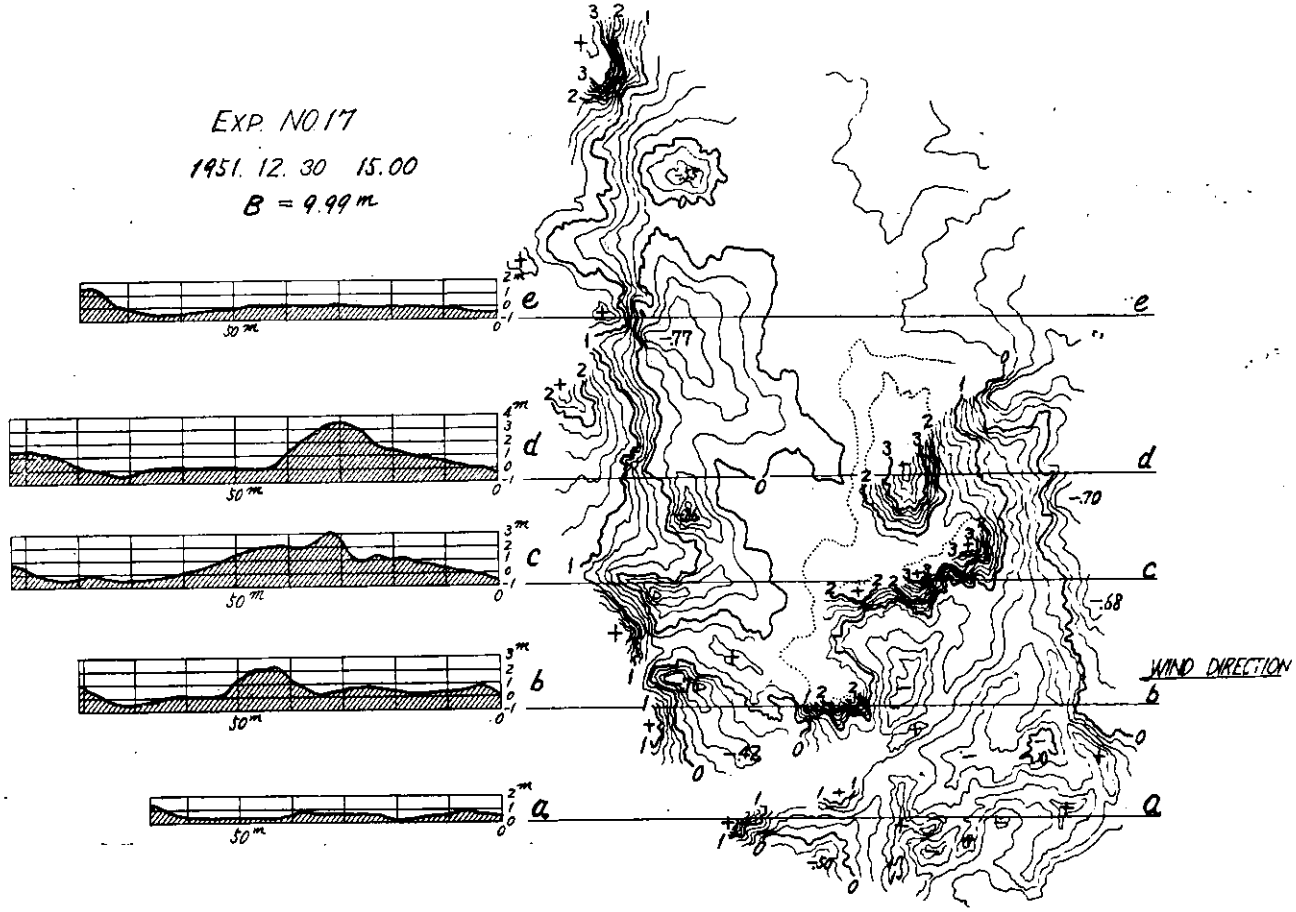

Fig. 17. Wave Pattern by Side Stereo-Camera

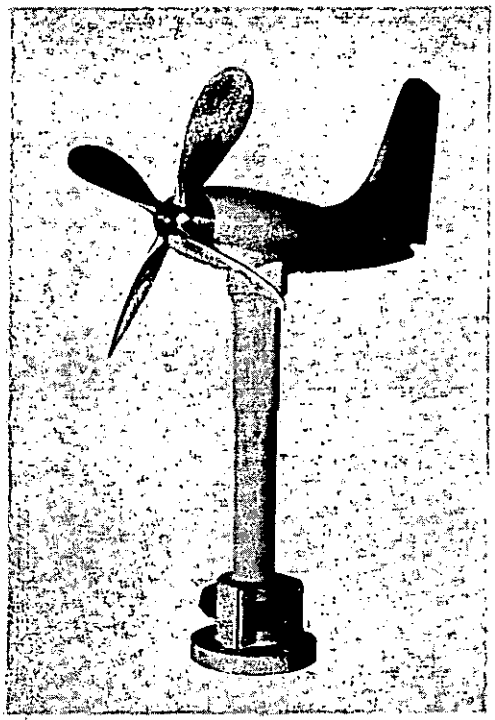

Fig. 18. Koshinvane

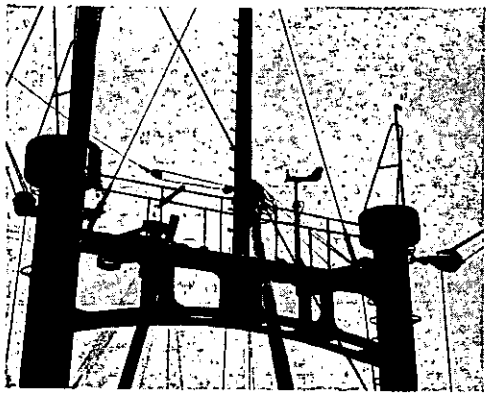

Fig. 19. Koshinvane on Portal

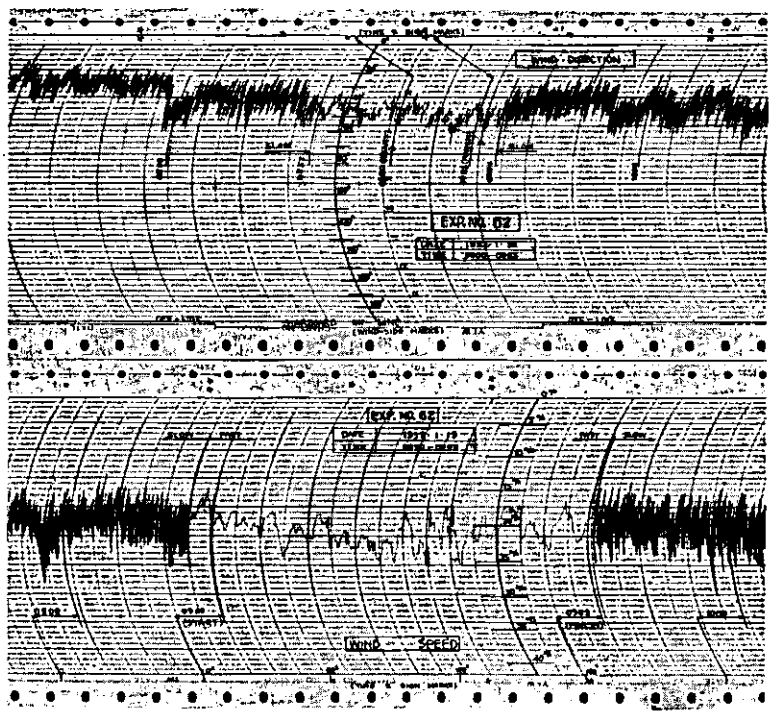

Fig. 20. An Example of Record by Koshinvane

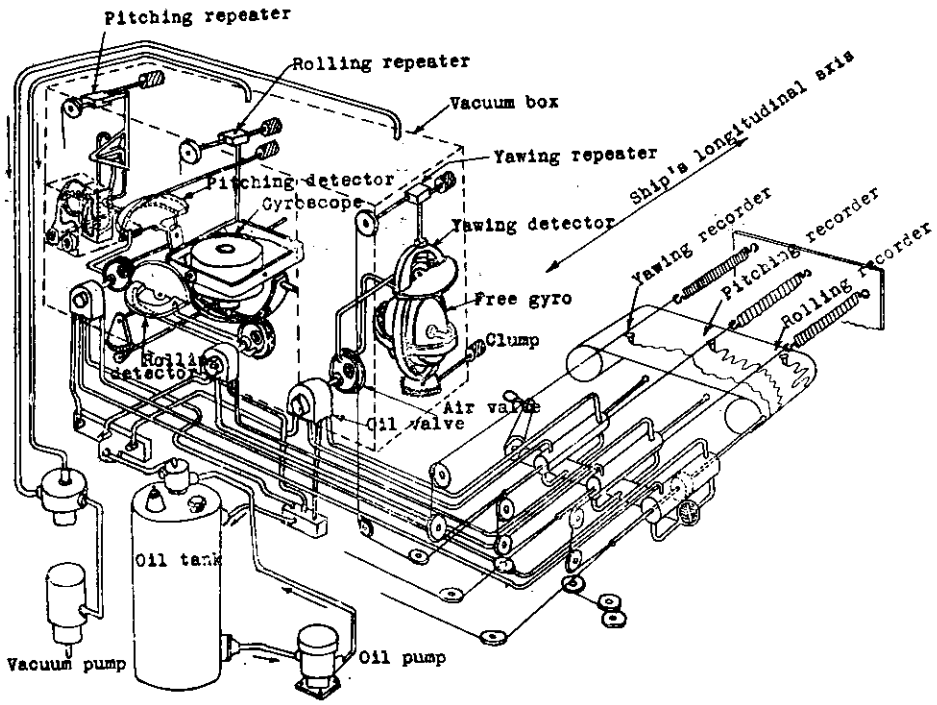

Fig. 21. Mechanism of the Air-Gyro Recorder

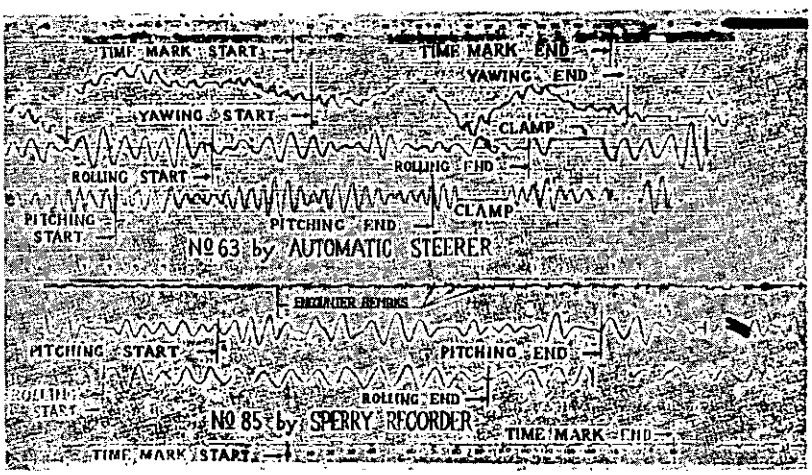

Fig. 23 An Example of Record by Air-Gyro Recorder

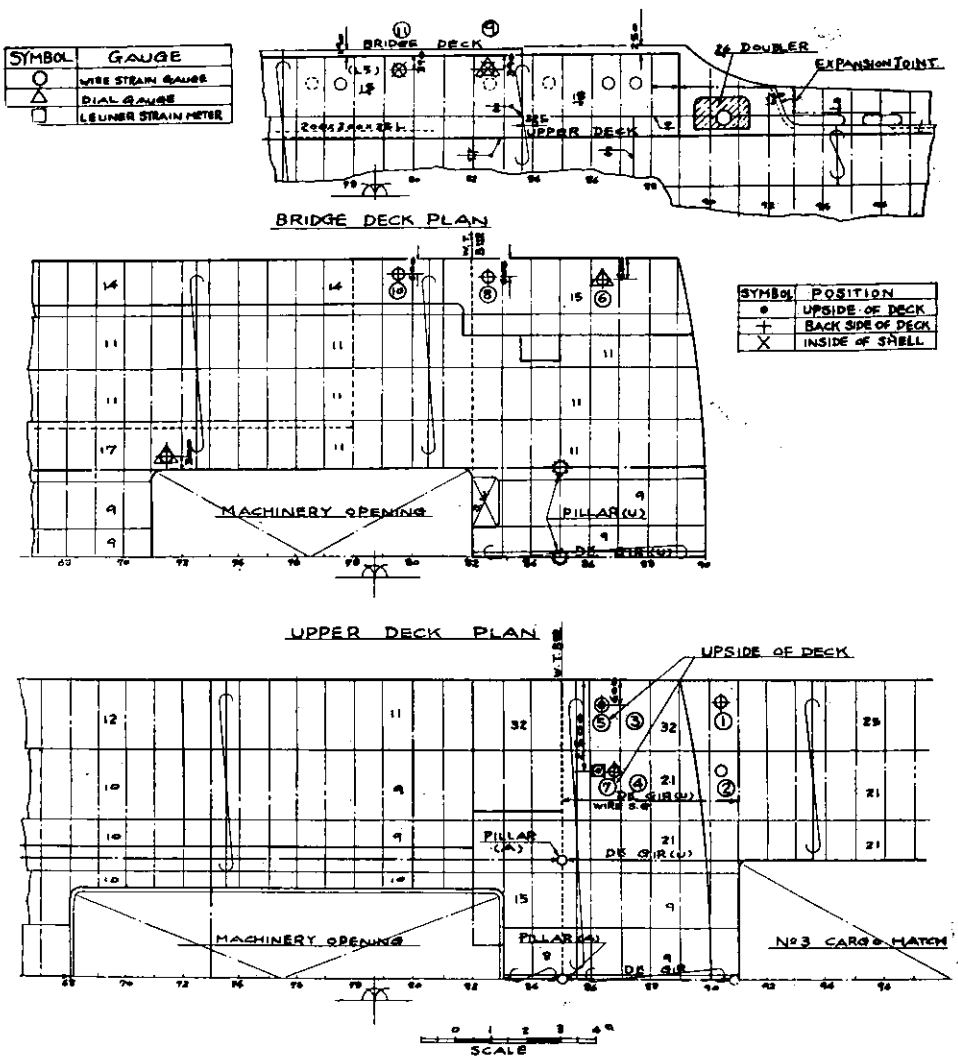

Fig. 24. Position of Strain Gauge

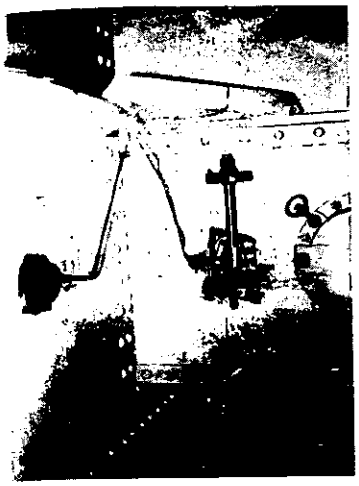

Fig. 25. Wire Strain Gauge and Giken Strain Gauge

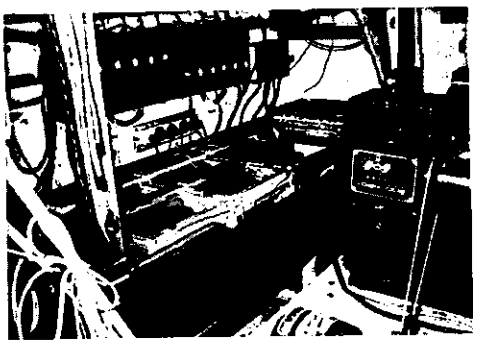

Fig. 26. Recorder of Wire Strain Gauge

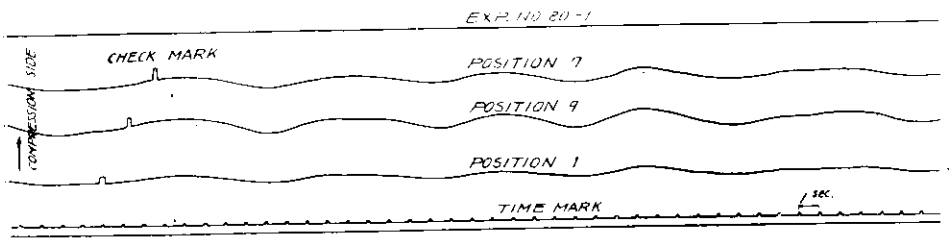

Fig. 27. An Example of Record by Wire Strain Gauge

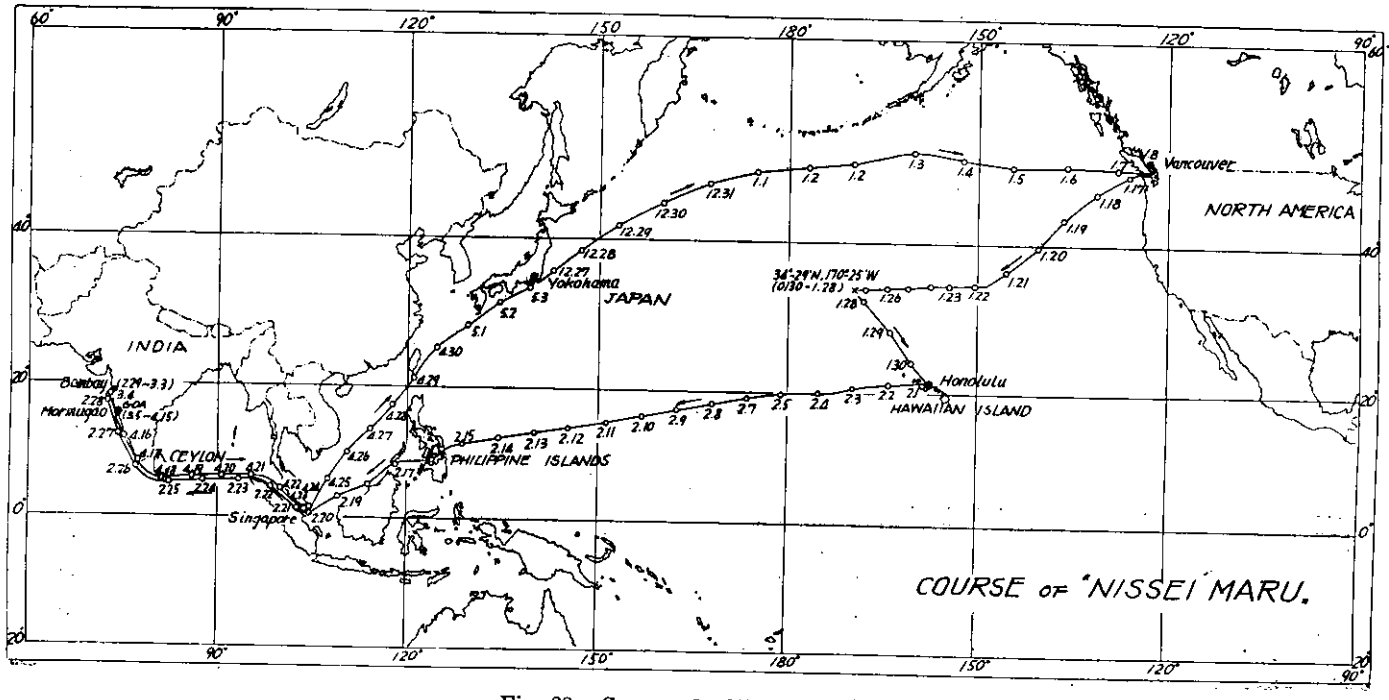

Fig. 28. Course of "Nissei Maru"

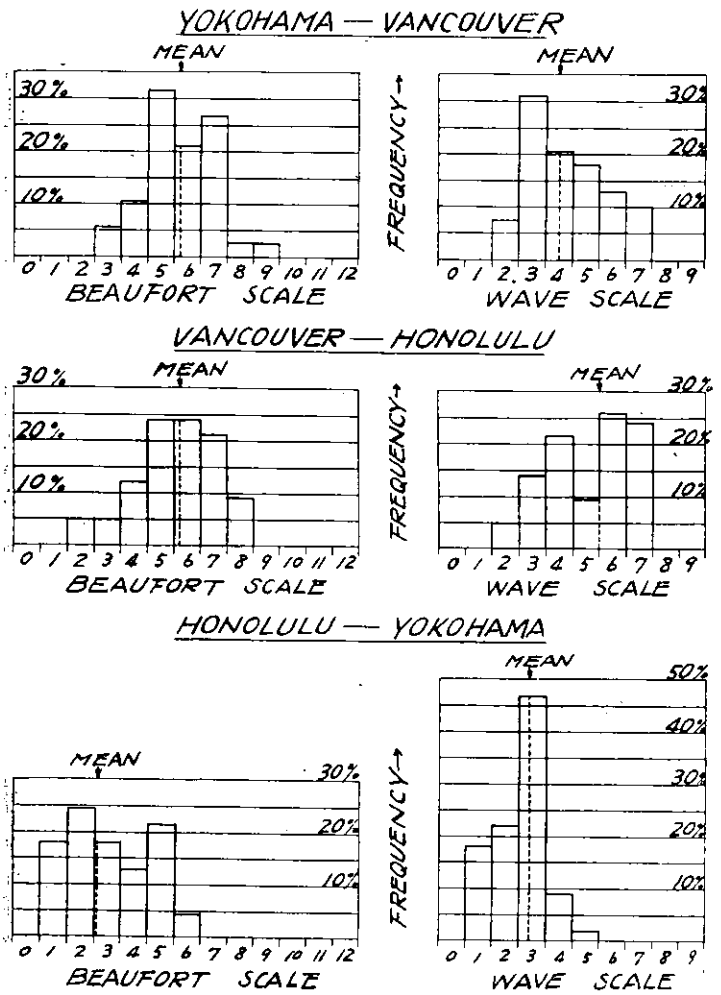

Fig. 29. Frequency Diagram for Wind and Wave Scales

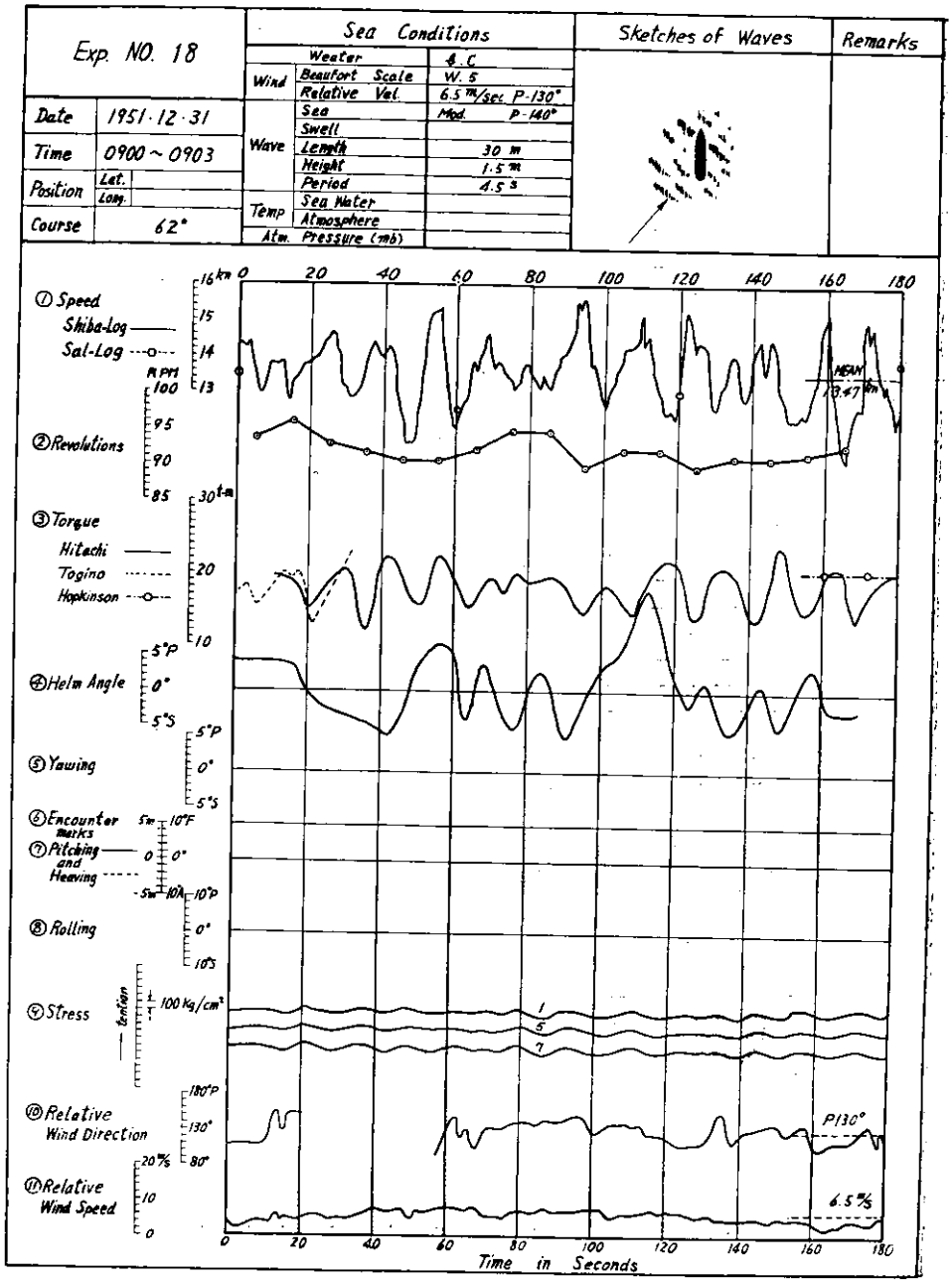

Fig. 30. An Example of Consolidated Graph of Simultaneously Measured Data

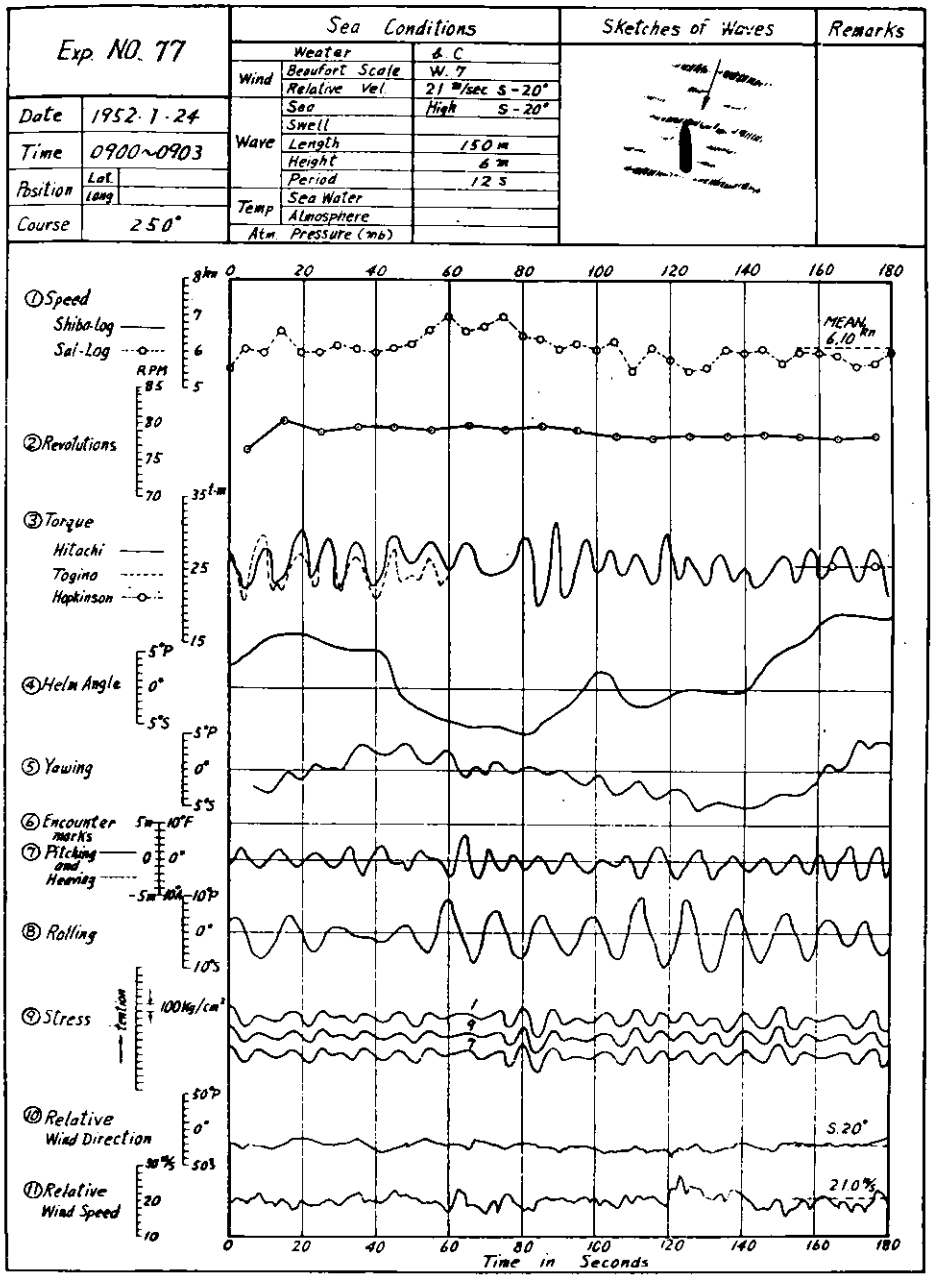

Fig. 31. An Example of Consolidated Graph of Simultaneously Measured Data

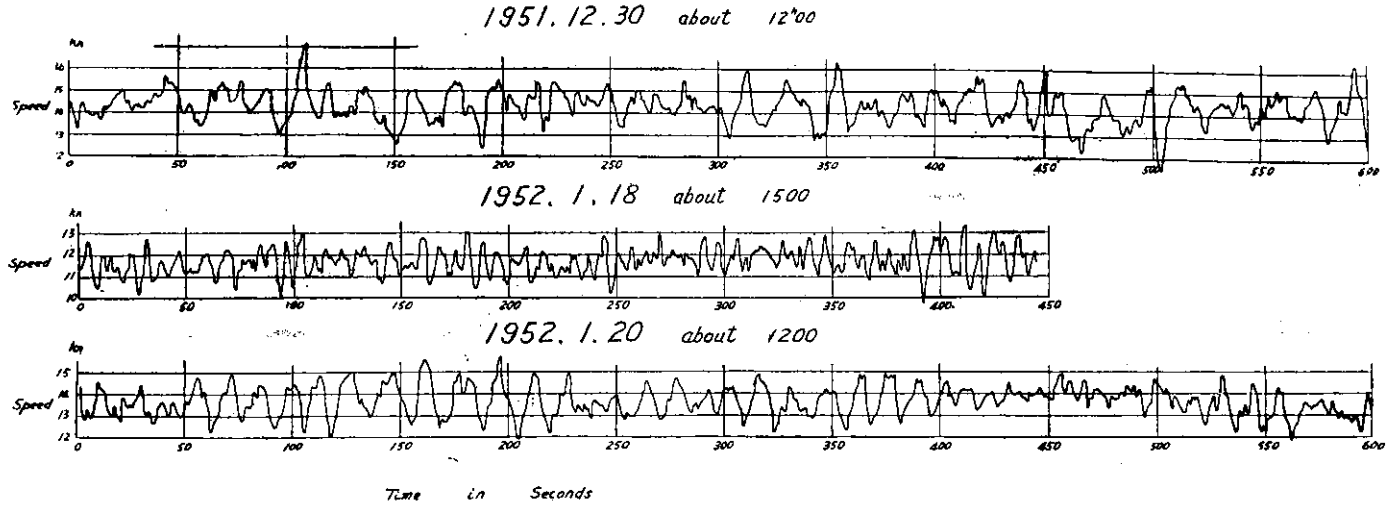

Fig. 32. Fluctuation of Speed measured by Shiba Log

CONDITION III

COND.	COURSE	DISPT.	WATER TEMP.
III	VANCOUVER – HONOLULU	13,700 t	4 ~ 14 °C

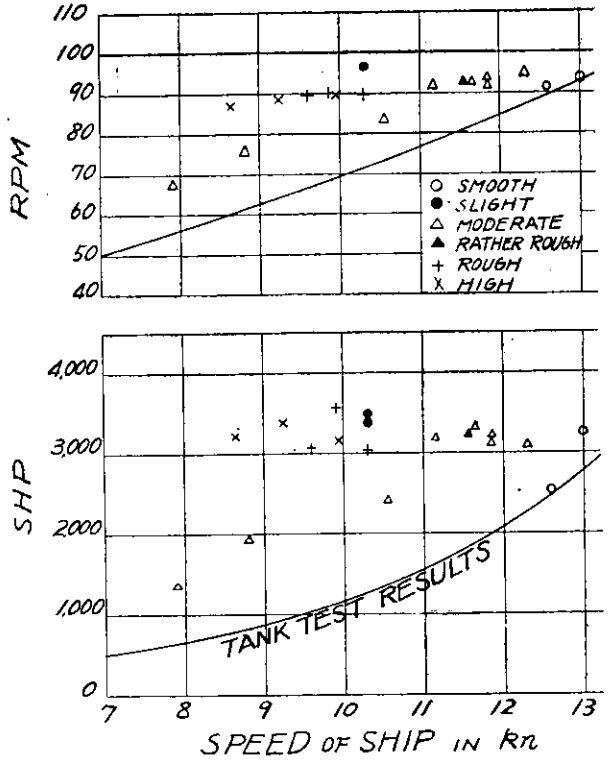

Fig. 34. SHP and RPM, Cond. III

CONDITION I & II

COND.	COURSE	DISPT.	WATER TEMP.
I	YOKOHAMA	6,440 t	3 ~ 17 °C
II	– VANCOUVER	6,130	4 ~ 7

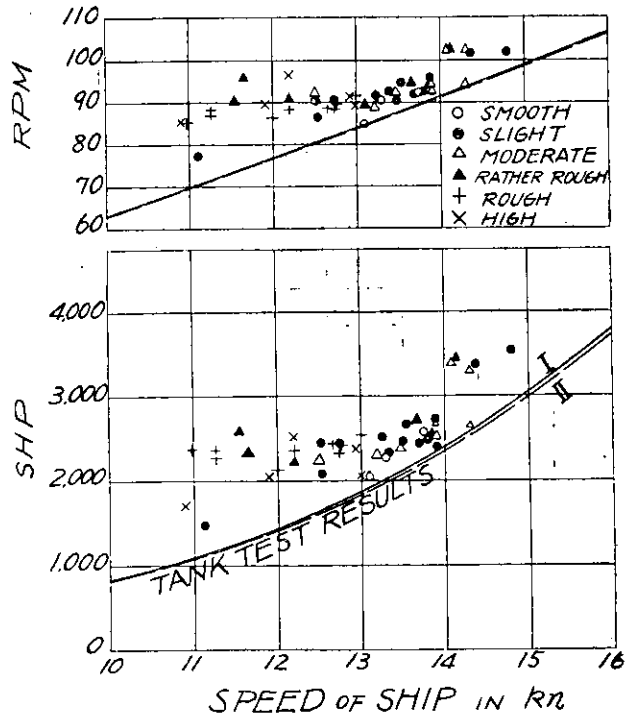

Fig. 33. SHP and RPM, Cond. I & II

CONDITION VI & VII

COND.	COURSE	DISPT.	WATER TEMP.
VI	HONOLULU-SING.	13,410 t	15 °C
VII	SING.- BOMBAY	13,840	27.5

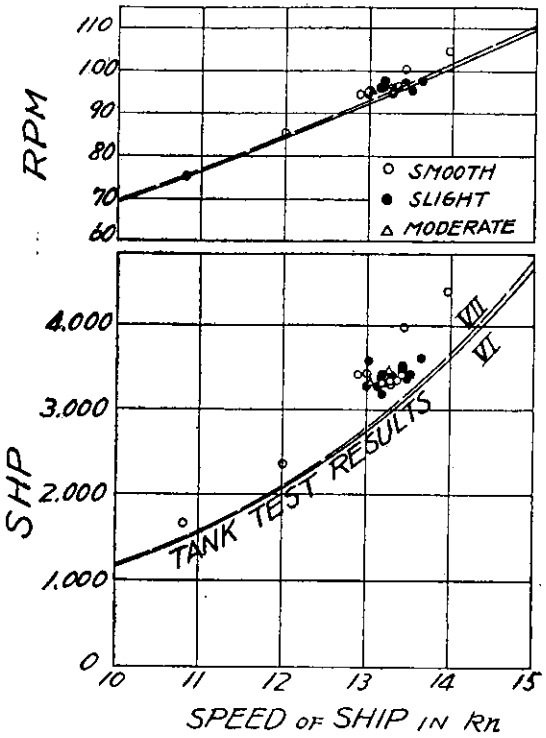

Fig. 36. SHP and RPM, Cond. VI & VII

CONDITION IV & V

COND.	COURSE	DISPLACEMENT	WATER TEMP
IV	VANCOUVER	13,450 t	14 ~ 16 °C
V	— HONOLULU	13,250	16 ~ 22

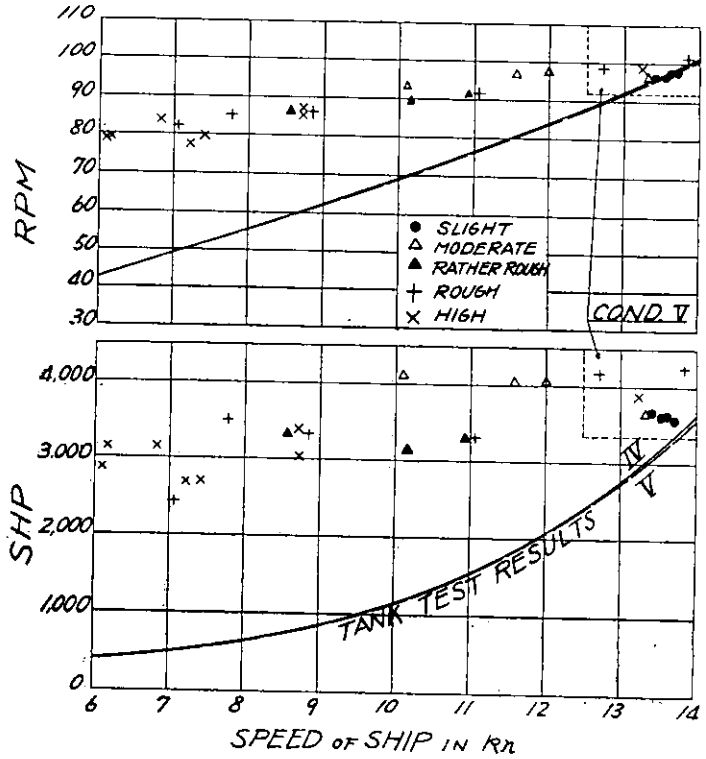

Fig. 35. SHP and RPM, Cond. IV & V

CONDITION IX & X

COND.	COURSE	DISPT.	WATER TEMP.
IX	MORMU. – SING.	13,540 t	28 °C
X	SING. – YOKOHAMA	13,850	17 – 29

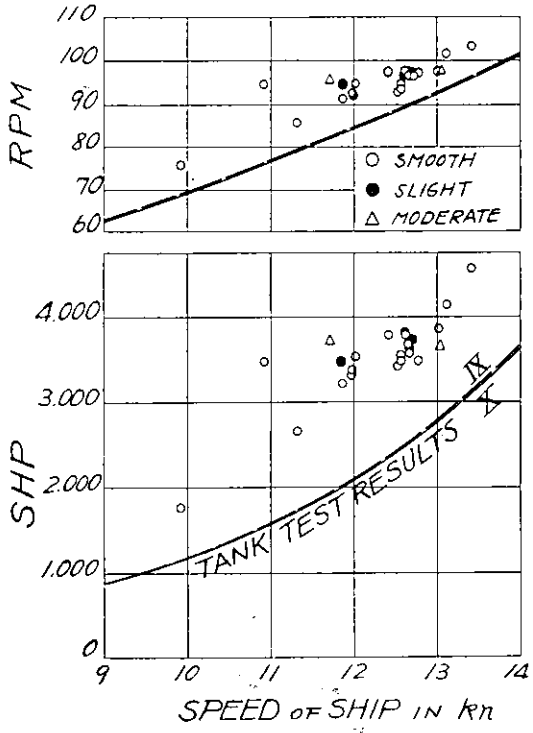

Fig. 38. SHP and RPM, Cond. IX & X

CONDITION VIII

COURSE	DISPLACEMENT	WATER TEMP.
BOMBAY-MORMUGAO	5,510 t	27 °C

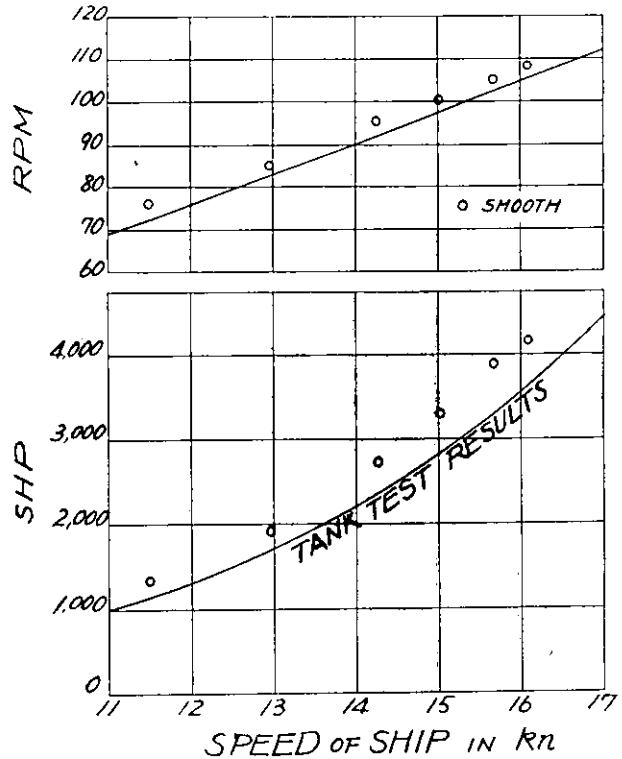

Fig. 37. SHP and RPM, Cond. VIII

Fig. 39. Exp. No. 3

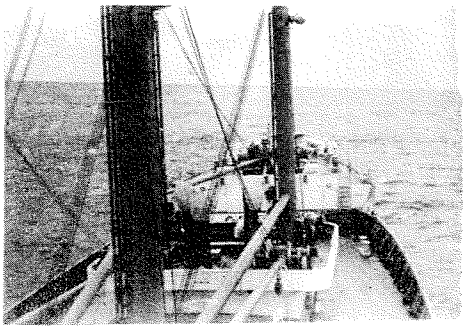

Fig. 40. Exp. No. 12

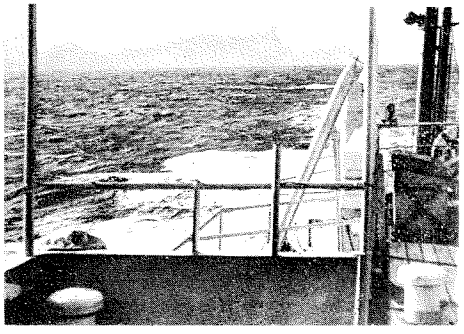

Fig. 41. Exp. No. 16

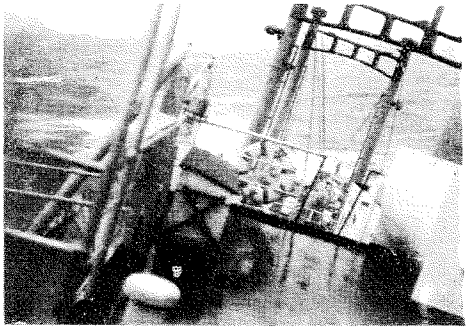

Fig. 42. Exp. No. 24

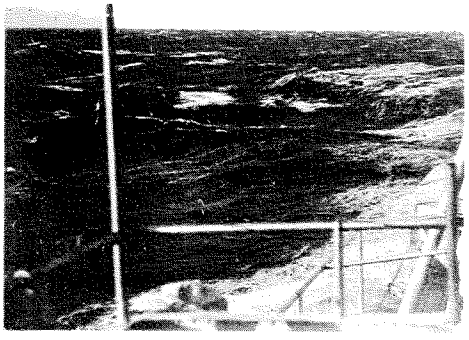

Fig. 43. Exp. No. 36

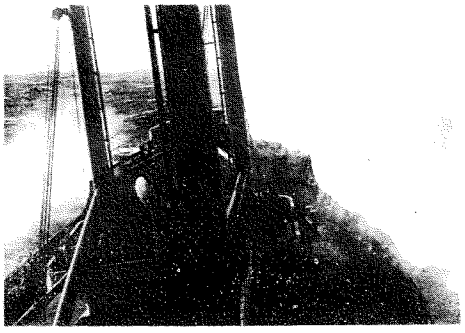

Fig. 44. Exp. No. 63

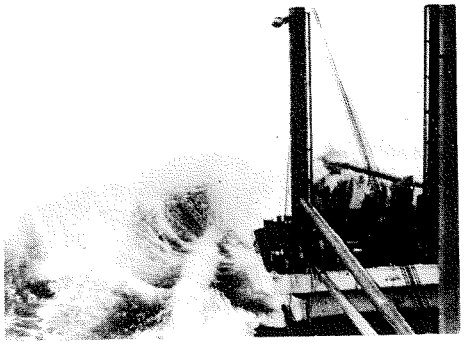

Fig. 45. Immediately after Exp. No. 69 (Slamming)

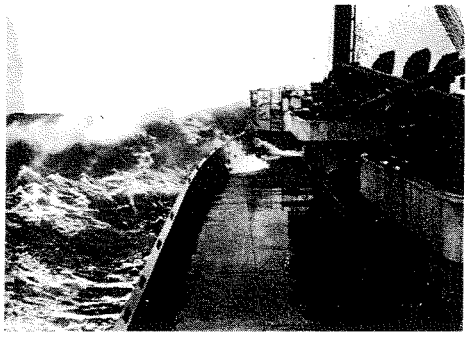

Fig. 46. One Hour before Exp. No. 70 (Slamming)

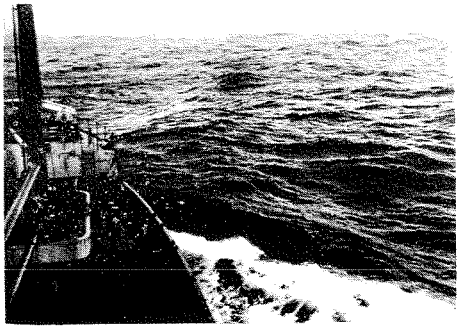

Fig. 47. Exp. No. 70

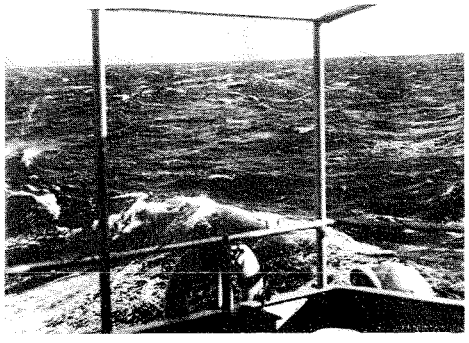

Fig. 48. Exp. No. 74

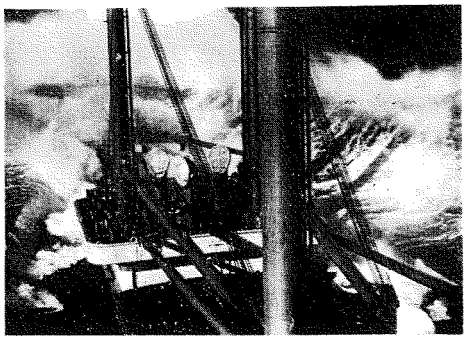

Fig. 49. One Hour after Exp. No. 74 (Slamming)

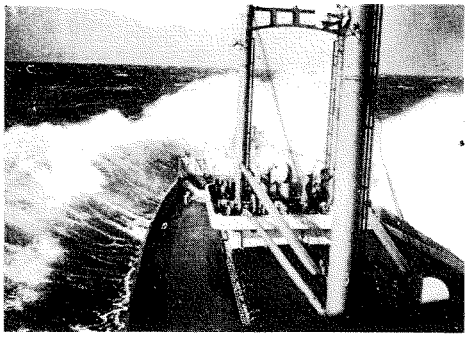

Fig. 50. One Hour after Exp. No. 74 (Slamming)

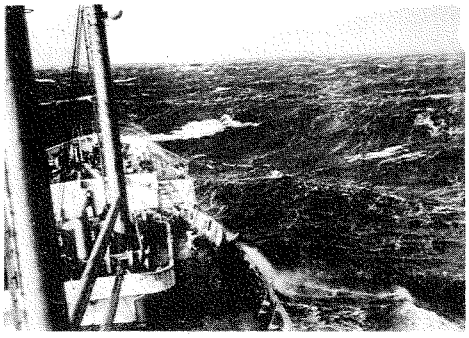

Fig. 51. Exp. No. 77

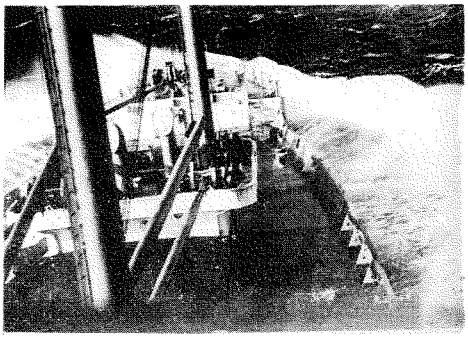

Fig. 52. Exp. No. 77

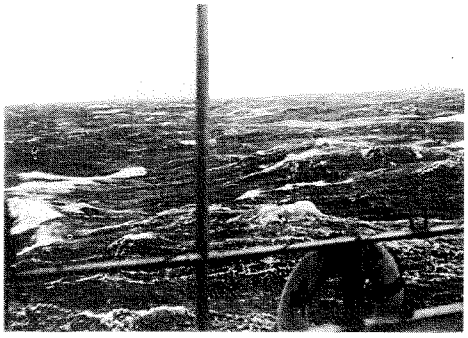

Fig. 53. Exp. No. 77

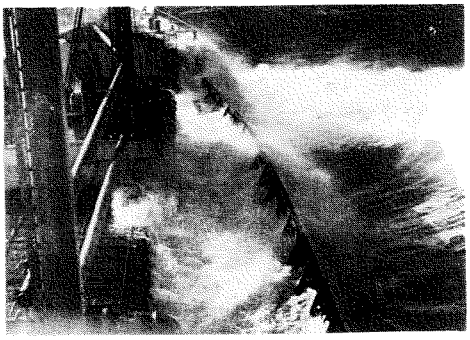

Fig. 54. One Hour before Exp. No. 79

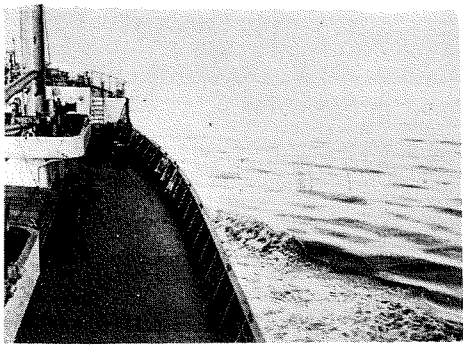

Fig. 55. Calm Sea in Maracca Strait

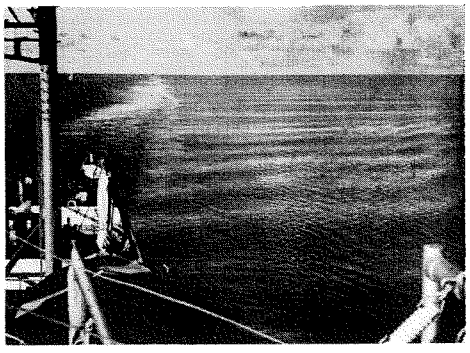

Fig. 56. Very Smooth Sea in Sulu Sea, Philippine Islands

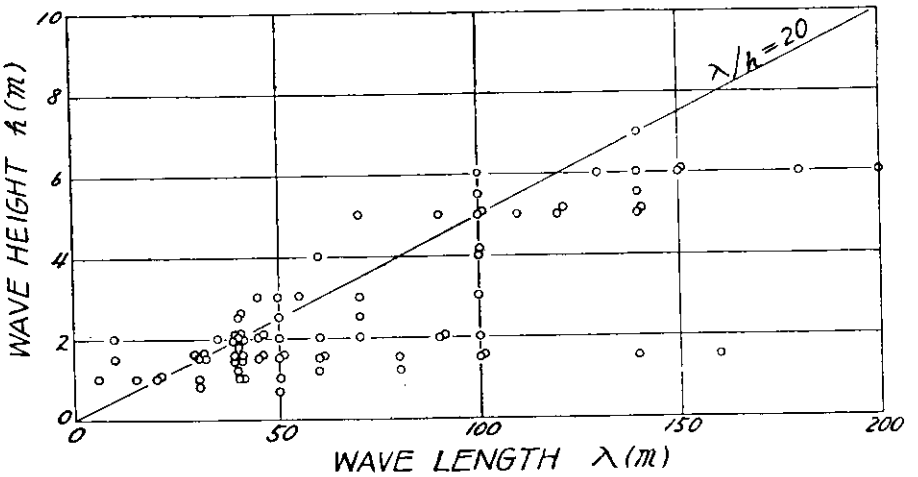

Fig. 57. Relation bet' Wave Height and Wave Length observed

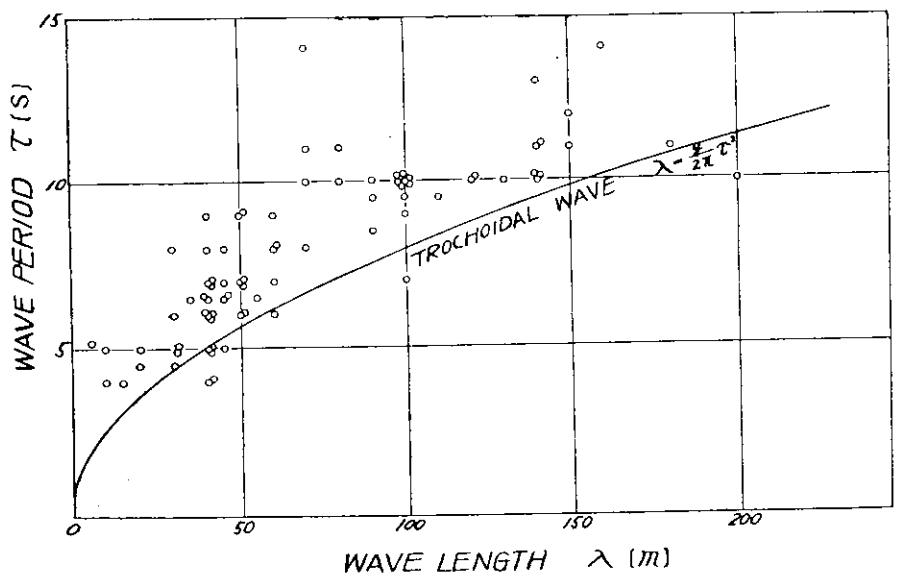

Fig. 58. Relation bet' Wave Period and Wave Length observed

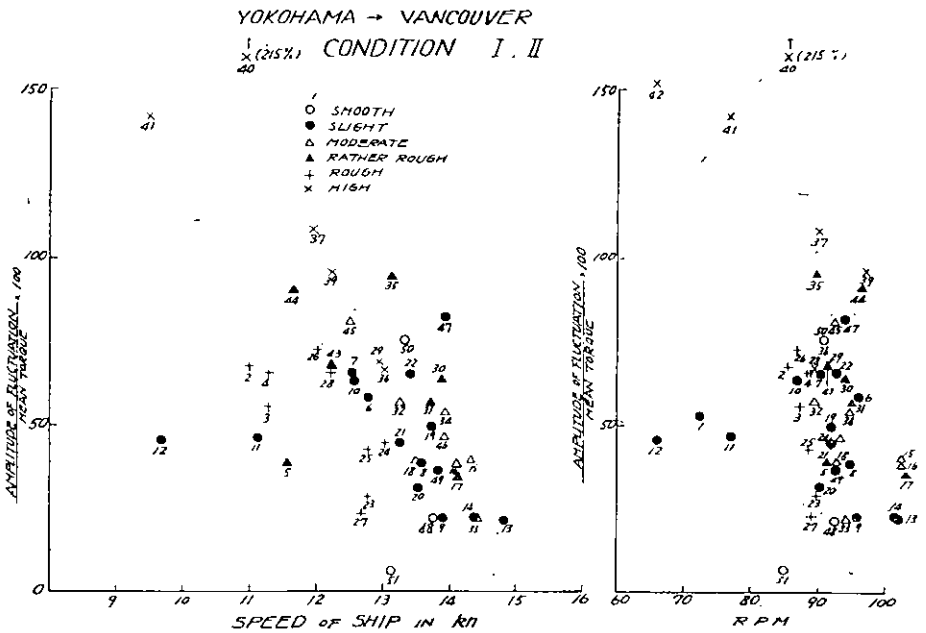

Fig. 59. Fluctuation of Shaft Torque, Yokohama–Vancouver

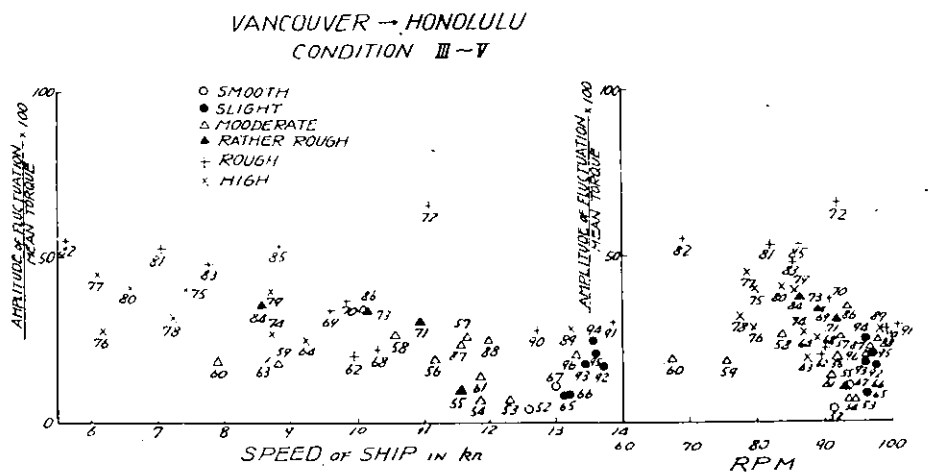

Fig. 60. Fluctuation of Shaft Torque, Vancouver–Honolulu

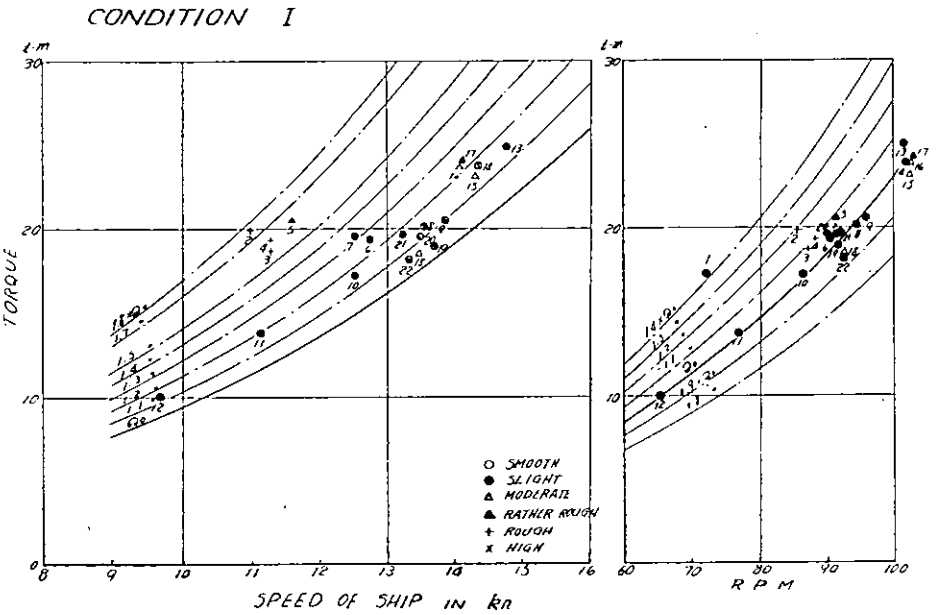

Fig. 61. Shaft Torque, Condition I

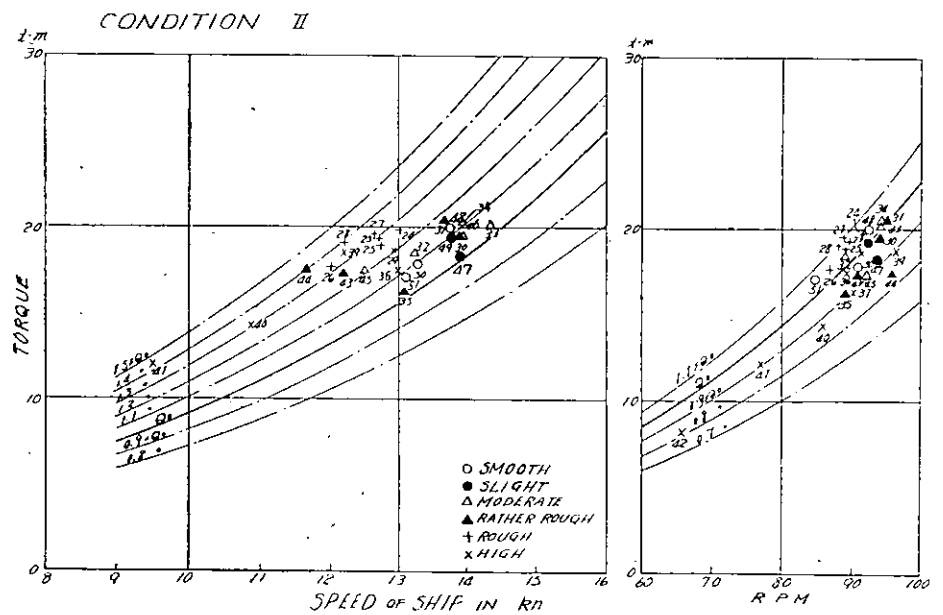

Fig. 62. Shaft Torque, Condition II

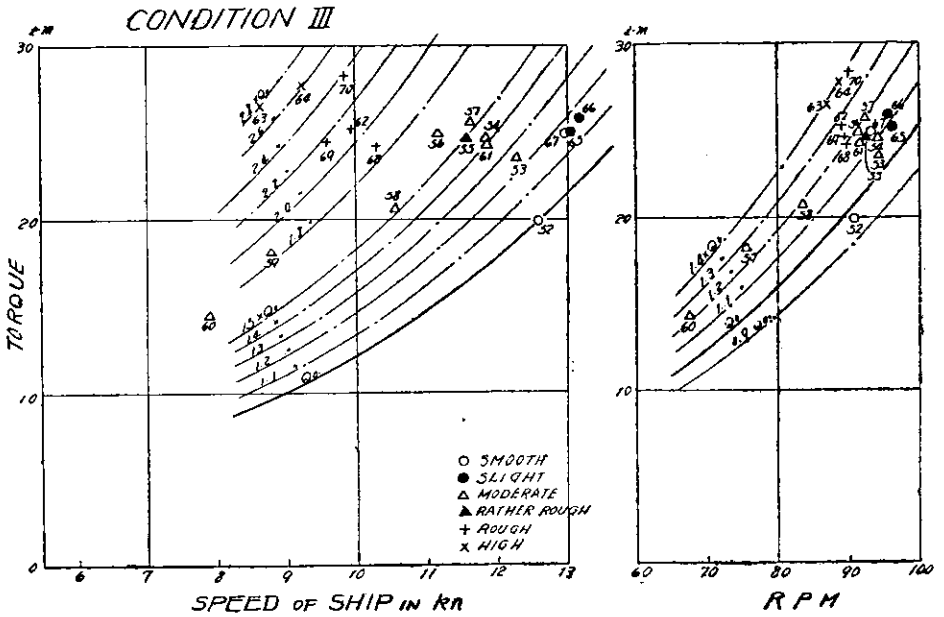

Fig. 63. Shaft Torque, Condition III

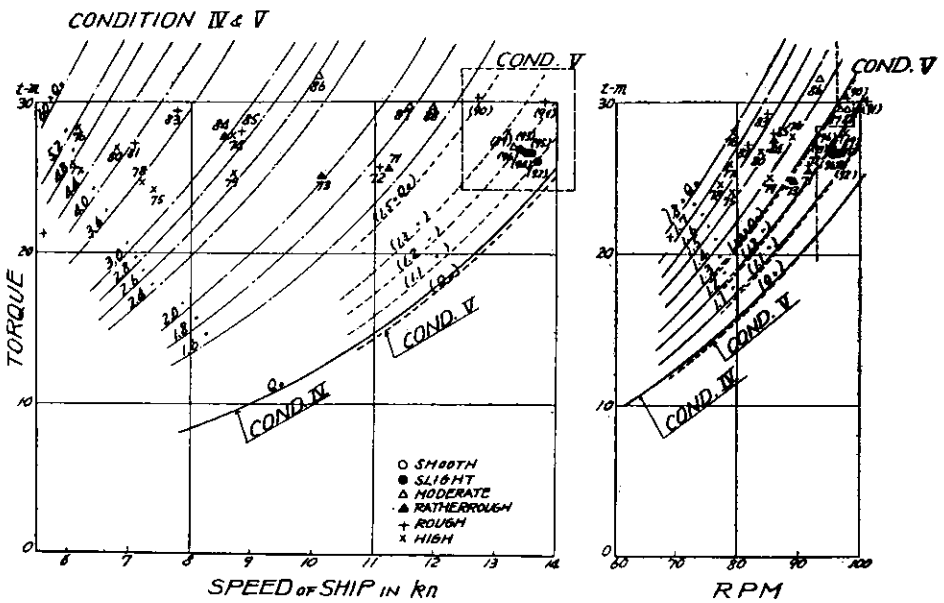

Fig. 64. Shaft Torque, Condition IV–V

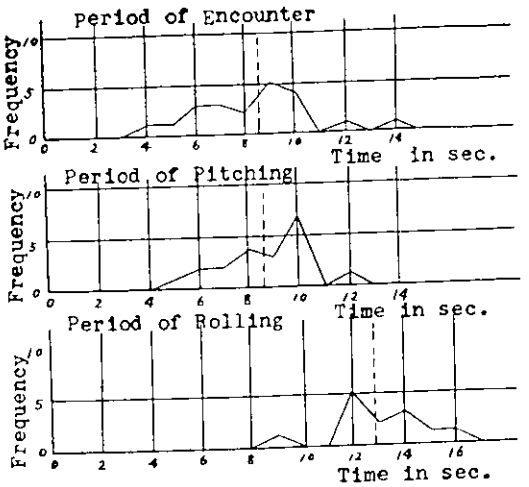

Fig. 65. Frequency Diagram of Period during One Measurement throughout 3 Minutes

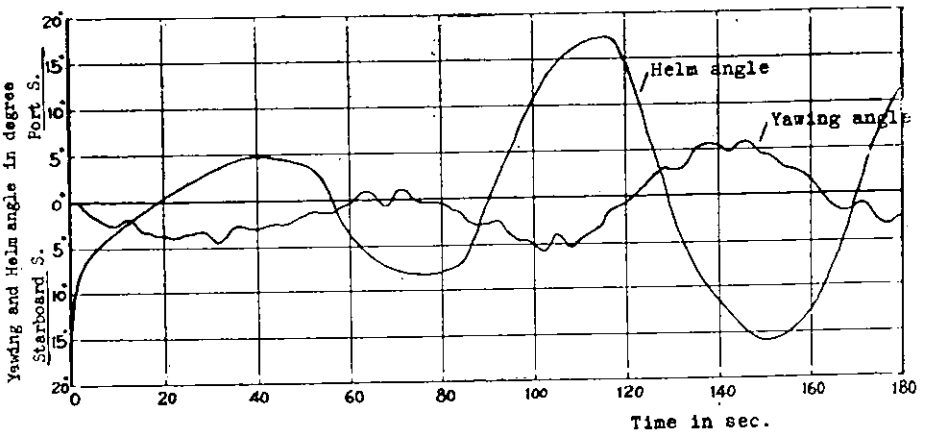

Fig. 70. An Example of the Relation between the Helm Angle and the hip's Heading Angle (Exp. No. 74)

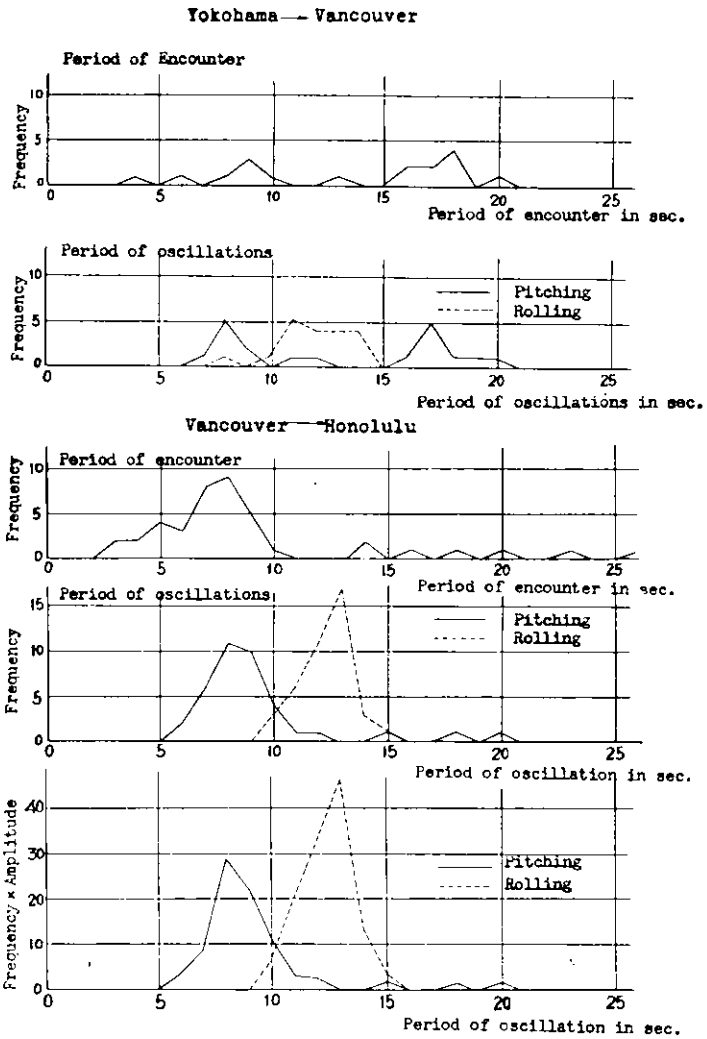

Fig. 66. Relation between the Period of Encounter of Waves and the Period of Oscillations of the Ship

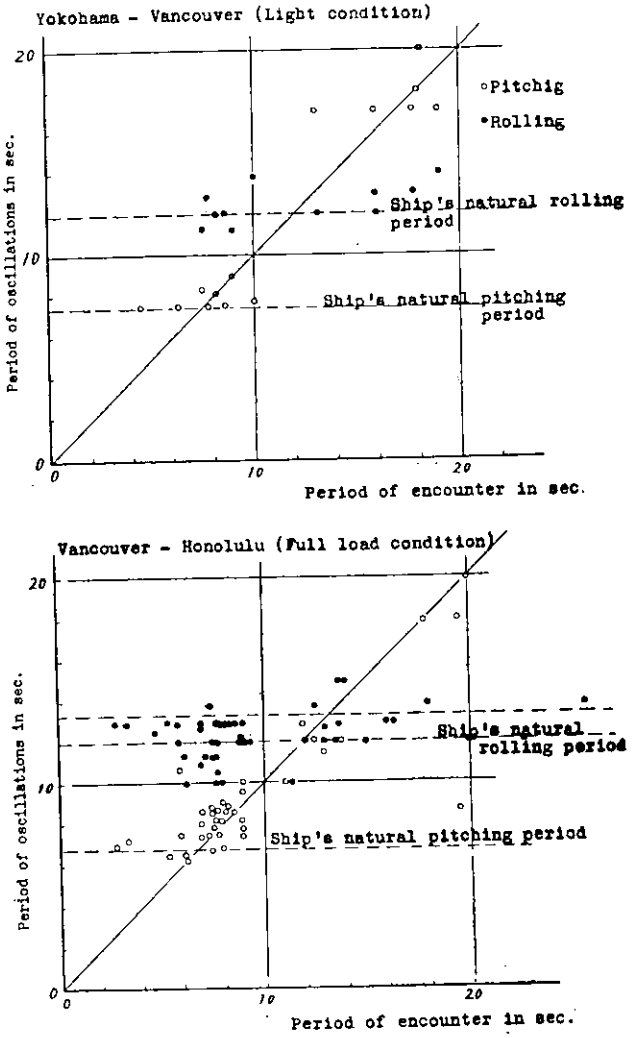

Fig. 67. Relation Between the Period of Encounter of Waves and the Period of Oscillations of the Ship

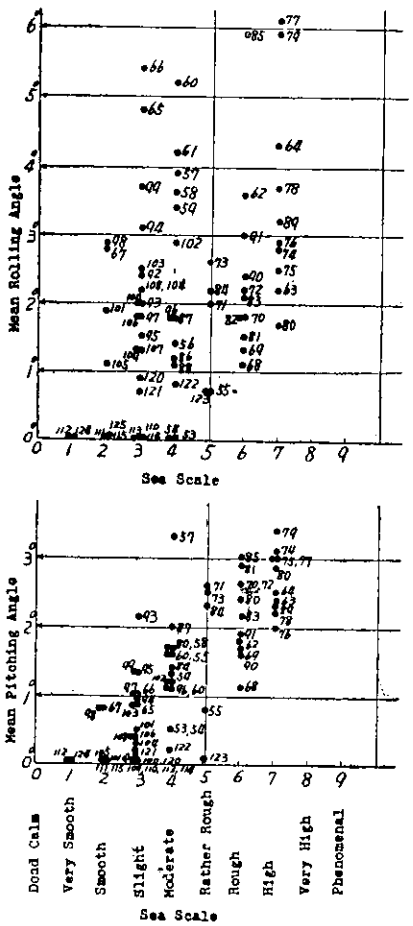

Fig. 69. Relation between Sea Scale and Angle of Oscillation

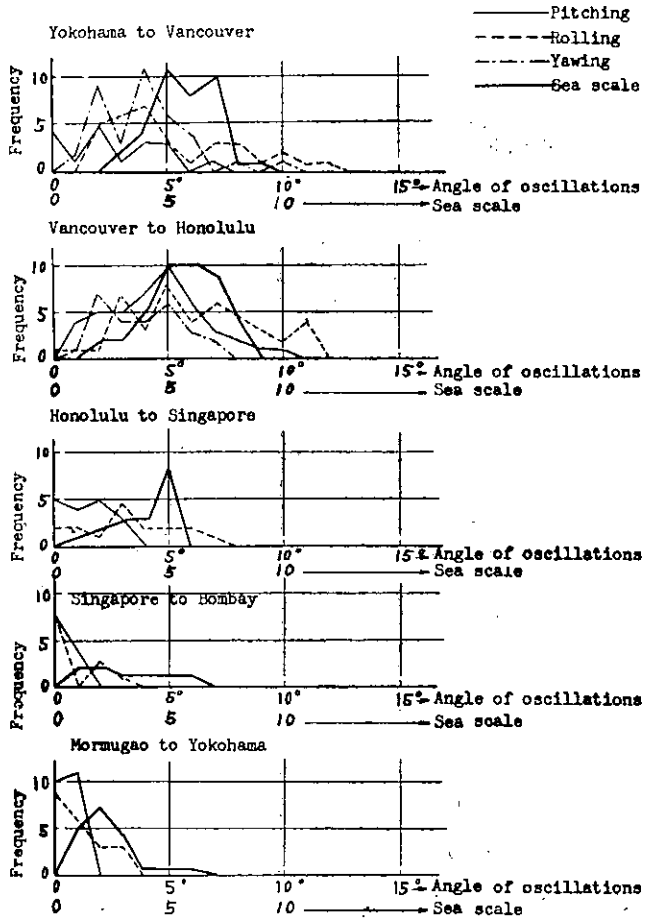

Fig. 68. Frequency Distributions of the Period of Oscillations and the Sea Scales on Each Course

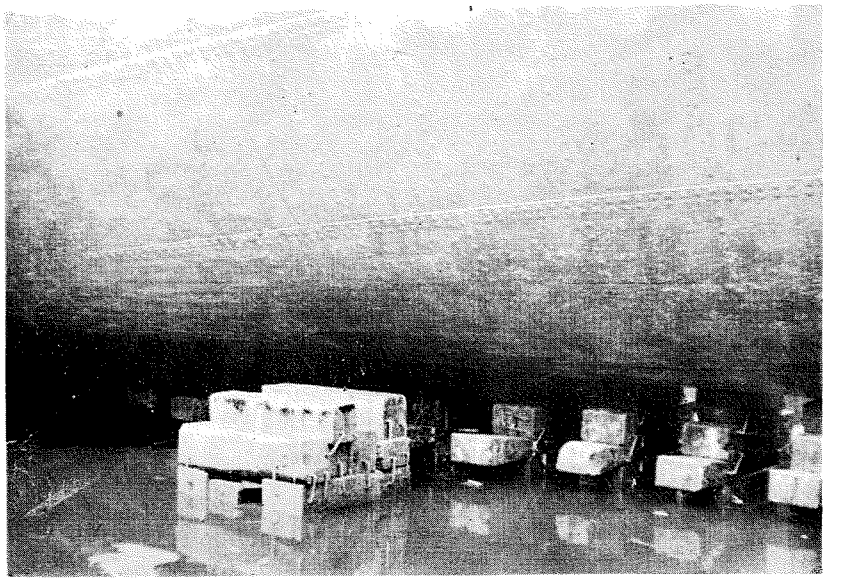

Fig. 71. Fouling of Shell Plate (Port side After Body)

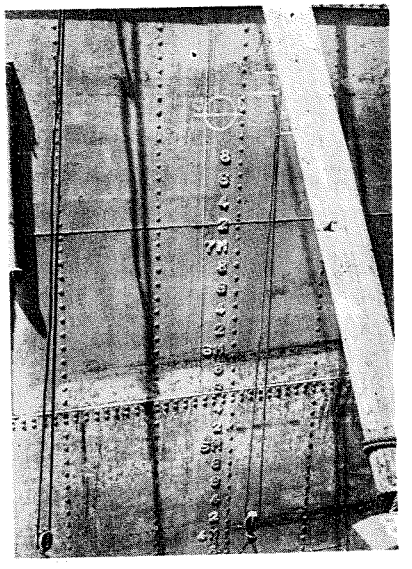

Fig. 72. Fouling of Shell Plate (Midship)

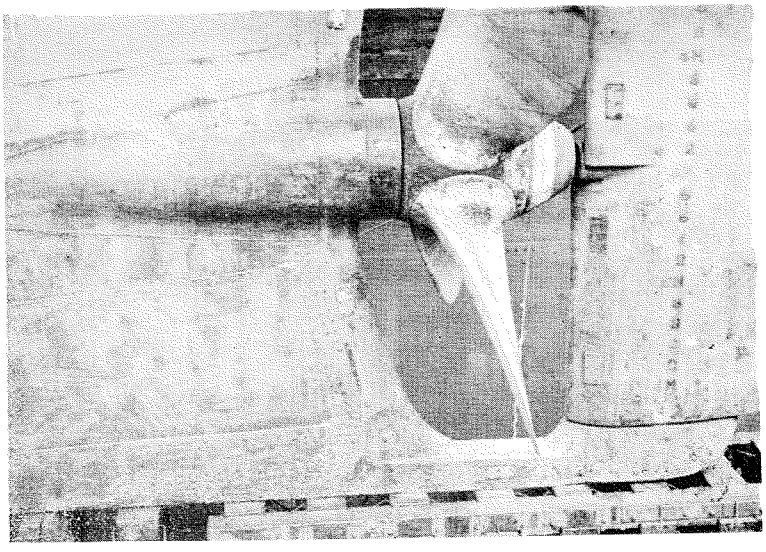

Fig. 73. Fouling of Propeller and Stern Frame

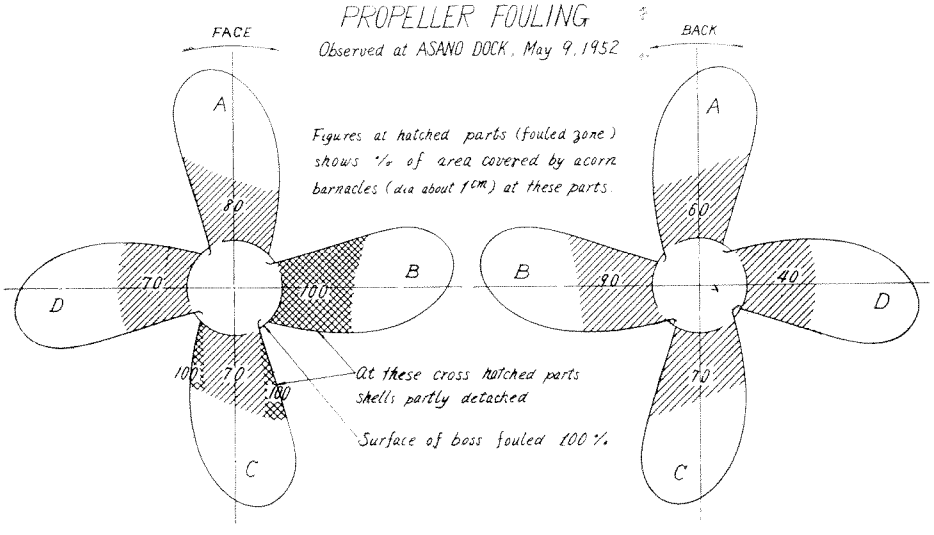

Fig. 74. Sketch of Propeller Fouling

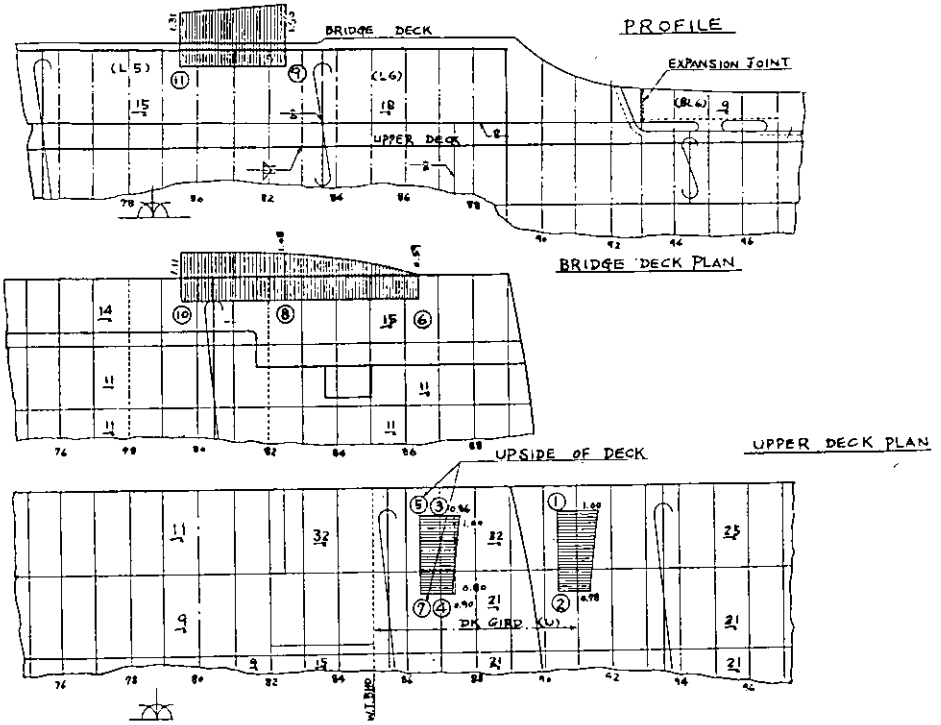

Fig. 75. Measured Stress Distribution

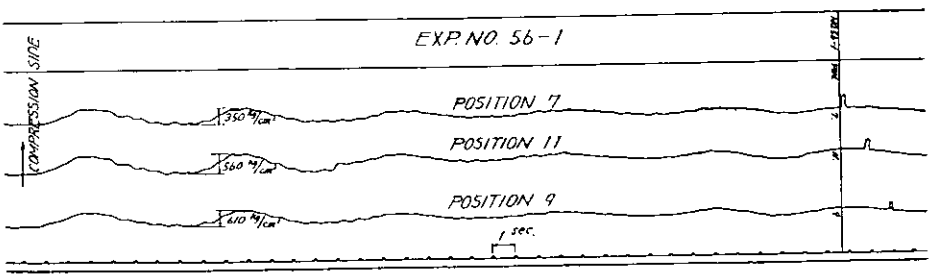

Fig. 76. A Stress Diagram at Slamming

PART II. MODEL EXPERIMENTS

Chapter 1

Introduction

Much valuable data and instructive experiences were secured by the actual ship experiments on the "Nissei Maru" as described in Part I of this paper, among which, it was specially noticed that the effects of wind and waves on the ship propulsive performance were far larger than had been expected.

From this fact, the Authors thought it to be an urgent matter to improve and establish the methods of tank experiments in waves and wind tunnel experiments, and then to clarify the nature of the speed loss of vessels in a seaway and the effect of wind and waves on the sea-worthiness of vessels under any weather and sea conditions, and hence, to direct their efforts in making several contributions towards the reduction of the wind resistance of vessels, and the improvements of the propulsive performance of vessels in a seaway and the navigating method in heavy storms.

To further the above mentioned investigations, the 1st Research Committee was set up in the Shipbuilding Research Association of Japan, and the following model experiments were carried out by the members of the committee*; the resistance, self-propulsion and oscilla-

* Members who took share in the experiments

Name	Division of work	Position
Shiro Kan Kiyoshi Tsuchida Tatsuo Ito	Resistance, self-propulsion and oscillation tests on a 4 m and 6 m models.	Transportation Technical Research Institute.
Takao Inui Seizo Motora	Resistance, self-propulsion and oscillation tests on 2.5 m model.	Faculty of Eng., University of Tokyo.
Masao Kinoshita Shojiro Okada	Wind tunnel experiments	Technical Res. Laboratory, Hitachi Shipbuilding & Eng. Co. Ltd.
Shoichi Nakamura	Do.	Faculty of Eng., University of Osaka.
Kaname Taniguchi	Prepeller open tests	Technical Department, Mitsubishi Shipbuild. & Eng. Co. Ltd.

tion tests in still and rough waters at the No. 1 Experiment Tank of the Transportation Technical Research Institute (200 m in length), and the experiment tank of Tokyo University (86 m in length); the wind tunnel experiments on a model of the above-water portion of the ship at the 3.5 m wind tunnel of Osaka University; the propeller open tests at the Experiment Tank of Mitsubishi Shipbuilding and Engineering Co., Ltd.. Precise descriptions of the methods and results etc. of the experiments are given in the following chapters.

Though there are still many additional untested cases and problems to be solved, such as the improvement of testing methods etc., the Authors consider that they have been able to clarify, to a considerable extent, the sea-going qualities of vessels—with regards at least to the "Nissei Maru" and other similar kinds of medium-speed cargo ships—through comparison between the model experiment data and those of the actual ship experiments.

The Authors are also thinking of promoting further experiments, and they believe that they will be able to present a way to the solution for many unsolved problems in the field of the sea-going qualities of vessels of general kind.

Chapter 2

Models used and Test Conditions

1. Description of models

Various kinds of tank tests were carried out principally on two wooden models, whose length between perpendiculars were 4 m (scale 1/32.00) and 2.5 m (scale 1/51.20). But the resistance and self-propulsion tests in still water were carried out on a 6 m paraffin model (scale 1/21.33) as well as the models above mentioned. Appendages such as rudder and bilge keels were fitted to these models, and the lines of modelship were corresponded to the moulded form (Fig. 1 of Part I) covered with mean thickness of shell plates (23 mm in actual ship).

Propeller open tests were carried out on model propeller of diameter 50 cm.

Wind tunnel experiments were carried out on a 1.707 m wooden image model (scale 1/75.00), consisted of two models of above-water portion which were joined together on the water plane symmetrically.

2. Test conditions

Concerning the loading condition of the models in tank and wind tunnel experiments, condition I and IV (Table 3 of part I) in the actual ship experiments were chosen as typical cases of light and full load conditions (see Table 1).

Table 1. Test Condition (Values for Actual Ship)

Load Condition		Light (Cond. I)	Full Load (Cond. IV)
Mean Draft (above Bottom of Keel)	m	4.25	8.04
Trim by the Stern	m	3.45	0.82
Displacement	t	6,440	13,450
Block Coefficient			0.728
Prismatic Coefficient			0.737
Midship Section Coefficient			0.988
Longitudinal centre of Buoyancy from ⊗	% of Lpp	3.96 aft	0.37 aft
Height of Centre of Gravity, KG	m	6.35	6.55
Transverse Metacentric Height, GM	m	1.69	0.39
Longitudinal Metacetric Height, GM_L	m	266.0	144.0
Wetted Area	m^2	2,446	3,475
Transverse Projected Area of Above-water Portion	m^2	370	285
Longitudinal ,, ,, ,, ,, ,,	m^2	1,490	999

Chapter 3

Wind Tunnel Experiments

1. Model

General view of the model used on the wind tunnel experiments is shown in Fig. 1. The model was made of lacquered Japanese cypress (Hinoki), and its length is 1.707 m and 1.842 m between perpendiculars

and over all respectively. A few kinds of metals such as copper plates are also used on some parts of the bridge and equipments.

To be able to test under both light and full load conditions, a layer part between two corresponding water planes are made removable. Superstructures and various kinds of equipments on deck were made removable also.

2. Method of the experiments

When the wind tunnel experiments are performed concerning wind resistance of ship, it is a question how to represent the sea surface. In these tests, besides a method of so called image model, consisted of the two models of the above-water portion which were joined together symmetrically, a method of representing the sea surface, as a new trial, by inserting a wooden circular plate (2 m diameter, 40 mm thick shown in Fig. 4) between the two models was adopted.

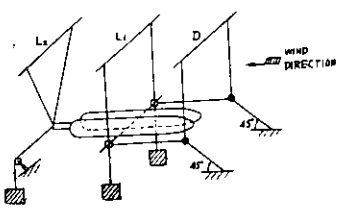

Fig. 2. Suspension of Ordinary Image Model

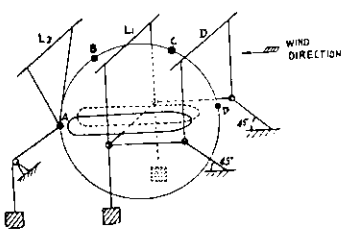

Fig. 3. Suspension of Model with Circular Plate

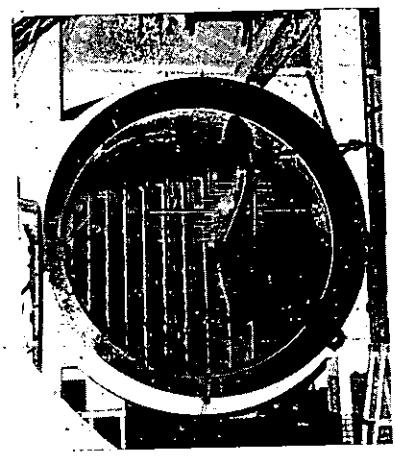

Fig. 4.

Setting condition of the model in the wind tunnel is shown in Figs. 2 and 3. At first, by a method inserting the circular plate between the models, in case of the direction of wind off bow 0°–35°, it was confirmed that aerodynamical coefficients reported as following were not changed substantially, even though the speed changed in the

the scope of 5-30 m/sec, and then drag and lift were measured, changing the direction of wind off bow every 5° in the range 0°-180° and keeping the wind speed constant about 23 m/sec, under the light and full load conditions.

During these tests, the circular plate was always vibrated slightly in the normal direction to the air flow. Particularly in the case near abeam wind, as the oscillation was excessive and appeared dangerous, so the experiments on these cases were performed reducing the wind speed down to 17 m/sec.

The method of inserting the plate is evidently convenient, on the occasion of changing continuously the direction of wind to the wide range. However, according to the results of the measurements of wind speed distribution around the wooden circular plate and the results of the comparative tests with case of no plate, the method is not always so effective and adequate in points of accuracy and others.

In Test No. 4, the speed distribution around the wooden circular plate was measured without the models. The boundary layer was extremely thin as was expected. The speed at 5 mm above the surface of the wooden circular plate was equal to the general speed, and its distribution may be recognized to be a constant distribution.

Then to know the ratio of the air resistance of principal equipments on decks to the total wind resistance, experiments were performed removing those equipments by turns. Some experiments were also carried out to know the influence of the alteration of shape and height of bridge on aerodynamical forces. In these cases, the experiments were carried out with no circular plate, increasing the wind speed up to about 30 m/sec, in order to increase accuracy of measurements. In these experiments, the direction of wind off bow were every 5° in the range of 0°-35°.

The details of the wind tunnel experiments are shown in Table 2. In Test No. 6, masts and derrick posts were removed from the original form. In Test No. 7, 8 and 9, more other principal equipments on decks were removed by turns. In Test No. 10, 11 and 12, first, second

and third floors were removed by turns from the bridge of the original ofrm which has five floors above the upper deck. In Test No. 13, the bridge has 4 floors and each story is stepped back as shown in Fig. 5. In Test No. 14, 15, 16 and 17, the bridge front was made semi-circle of radius equal to the half breadth of ship, with 5, 4, 3 and 2 floors respectively. In Test No. 19, the bridge was reformed to the mode of the cargo vessel "Nikko Maru" whose bridge is somewhat stream-lined, as shown in Fig. 6.

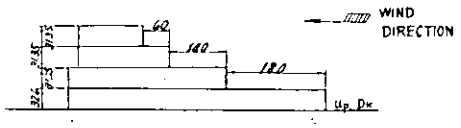

Fig. 5.

Table 2. Details of Wind Tunnel Experiments

Test No.	Load Cond.	Circular Plate	Condition of Model	Measured Items	Range of Wind Direction
1	Light	With	Original form	L_1, L_2, D	0°-180°
2	Full	〃	〃 〃	〃	〃
3	/	Circular plate only		D	0°
4	/	〃	〃 〃	Velocity Distribution	〃
5	Light	Without	Original form	L_1, L_2, D	0°– 35°
6	〃	〃	Derrick posts and masts removed	〃	〃
7	〃	〃	Ventilators, winches and windlasses removed from No. 6	〃	〃
8	〃	〃	All equipments, bulwarks and handrails removed	〃	〃
9	〃	〃	Winch platforms removed from No. 8	〃	〃
10	〃	〃	One floor of bridge removed from No. 9	〃	〃
11	〃	〃	Two floors 〃 〃 〃 〃 〃	〃	〃
12	〃	〃	Three 〃 〃 〃 〃 〃 〃	〃	〃
13	〃	〃	Bridge stepped back	〃	〃
14	〃	〃	Bridge front rounded	〃	〃
15	〃	〃	One floor of bridge removed from No. 14	〃	〃
16	〃	〃	Two floors 〃 〃 〃 〃 〃 〃	〃	〃
17	〃	〃	Three 〃 〃 〃 〃 〃 〃 〃	〃	〃
18	〃	〃	F'cle and Poop removed from No. 17	〃	〃
19	〃	〃	With "Nikko Maru" type bridge	〃	〃
20	〃	〃	All equipments removed from No. 19	〃	〃

Besides above mentioned experiments at the 3.5 m wind tunnel of Osaka University, the wind speed distributions around the ship were

measured at the 1.0 m wind tunnel of the Department of Naval Architecture, Osaka University. On the single model, not the image model, of the original form, the relative wind speed was measured by hot-wire anemometer under the general wind speed of 11 m/sec. At first, in case of the direction of wind off bow 0°, the speed distribution on the centre line plane was measured, and then wind speed was measured, turning the model by the interval of 15°, at the position of 750 mm above the top of fore derrick post, the top of fore mast, rader post and middle point of the starboard half of the fore mast portal respectively.

3. Results of the experiments and discussions thereon

As for the expression of the results of experiments, for the convenience of comparison, an usual expression by the following non-dimensional form was adopted.

Coefficient of resultant wind force

$$C_{F\,\mathrm{wind}}=\frac{F_{\mathrm{wind}}}{\frac{1}{2}\rho_{\mathrm{air}}V^2_{\mathrm{wind}}(A\cos^2\varphi_{\mathrm{wind}}+B\sin^2\varphi_{\mathrm{wind}})}$$

Position of centre of pressure of the resultant wind force

$$a/L_{oa}$$

Wind resistance coefficient

$$C'_{F\mathrm{wind}}=\frac{F_{\mathrm{wind}}\cos(\alpha_{\mathrm{wind}}-\varphi_{\mathrm{wind}})}{\frac{1}{2}\rho_{\mathrm{air}}V^2_{\mathrm{wind}}(A\cos^2\varphi_{\mathrm{wind}}+B\sin^2\varphi_{\mathrm{wind}})}$$

Wind direction effect coefficient

$$k=\frac{R_{\mathrm{wind}}}{\frac{1}{2}\rho_{\mathrm{air}}V^2_{\mathrm{wind}}C_{F0}A}$$

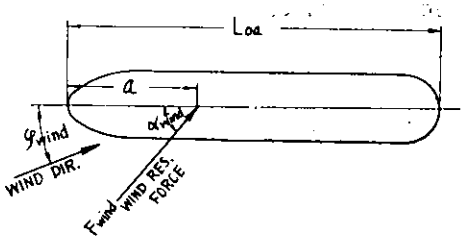

Fig. 7.

where, V_{wind} : relative wind speed (m/sec)

ρ_{air} : density of air (kg. sec²/m⁴)

φ_{wind} : relative direction of wind off bow

α_{wind} : direction of resultant wind force off bow

F_{wind} : resultant wind force (kg)

R_{wind} : wind resistance (kg)$=F_{wind}\cos\alpha_{wind}$

L_{oa} : over all length of ship (m)

a : position of centre of pressure of the resultant wind force on the centre line plane from bow (m)

A : transverse projected area of above-water portion (m^2)

B : longitudinal projected area of above-water portion (m^2)

C_{F0} : C_{Fwind} at $\varphi_{wind}=0$

In the experiments, as reported above, measurements were performed in the cases of both with and without the circular plate in the scope of $\varphi_{wind}=0°$–$35°$. The wind resistance in the case of no plate is about 9% less than that in the case of with plate at $\varphi_{wind}=0$. This difference decreases as φ_{wind} increases and almost coincides when φ_{wind} is about 30°. Though the causes of such difference is not clear yet, the values in the case of no plate were taken as correct values.

The direction of resultant wind force off bow, the position of centre of pressure of the resultant wind force, the wind resistance coefficient and the wind direction effect coefficient, obtained from these experiments, were plotted to a base of the direction of wind off bow in Figs. 8–11. For reference, data of several kinds of ships, which were already published, are contained in these figures. Though these data are not always comparable strictly, many interesting tendencies can be conjectured through them. Among the experiments on the model of the "Nissei Maru", it is a note-worthy fact that the wind direction effect coefficient is considerably different from that expected. That is, the values of this vessel are generally large, comparing with the values (shown by a thick line in Fig. 11) which we have thought as the standard for ordinary cargo vessels, and the difference of the values is remarkable in the case with oblique after wind at full load condition. The angles, at which the wind direction effect coefficient attains maximum, are generally about 30° and 160°. But, in this test of the "Nissei Maru" they are 45° and 150°.

In Fig. 12, head resistance coefficients are plotted to a base of Reynolds Number. Values of the "Nissei Maru" are smaller than

those of express cargo carrier "London Mariner" and oil tanker "San Gerardo", and are equal to those of tuna fishing boat. Therefore, it seems that the values are not so large particularly as a cargo vessel.

Tests were carried out for the purpose of investigating the effect of the shape and height of a bridge upon the resultant wind force, and also for the purpose of investigating the ratio of the resistance of the main fittings on decks such as masts, derrick posts, windlasses, winches, ventilators, bulworks, handrails, bollards, fair-leaders, winch platforms and etc. to the total wind resistance. The results of these tests are shown in Fig. 13 by percentage of resultant wind force for the original form of the "Nissei Maru".

From these results, following conclusions may be deduced on the whole.

(1) In model tests, masts, derrick posts, ventilators and etc. have little influence on the resultant wind force.

(2) By decreasing floors of the bridge the resultant wind force is decreased by more than the ratio of the decrease of projected area, in the scope of relative wind direction $\varphi_{wind}=0°-15°$. But, at more than 15° of φ_{wind}, the decrease of the resultant wind force is resulted only from the decrease of projected area.

(3) Facts stated in (2) can be said also in case that the bridge front is round.

(4) On the contrary, the influence of remove of fittings has no connection with the angle of wind direction.

(5) To decrease the number of bridge decks, to round up the bridge front, and to make the upper part of the bridge front round like a going-back curved surface are all effective means to decrease the resultant wind force. Above all, to decrease the number of bridge decks is the most effective means.

Making use of those results of tests above related, wind resistance in case of the actual ship experiments was calculated and shown in Table 3. In the actual ship experiments, the ship received generally a fair wind in light condition, but received frequently a strong head

Table 3. Calculated Wind Resistance in the Case of Actual Ship Experiments

Exp. No.	Relative Wind Speed, m/sec.	Wind Direction, degree	Wind Resistance, ton	Exp. No.	Relative Wind Speed, m/sec.	Wind Direction, degree	Wind Resistance, ton
1				49	1.5	P 135	− 0.042
2	16.0	P 85	1.260	50	3.0	〃 30	0.196
3	〃	〃 〃	1.265				
4	10.0	〃 70	1.110	51	11.0	S 70	1.354
5	14.5	〃 65	3.540	52	10.0	P 35	2.270
				53	17.5	〃 25	5.705
6	10.0	〃 70	1.143	54	19.0	〃 25	6.710
7	7.5	〃 55	1.202	55	20.5	〃 20	7.300
8	1.0	〃 140	− 0.020				
9	5.0	〃 70	0.286	56	13.5	S 45	4.115
10	1.5	〃 〃	− 0.026	57	12.0	〃 25	2.618
				58	10.5	〃 25	2.030
11	3.0	〃 175	− 0.218	59	10.0	〃 25	1.843
12	〃	〃 〃	− 0.218	60	11.0	〃 35	2.345
13	2.0	〃 125	− 0.044				
14	9.0	〃 75	0.804	61	13.0	〃 15	2.735
15	7.5	〃 100	− 0.052	62	22.0	〃 50	10.650
				63	20.0	〃 45	9.100
16	9.0	〃 105	− 0.126	64	19.5	〃 35	7.410
17	8.0	〃 115	− 0.481	65	10.0	〃 30	1.958
18	6.5	〃 130	− 0.668				
19	10.0	〃 135	− 1.934	66	9.0	〃 10	1.135
20	6.0	〃 155	− 0.620	67	8.0	P 20	1.105
				68	17.0	〃 75	2.010
21	4.5	S 160	− 0.538	69	15.0	〃 50	4.970
22	6.0	〃 130	− 0.569	70	14.5	〃 37	4.150
23	17.5	〃 70	3.562				
24	17.0	〃 77	2.760	71	16.5	S 5	3.705
25	16.0	〃 80	2.253	72	17.0	〃 10	3.885
				73	16.5	〃 10	3.670
26	15.0	〃 85	1.091	74	19.5	〃 12	5.680
27	〃	〃 〃	〃	75	17.0	〃 7	3.970
28	〃	〃 〃	〃				
29	〃	〃 〃	〃	76	22.0	〃 17	7.575
30	7.0	〃 95	0	77	21.0	〃 20	7.320
				78	19.0	〃 15	5.698
31	10.0	〃 110	− 0.564	79	15.0	〃 20	3.770
32	5.0	P 105	− 0.038	80	18.0	P 20	5.425
33	10.0	〃 180	− 2.377				
34	13.0	〃 120	− 1.558	81	17.5	〃 5	4.030
35	14.0	〃 140	− 3.870	82	16.0	S 10	3.460
				83	19.0	〃 15	5.660
36	19.0	〃 145	− 7.940	84	17.5	〃 5	4.255
37				85	18.0	〃 5	4.500
38	13.0	〃 140	− 3.338				
39				86	13.0	P 8	2.305
40	10.0	〃 115	− 0.745	87	15.0	〃 20	3.755
				88	16.0	〃 30	4.815
41	13.0	〃 135	− 3.260	89	16.0	S 110	− 2.410
42				90	16.0	〃 120	− 4.025
43	11.0	〃 110	− 0.566				
44	9.0	〃 130	− 1.271	91	10.0	〃 105	− 0.585
45	6.0	〃 110	− 0.198	92	7.5	〃 110	− 0.530
				93	6.0	〃 115	− 0.504
46	6.5	S 150	− 0.928	94	6.0	〃 150	− 0.955
47	9.0	P 130	− 1.246	95	6.5	〃 85	− 0.047
48	4.0	〃 80	0.143	96	7.0	〃 75	0.323

wind in full load condition. So the maximum wind resistance is about 10 tons in Test No. 62 under the full load condition.

We calculated the wind resistance R_{wind} when this vessel sails receiving a wind of relative wind speed 15 m, 20 m and 25 m per second from dead ahead and the direction of maximum wind resistance. These results are shown in Figs. 14 and 15 in the ratio of wind resistance to water resistance in still water. The maximum value of the ratio on the actual ship experiments is 1.47 in Test No. 79 under the full load condition. By the figures it is evident how the wind resistance can be large, and it is very important to pay attention on the wind resistance even in this kind of cargo ship.

In Fig. 16 is shown the wind speed distribution on the centre line plane at $\varphi_{wind}=0$. By this figure, it can be known that the existence of the hull influences up to the upper parts as it goes to the stern of the hull, and moreover, the effect of fore mast portal and other interesting facts can be known. In Fig. 17, it is shown how the wind speed, in a spot where it can be thought as a place to fit up the anemometer, changes by the wind direction. Thus the wind speed is influenced in any place by obstacles nearby and is not always equal to general wind speed. The wind directions were not nearly different from general wind direction and its deviation was not over 5°.

Chapter 4

Oscillation Tests

I. Rolling

1. Method of experiments and apparatus used

In the actual ship experiments on "Nissei Maru", very few abeam seas were encountered being in most cases oblique or nearly ahead seas. For this reason, the model rolling experiments were conducted mainly in oblique waves.

The experiments were carried out in the experiment tank of the Tokyo University on a 2.5 m wooden model, similar to the one used for the resistance experiment, at full load condition (Condition IV). The model ship's natural rolling period T_0 was adjusted to 1.72 sec. and the pitching period to 0.92 sec. respectively, and the damping factors measured in an experiment in still water were; $a=0.0298$, $b=0.0374$ respectively.

In the ordinary rolling experiments in abeam waves, the model

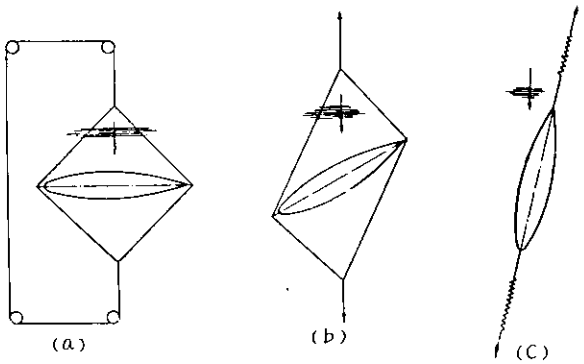

Fig. 18. Methods to hold the Model in Rolling Experiments

ship was held in its direction by cords fixed to its fore and aft ends and stretched in a diamond shape as shown in Fig. 18 (*a*), allowing for free drifting. In this experiment, in a range of 30°–150° of the angle of encounter, this method was used in a somewhat deformed condition as shown in Fig. 18 (*b*), and among 0°–30° and 150°–180° the model was held successively by two weak springs stretched in fore and aft directions as shown in Fig. 18 (*c*), permitting free drifting and surging motions.

2. Results of experiments and discussions thereon

The rolling experiment was conducted in oblique waves, their angle of encounter being varied as 90°, 75°, 60°, 45°, 30°, and 15°, the wave period T being chosen as 1.30 sec. ($T/T_0=0.76$), 1.54 sec. (0.90), 1.72 sec. (1.0), 1.79 sec. (1.04), and 1.90 sec. (1.10), wave slope as 1°, 2°, 3°, 4°, and 5° for each angle of encounter respectively.

(1) Effect of wave slope on rolling angle

As shown in Fig. 19, the rolling angle θ_s varies almost proportionally to the wave slope θ_w, and as seen in Fig. 20, the ratio θ_s/θ_w has a large value for small θ_w, decreasing when θ_w becomes large, and becomes almost constant for larger θ_w than 5°. Hence, the θ_s/θ_w value for $\theta_w=5°$ was employed as θ_s/θ_w for larger θ_w than 5° in analysing the actual ship experiment results.

(2) Effect of angle of encounter

An example of the effect of changing the angle of encounter is shown in Fig. 21, in which θ_s/θ_w values for $\theta_w=5°$ are plotted against the angle of encounter α, showing that the rolling angle varies proportionally to sin α. In addition, θ_s/θ_w varies for different θ_w when T/T_0 is kept constant, an example being shown in Fig. 22.

(3) Corresponding wave slope in oblique waves

Considering θ_s/θ_w curve vs α to be a sine curve, the wave slope θ_w of the abeam waves necessary to cause the above θ_s are obtained from Fig. 19 as shown in Fig. 23, and we call such a θ_w to be "corresponding wave slope." The corresponding wave slope $\theta_{w\alpha}$ in the oblique waves is usually expressed as follows;

$$\theta_{w\alpha}=\theta_{w90°}\sin\alpha$$

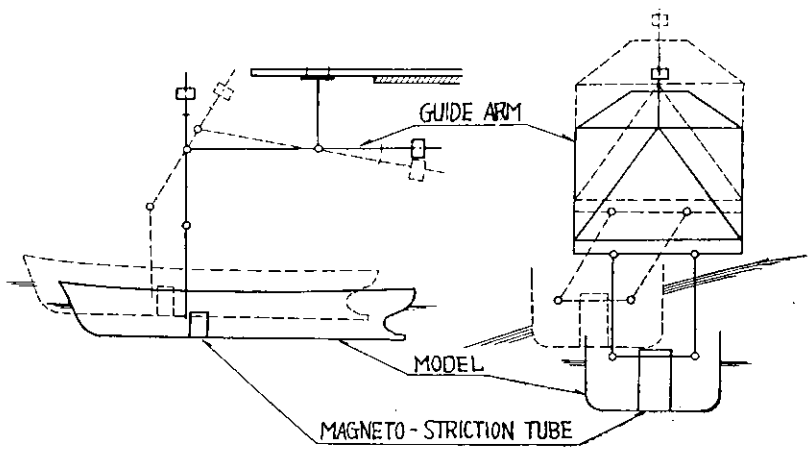

Fig. 24. Illustration of an Apparatus used for Measuring the Wave Force Acting on Ship

but as can be seen in Fig. 23, $\theta_{w\alpha}$ for small α (nearly ahead waves) is smaller than is expressed in the above formula.

On the other hand, the wave force acting on a model ship was measured directly by using the instrument shown in Fig. 24, the corresponding wave slope being computed by the following formula;

$$\text{wave force (moment)} = W \cdot GM\gamma\theta_{w\alpha}$$

where W: displacement
GM: transverse metacentric height
$\theta_{w\alpha}$: corresponding wave slope
γ: effective wave slope factor for $\alpha=90°$

The results obtained are given in Fig. 25 and are thought to agree closely with Fig. 23.

(4) Effect of ship's speed

The period of encounter in oblique waves changes when the ship's speed is altered, viz.

$$T_e = \lambda/(V_w + V_s \cos\alpha)$$

where λ: wave length
V_w: wave speed
V_s: ship's speed

Therefore, the rolling angle will deviate from the result in Fig. 21, where the ship's speed was kept as zero, and deviation can be got as follows; supposing the ship encounters waves, the period of which is T_{w0}, and the wave slope θ_w, the corresponding wave slope $\theta_{w\alpha}$ will easily be secured from Fig. 26, and also T_e from the above formula. Hence the rolling angle corresponding to $\theta_w = \theta_{w\alpha}$, $T = T_e$ will be found on the equi-period diagram in Fig. 27. The results are shown in Fig. 28.

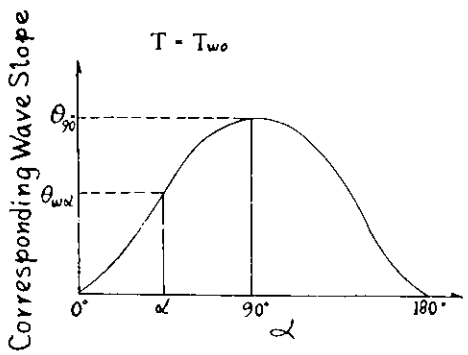

Fig. 26.

(5) Comparison between model experiment results and actual ship data

It is necessary to consider the irregularity of the waves in comparing the model experiment with the actual ship data. Two kinds of effects of the irregularity of the waves on the ship's rolling angle will be noticed. First, as is shown in Fig. 28, in regular waves the resonance curve has a sharp peak at the synchronism, and the amplitude decreases rapidly when the wave period deviates from synchronism. On the contrary, in irregular waves, the resonance curve will not have such a sharp peak at the synchronism (when the period of the ship coincides with the average wave period), and the amplitude does not decrease so rapidly as in regular waves at the outside of the synchronism (see Fig. 29).

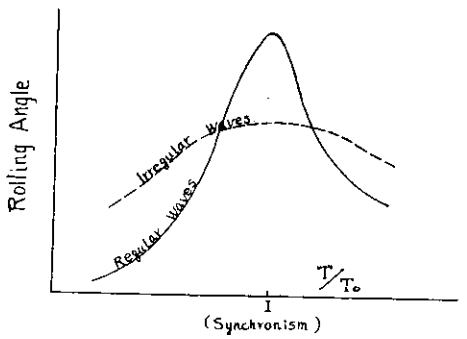

Fig. 29. Effect of the Irregularity of the Waves on the Ship's Rolling Angle

In the actual ship experiments on "Nissei Maru", there were so few cases when the ship encountered abeam waves likely to cause synchronous rolling, that it is difficult to discuss the effect quantitatively. The ratio $\theta_{s\,max}/\theta_w$ measured on the actual ship in a range $\alpha=$ 10°-20°, and $\alpha=160°$-170°, is plotted against the period of encounter as shown in Fig. 30. As the actual ship data were obtained from various wave slopes, it is difficult to arrive at a definite conclusion from them. Nevertheless, it can be said that the ship rolled considerably outside of synchronism, and its rolling diagram does not show a clear peak at the resonance.

In Fig. 30, it will be noticed that the $\theta_{s\,max}/\theta_w$ values for the actual ship are on the average larger than those of the model ship, due it is thought to lack of accuracy in measuring the wave slope, and by neglecting the correction for scale effect to the model experiment results.

Secondly, as shown in Fig. 31, in regular waves a ship rolls proportionally to the sin α, when the angle of encounter α varies from 90°, while in irregular waves, according to the record obtained, the ship rolled to a considerable degree even for small α, say in almost ahead waves. This phenomenon can be explained as follows; in waves having sufficiently long crest lines, the corresponding wave slope must be 0 when $\alpha=0$, and consequently a ship will not roll in such cases, while in actual ocean waves, which are formed from isolated waves having short crest lines, and are distributed quite at random, there is therefore some probability for the existence of a finite corresponding wave slope which will cause the ship's rolling.

II. Pitching and Heaving

1. Method of experiments and apparatus used

Measurements on pitching, heaving and surging were conducted on the occasion of the resistance and self-propulsion tests in waves on a 4 m model ship at the Transportation Technical Research Institute. The natural pitching and heaving period of the model used for those experiments (see Chapter 5) are shown in Tables 4 & 5.

Table 4. Natural Pitching Period of the 4 m Model

	Period at the Actual Ship Experiments		Period at the Model Experiments	
	Mean Value	Corresponding Value for the Model	Value obtained by Bifilar Suspension Tests in Air	Value obtained by Free Oscillation Tests in Still Water
Light Condition	7.28 sec.	1.29 sec.	0.72 sec. (172 kg. m²)	about 1.20 sec. (484 kg. m²)
Full Load Condition	7.02 sec.	1.24 sec.	0.87 sec. (343 kg. m²)	about 1.30 sec. (759 kg. m²)
			—	1.20 sec.

Remarks: Figures in brackets show the values of $I \times g$.

Table 5. Natural Heaving Period of the 4 m Model

	Theoretical Value taking no Account of the Virtual Mass Effect	Value obtained by Free Oscillation Tests in Still Water
Light Condition	0.683 sec.	1.2 sec.
Full Load Condition	0.937 sec.	1.3 sec.

Oscillation Tests

The oscillation recorder shown in Fig. 32, based on the "principle of a parallelogram", and composed of light metal tubes, was employed in the experiment. The pitching angle, heaving and surging amplitude are recorded simultaneously on a recording drum. Corrections are needed for the recorded values for the heaving and surging, because they are affected by each other.

As the recorder was attached to the model's centre of gravity, the recorded motion represents the motion of the model's centre of gravity.

For recording the wave profile, an electric wave height recorder was employed, which is composed of two brass pole plates placed against each other in the water, so as to convert the variation of the water level to the variation of electric current exerted by a 20 volts potential difference between the two poles. The variation of the electric current is recorded by a pen-writing oscillograph.

In addition, the encounter marks, showing the time at which the model encountered the waves, were recorded on the drum of the oscillation recorder, and simultaneous time marks were also made on every recording apparatus, so as to make it possible to secure a relation between the phase of waves and the pitching, heaving and resistance of the model.

2. Results of experiments and discussions thereon

The period of pitching and heaving coincided with the period of encounter as far as the experiments went, showing that they are all forced oscillations, and are thought to be a matter of course on account of the large damping force in the pitching and heaving motions.

The pitching angle and the heaving amplitude obtained by the experiment as well as the period of encounter and the resistance of the model are shown in Figs. 43-46, according to which the resonance curves for pitching and heaving do not show a sharp peak as those for rolling do, only indicating a low hump at the synchronism. The wave slope is also shown Figs. 45-46, by way of comparison, demonstrating that when the wave length becomes large, as is naturally expected, the angle of pitching approaches to the wave slope.

The pitching angle is very small when the wave length is shorter than the model length, and changes almost proportionally to the wave height when the model speed and wave length are kept constant.

The heaving amplitude increases as the ship's speed is increased, when the wave length is kept constant and the period of encounter is kept larger than the ship's natural period. It approaches to a constant value as the wave length (say the period of encounter) increases when the ship's speed is kept constant. For instance, in a full load condition, the ratio double amplitude of heaving to the wave height tends to a constant value of 0.5-0.6. The heaving amplitude is small when the wave length is small and therefore the period of encounter is shorter than the ship's natural period.

In Fig. 34, the pitching angle measured on the actual ship (values obtained in the case of head on waves α being less than 20°, and the corresponding wave length of the oblique waves were computed by the following formula, $\lambda_s=\lambda_{\text{observed}}/\cos\alpha$), as well as the model experiment results are shown by way of comparison. The natural period of pitching for the actual ship was about 7 sec. which lies between 6.8 sec. and 7.3 sec., chosen as the natural periods for the model.

The pitching angle of the actual ship was very small compared to the model data when the wave length was large, and was large compared to the model data when the wave length was as short as 100 m. This difference is thought to be caused by the irregularity of the actual ocean waves, and is considered to be an important problem.

III. Surging Motion

1. Method of experiments and apparatus used

Surging was measured on the occasion of the resistance and self-propulsion tests on a 4 m model as stated before, as well as on a 2.5 m model at the experimental tank of the Tokyo University. As to the latter, several analytical tests containing measurements on surging and resistance of the model in waves when it was at rest, were carried out by the gravity dynamometer method.

2. Results of experiments and discussions thereon

(1) Difference between surging motion in resistance tests and that in self-propulsion tests

The results of the measurement on the 4 m model are shown in Fig. 35, (as to half swing amplitude of the surging S, see Fig.33). Though there is some difference between the resistance test and self-propulsion test in regard to the propelling force or towing force applied to the model, no clear difference in surging motion was detected in those two kinds of experiments.

(2) Relation between surging and period of encounter

As there is no natural period in the surging motion, no synchronous oscillation such as in rolling will occur, the amplitude of the surging simply increasing or decreasing when the period of encounter increases or decreases.

When the model speed approaches to the wave velocity in the following waves, the surging amplitude will increase to a considerable amount, even larger than the amplitude of the orbital motion of the waves. These relations on a 2.5 m model are shown in Fig. 36, in which a fair curve shows a theoretical value, assuming the surging force to be constant and independent of the period of encounter.

viz. theoretical surging amplitude $a=a_0\left(\frac{\lambda}{V_w+V_s}\right)^2\Big/T_w^2$

where, λ: wave length
V_w: wave velocity
V_s: model velocity
T_w: period of the wave
a_0: surging amplitude when $V_s=0$

In spite of the said assumption, this theoretical value is found to coincide fairly with the experiment data.

(3) Effect of wave height

The variation of the surging amplitude of the model at rest when the wave length is kept constant, and the wave height varied, are shown in Fig. 37, in which it will be noticed that the amplitude varies

almost proportionally to the wave height, the average resistance varying almost proportionally to the square of the wave height, the latter conforming to Prof. Havelock's theory.

(4) Effect of wave length

When the wave length is changed by keeping the ratio wave height to wave length constant, the surging amplitude varies in the mode shown in Fig. 38, from which it will be seen that when the ratio wave length to model length exceeds the unity, the surging amplitude rapidly grows large. This phenomenon can easily be explained by assuming the surging force to be an integrated value of the horizontal component of the buoyancy, which is proportional to the wave slope, and is acting on the ship in every position. A fair curve in Fig. 38 shows a theoretical surging amplitude computed on a ship having a prismatic curve represented by $\eta=1-\xi^4$, and can be assumed to be in good agreement with the experiment data.

(5) Phase of surging motion

The phase of the surging motion varies with the ratio wave length to the model length. The direction of the surging motion at the instant a wave crest passes the midship, is shown in Fig. 39, from which it will be seen that in wave having a wave length comparable to the model length, the relative velocity of the model against the water due to surging will be reinforced by the velocity of the orbital motion of the wave at the stern, which means that in such waves the propeller slip will fluctuate in a large amplitude. From this feature, the surging motion is regarded to be one of the causes for speed loss of ships in waves.

Some examples of the fluctuation of the stream speed at the model's stern were computed and are shown in Table 6, the values given in which are computed on very steep waves; hence it will be too severe to apply these values to an actual ship without any reduction. However, it can be said that at a low speed, the propulsive efficiency will be adversely affected by a large fluctuation in the propeller slip as stated above. In fact, according to the actual ship ex-

periment results, great fluctuations in measured torque are recorded, one of the causes of which the said feature can be considered.

Table 6. Examples of Speed Fluctuation due to Surging Motion
2.5 m Model $\lambda = 3.0$ m $h/\lambda = 1/20$

Ship's Speed, kn	Model Speed, m/sec.	Surging, cm	Surging Speed, m/sec.	Speed of Orbital Motion of Waves m/sec.	Combined Speed / Model Speed
8	0.575	1.0	0.056	0.163	0.380
13	0.934	0.6	0.040	〃	0.217
13 (following seas)	〃	3.8	〃	〃	〃

Chapter 5

Resistance Test

1. Description of models

A paraffine model ship and a wooden model ship of Japanese cypress painted by white lacquer paint were used for the tests in the tank of Transportation Technical Research Institute, and another wooden model of Japanese cypress painted by white lacquer paint was used in the tank of the Tokyo University. Their length between perpendiculars were 6.0, 4.0 and 2.5 m respectively. The forecastle, foreward upper deck and bridge front for the wooden models were made similarly to those of the actual ship from the necessity to perform the tests in waves. All the models were fitted with appendages as rudder, bilge keels and etc. and with a trip wire of 0.9 mm dia. for turbulence stimulation, which was fixed slopwise on No. $9\frac{1}{2}$ station at L.W.L. and on No. 9 station at the bottom. Moreover, in the tests in waves, KG, GM and GM_L of the models were corresponded to the values shown in Table 1 (see Chapter 4 concerning the natural periods of pitching and heaving).

2. Method of experiments and apparatus used

Resistance was measured in both still and rough waters for the

4.0 and 2.5 m models. A gravity dynamometer*[6] shown in Figs. 40 and 41, which was made by adding some improvements to the gravity dynamometer proposed at the Sixth International Conference, was used as a resistance dynamometer. B in this figure is a compound pulley consisted of concentric big and small pulleys. Errors due to vertical accelerations of weight W_1 resulted from surging of the model ship may be made very small by the presence of this pulley. Radius ratio of the pulley B was taken as 2.5 for the 4 m model and 5.0 for the 2.5 m model. Guides for the 4 m model were of a roller type and those for the 2.5 m model were consisted of ball bearings and plates fixed to the towing carriage. Moreover, for the 4 m model, resistance in still water was measured by both the gravity dynamometer above mentioned and ordinary balance type of dynamometer, and the results were compared with. Resistance of the 6 m model was measured only in still water by the balance type of dynamometer.

In the resistance tests in wave, pitching, heaving and surging of the model and wave profiles were measured by the oscillation recorder and wave profile recorder described in the Chapter 4.

3. Results of Experiments and Discussions thereon

(1) Resistance tests in still water

Resistance values for the 4 and 6 m models in still water are shown in Fig. 42. For the 4 m model, resistance values measured by both dynamometers well coincided with each other. Wave making resistance of the 4 m model has a little greater value than that of the 6 m model, and it is considered to be resulted from the difference between the model surfaces and etc.

Notations in the figures are as follows;

Relative wavemaking resistance $r_w = R_w/\rho\nabla^{\frac{2}{3}}V^2$

Relative frictional resistance $r_f = R_f/\rho\nabla^{\frac{2}{3}}V^2$

Froude number $F = V/\sqrt{Lg}$

*6. Seizo Motora, "On Resistance Test in Rough Waters measured by Gravity Dynamometer and Surging of a Ship", Journal of the Society of Naval Architects of Japan, Vol. 94, 1954.

where, R: total resistance (kg)

R_w: wavemaking resistance $=R-R_f$ (kg)

R_f: frictional resistance, calculated from the Froude's formula (kg)

ρ: density of water (kg. sec^2/m^4)

∇: displacement (m^3)

V: advance speed (m/sec.)

L: length on L.W.L. (m)

g: acceleration of gravity (m/sec^2)

Suffix m and s are added for the model and ship respectively.

(2) Resistance tests on the 4 m model in waves

Resistance tests were performed under the conditions against various kinds of waves shown in Table 7. Natural pitching period of the model in this test was 1.30 sec. for the full load condition (Cond. IV) and 1.20 sec for the light condition (Cond. I), corresponding to about 7.3 and 6.8 sec. of the actual ship respectively. At the full load condition, in order to realize a more approximate condition to the test condition of the actual ship, the model with natural period of 1.20 sec. (corresponds to 6.8 sec. of the actual ship) was tested for two kinds of waves with $\lambda=4.0$ m, $h=0.06$ m and $\lambda=5.0$ m, $h=0.06$ m.

Table 7. Length and Height of Waves in Resistance Tests on the 4 m Model

Load Condition	Light							Full Load							
Wave Length, λ in m	2 (64)	3 (96)		4 (128)		5 (160)		3 (96)		4 (128)		5 (160)		6 (192)	
λ/L	0.50	0.75		1.00		1.25		0.75		1.00		1.25		1.50	
Wave Height, h in m	0.10 (3.2)	0.06 (1.92)	0.10 (3.2)	0.06	0.10	0.10 (3.2)	0.15 (4.8)	0.06 (1.92)	0.10 (3.2)	0.06	0.10	0.06	0.10	0.06	0.10
h/λ	1/20	1/50	1/30	1/67	1/40	1/50	1/33	1/50	1/30	1/67	1/40	1/83	1/50	1/100	1/60

Remarks: Figures in brackets show the corresponding values for actual ship.

The results of the tests are shown in Fig. 43 (light condition) and Fig. 44 (full load condition). Values of total resistance of the model are shown to a base of model speeds with values of pitching and heav-

ing. In Fig. 45 (light condition) and Fig. 46 (full load condition with a natural period of 1.30 sec.), values of resistance are shown to a base of wave length. In the neighbourhood, where the period of encounter coincides with the natural pitching period, resistance is increased remarkably by their resonance, and decreased greatly with departure from the point of resonance. However, it can not be cleared by this test only, which of pitching and heaving has a important effect upon such increase of resistance, as the natural pitching period equals nearly to the natural heaving period.

EHP for the actual ship, calculated from the results of the resistance tests, is shown in Figs. 47 and 48. In calculations of frictional resistance, Froude's constants were used for both model and ship and values at rest taken as wetted area. EHP for still water calculated from the results of resistance tests in still water and rate of increase of EHP due to waves are shown in these figures.

From the results above mentioned, it will be cleared that resonance of pitching (or heaving) is a most important cause for increase of resistance, and that a slight difference of natural pitching period has a great effect upon increase of resistance, if it were a same system of wave. Therefore, for resistance tests, it is essential for natural pitching period to make exact correspondence to the value of the actual ship. In spite of such a remarkable change of resistance with the natural period, pitching and heaving do not show such a clear difference, as mentioned in the Chapter 4. Therefore, even if states of pitching and heaving were almost same at first sight, resistance and therefore speed may show a considerable quantity of difference.

(3) Resistance tests on the 2.5 m model in waves

Resistance tests for the full load condition on the 2.5 m mode were performed with and against waves show in Table 8. Natural pitching period of the model in this

Table 8. Length and Height of Waves in Resistance Tests on the 2.5 m Model

Wave Lenght, λ in m	2	3
λ/L	0.8	1.2
Wave Height, h in m	0.091	0.091
h/λ	1/22	1/33

test was 0.94 sec., which corresponds to 6.73 sec. of the actual ship.

The results of the tests are shown in Fig. 49. Tendency of the results is in near coincidence with that of the results for the 4 m model. Pitching or heaving does not synchronize in the case of following waves, and resistance curve has not such a hump as in the case of head-on waves.

(4) Comparison with the actual ship data

As mentioned in the former chapter, ocean waves encountered by the actual ship are not so regular as artificial waves in the experiment tank, and if mean length and height of wave were corresponded to those in ocean, there would be a considerable quantity of difference in

Table 9. Some Examples of Comparison between EHP obtained from Model Experiments and SHP obtained from Actual Ship Experiments

	Load Condition		Light			Full Load	
Actual Ship Exp.	Experiment No.		6	7	8	55	87
	Sea Condition		Slight	Slight	Slight	R. Rough	Moderate
	Wave Length in m		40	150	40	54	100
	Wave Height in m		2	1.5	1.5	2	2
	Pitching Period in sec.		8.2	7.5	7.8	6.9	7.8
	Speed of Ship in kn		12.74	12.51	13.54	11.55	11.57
	Speed of Rev. of Propeller in rpm.		90.6	90.1	94.7	92.5	96.8
	Shaft Horse Power	SHP	2437	2453	2656	3211	4026
	Delivered Horse Power	DHP*1	2389	2405	2604	3148	3946
Model Exp.	E.H.P. in Still Water	EHP_0	1443	1363	1720	1395	1401
	Natural Pitching Period of Model in sec	*2	1.3(7.3)	1.3(7.3)	1.3(7.3)	1.2(6.8)	1.2(6.8)
	E.H.P. in Waves/E.H.P. in Still Water	*3	1.274	1.284	1.176	1.118	1.506
	E.H.P. in Waves	EHP′	1838	1750	2022	1560	2110
	Air Resistance in ton		1.143	1.202	− .020	7.300	3.755
	E.H.P. due to Air Resistance	EHP_{wind}	100	103	− 2	580	300
	E.H.P. in Waves & Wind	EHP*	1938	1853	2020	2140	2410
	EHP/DHP		.811	.771	.776	.680	.611
	EHP_0/DHP_0	*5	.812	.815	.804	.780	.780

*1. Assumed, DHP = SHP/1.02
*2. Figs. in brackets show the corresponding values for ship
*3. Estimated from Figs. 47 & 48
*4. EHP = EHP′ + EHPwind.
*5. DHP_0 = Delivered horse power obtained by self-propulsion test in still water

pitching and heaving, and therefore in rate of augument of resistance between the model and ship.

Only shaft horse power was measured in the actual ship experiments of the "Nissei Maru". Therefore, it is difficult to estimate EHP of the actual ship exactly, until ample data concerning propulsive efficiency in waves will be obtained. The results from rough calculations, however, show that augument of resistance of the model due to waves seems to be greater than that of the actual ship, and that the results of the model seems to be in well coincidence with those of the ship in the case where wave height is below 2 m. Some examples are shown in Table 9. Values of EHP/DHP obtained here will be not so irrational. It will be considered that the ocean wave approaches to a regular trochoidal wave in the case of small wave height, and that the greater the wave height irregularity is likely to become remarkable.

Chapter 6

Propeller Open Water Test

In order to obtain propeller characteristics used in analysis of propulsive performances of the "Nissei Maru", open water tests on a bronz model propeller of 500 mm dia. (scale ratio is 1/10.5) were performed in the tank of Mitsubishi Shipbuilding & Engineering Co., Ltd. The model propeller was tested by a method of constant revolution, and the results were corrected for idle force of the boss. Characteristic curves of the propeller obtained are shown in Fig. 50. These tests were carried out, varying immersions and revolutions of the propeller, and the results of them agree very well each other.

Moreover, open water tests in waves will be performed in near future successively.

Chapter 7

Self-Propulsion Test

1. Description of Models

Model ships used in self-propulsion tests are the same models that used in resistance tests (see the Chapter 5). Three model propellers were made with diameters of 24.61, 16.41 and 10.25 cm for the 6, 4 and 2.5 m model ships respectively. Composition of the propeller metal is 70% *Sn*, 15% *Pb*, 10% *Bi* and 5% *Sb*.

2. Method of experiments and apparatus used

(1) Self-propulsion tests on the 6 m model in still water

In order to estimate propulsive performances in still water exactly as a base of investigations for propulsive performances in rough waters, self-propulsion tests for the 6 m paraffine model ship in still water were performed in the tank of Transportation Technical Research Institute. Quantities of friction correction were calculated by the Froude's formula. But, self-propulsion tests were carried out with not only Froude value itself but also 1.15 and 1.30 times of Froude value as friction constant of the actual ship. A Gebers' type of propeller dynamometer was used in these tests.

(2) Self-propulsion tests on the 4 m model in still and rough waters

Self-propulsion tests on the 4 m wooden model in still and rough waters were performed in the tank of Transportation Technical Research Institute. In both cases of still and rough waters, quantities of friction correction were calculated, using Froude's friction constants. Self-propulsion tests with additional resistance corresponding to wind resistance will be performed in near future.

Pitching, heaving and surging of the model and wave profiles were also measured in self-propulsion tests as in resistance tests.

In self-propulsion tests in waves a magneto-striction type of propeller dynamometer was used in general. (At earlier stage of the tests

some tests were performed using a wire strain gauge type of dynamometer, but friction of the slip ring picking up torque was found to exert some effects upon measured values of thrust. Even after several times of improvements, satisfactory results could not be obtained. And, torque and thrust should be measured separately by two runs of the same condition.)

A Gebers' propeller dynamometer, besides two kinds of dynamometers above mentioned, was used in self-propulsion tests in still water, and all of their results were found to give nearly same values.

(3) Self-propulsion tests on the 2.5 m model in still and rough waters

Self-propulsion tests on the 2.5 m wooden model in still and rough waters were carried out in the tank of the Tokyo University. A magneto-striction type of dynamometer was used, and friction correction was calculated by the Schoenherr's formula.

3. Results of experiments and discussions thereon

(1) Self-propulsion tests in still water

The results of self-propulsion tests on the 6 m model in still water are shown in Fig. 51, in the non-dimensional form used in the tank of Transportation Technical Research Institute.

Relative total resistance $r'=R/\rho\nabla^{\frac{2}{3}}V^2$

Relative thrust $t'=T/\rho\nabla^{\frac{2}{3}}V^2$

Relative power $p'=2\pi NQ/\rho\nabla^{\frac{2}{3}}V^3$

Relative revolution $n=\nabla^{\frac{1}{3}}N/V$

Froude Number $F=V/\sqrt{Lg}$

where, R: total resistance (kg)

T: thrust of the propeller (kg)

Q: torque of the propeller (kg-m)

N: number of revolutions of the propeller (1/sec.)

V: advance speed of the ship (m/sec.)

∇: displacement of the ship (m^3)

L : length of the ship at L.W.L. (m)

ρ : density of water (kg. sec^2/m^4)

g : acceleration of gravity (m/sec^2)

Suffix m and s were added to the model and ship respectively. Friction constants used in the calculations of friction correction were also utilized in calculating frictional resistance of the actual ship.

As these tests were performed with three kinds of friction corrections, the results with any friction correction can be obtained from the results of these tests. Moreover, it was intended to investigate to what extent the effects of fouling of hull surface and wind resistance can be expressed by such increase of resistance correction, but the analysis has not yet been completed.

Delivered horse power DHP — shaft horse power at the position of the propeller — for the actual ship, number of revolutions of the propeller and etc., calculated from the above results in the case where Froude's value was taken as friction constant of the actual ship, are shown in Fig. 52. SHP (SHP=1.02 DHP, assuming the power loss due to the friction of the stern tube as 2% of DHP) and RPM, shown as the results of the tank tests in the figures and tables of Part I, are based upon this figure.

Moreover, the results of the self-propulsion tests for the 4 m model in still water, as shown in Figs. 53 and 54, agree well with the results for the 6 m model with a small difference. Therefore, the values of the 6 m model were adopted as the results in still water.

(2) Self-propulsion tests in wave

On the 2.5 m model, only a few tests under the full load condition were carried out, and therefore, the results of the tests for the 4 m model will be described in the following.

For the 4 m model, self-propulsion tests were performed under the conditions against various kinds of waves shown in Table 10. Natural pitching period of the model and kind of propeller dynamometer are also shown in this figure.

Table 10. Length and Height of Waves, Natural Pitching Period and etc. in Self-propulsion Tests on the 4 m Model

Load Condition	Light			Full Load					
Wave Length, λ in m	3 (96)	4 (128)	5 (160)	3 (96)	4 (128)		5 (160)	6 (192)	
λ/L	0.75	1.00	1.25	0.75	1.00		1.25	1.50	
Wave Height, h in m	0.06 (1.92)			0.06 (1.92)					0.10 (3.2)
h/λ	1/50	1/67	1/83	1/50	1/67		1/83	1/100	1/60
Natural Pitching Period in sec.	1.20 (6.8)			1.20 (6.8)		1.30 (7.4)	1.20 (6.8)		1.30 (7.4)
Propeller Dynamometer used*	M-S			M-S	M-S W.S.G.	M-S	M-S W.S.G.		M-S

Remarks: 1) Figures in brackets shows the corresponding values for actual ship.
2) * M-S: Magneto-striction type
W.S.G.: Wire Strain Gauge type

Measured values in the above tests are shown in Figs. 53 and 54. Pitching, heaving and etc., measured at the same time, are shown in Figs. 43 and 44 with the values measured in the resistance tests in waves.

DHP and RPM for the actual ship, calculated from the above results, are shown in Figs. 55 and 56. The ratio DHP in waves to DHP in still water are also shown in these figurs. According to the results of preliminary analysis by using the characteristic curves of the propeller in still water, as naturally expected, the lowering of propulsive efficiency in waves is mainly due to the lowering of the propeller efficiency itself resulted from increase of the propeller load. Effects of fluctuations in advance speed of the propeller, due to surging of the ship and orbital motion described in the Chapter 4, and lowering of efficiency by pitching, heaving and etc. do not seem to be so important. The effects of length and height of waves, natural pitching period and etc. upon increase of shaft horse power are considered to be nearly same as in the case of the resistance tests in waves (see the Chapter 5).

Further more, various kinds of tests in waves are now being carried

out successively for this model, and as propeller open tests in waves, on the other hand, are about to be performed, detailed analysis will be done after their completion.

(3) Comparison with the actual ship data

a. Sea-going qualities in still water

SHP and RPM calculated from the results of the self-propulsion tests for the 6 m model in still water, as shown in Figs. 3, 35 and 36 of Part I, may be recognized to agree nearly with the results of the actual ship experiments in the case near the ideal condition—no wind, no wave, clean bottom and no effect of shallow water and etc. Therefore, the usual method of self-propulsion tests, in which friction correction is calculated by using Froude's friction constants, is considered to give a nearly valid result for medium speed and size of cargo boats with welded shell plates of same proportions as this ship.

b. Sea-going qualities in waves

Self-propulsion tests in waves, with additional resistance correction corresponding to wind resistance, has not been completed. However, according to the comparison of the results, estimated roughly from the data above described, with the results obtained by the actual ship experiments, a remarkable effect of irregularity of actual waves can be recognized, as described concerning oscillation and resistance. That is, SHP and RPM of the actual ship are rather lower than those of the corresponding results of the model in the case for large length and height of waves. However, in the case for small height of waves, the results of tank tests seem to be near the results of the actual ship. Therefore, in investigations on sea-going qualities in waves it will be very important to grasp noumenon of irregularity of ocean waves and to investigate its effect.

Acknowledgement

At the conclusion of this report, a word of thanks is due to all those who have lent their assistance during the carrying out of the

experiments. It is desired to record an expression of thanks in particular.

Ministry of Transportation, for hastening the realization of this research with a subsidy.

The Shipbuilders' Association of Japan, for bearing the research finance.

Nissan Kisen Kaisha, shipowner, for placing the Nissei-maru at their disposal and affording much convenience.

The Japanese Ship Owners' Association, for selecting a suitable ship for the experiments and bearing the greater parts of passage-money.

Tsurumi Shipyard, Nippon Steel Tube Co. Ltd., for paying dearly for fitting measuring apparatus and making the ship model, and for the direct co-operation into the experiments.

Captain, chief engineer and other crews of the "Nissei-maru", for the co-operation with good intentions.

Transportation Technical Research Institute; Department of Naval Architecture, Faculty of Technology, Tokyo and Osaka University; Technical Department, Mitsubishi Shipbuilding & Engineering Co. Ltd.; Technical Research Laboratory, Hitachi Shipbuilding & Engineering Co. Ltd.; for their direct co-operation.

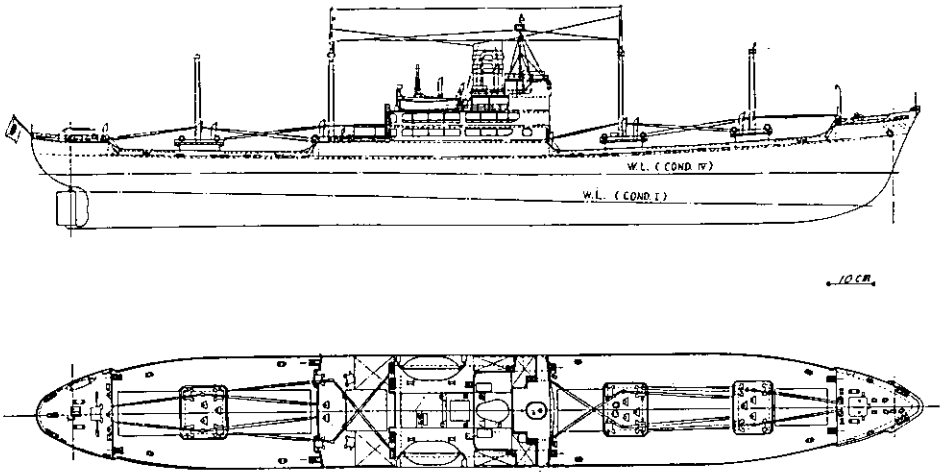

Fig. 1. Model of "Nissei Maru" for Wind Tunnel Experiments

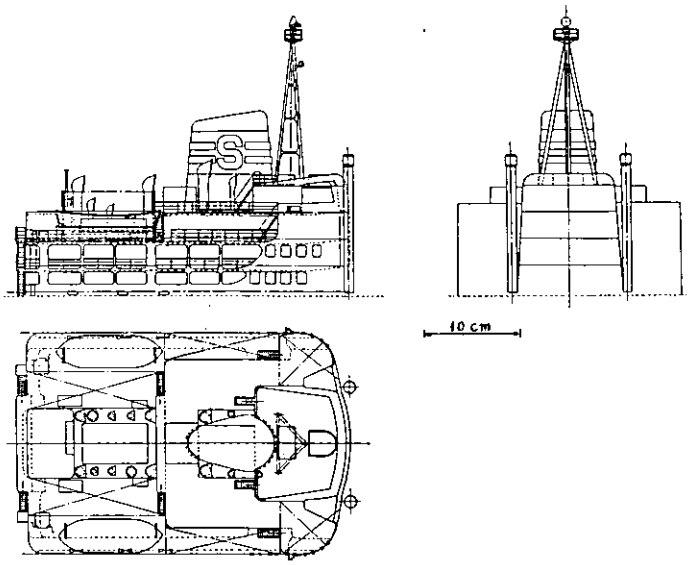

Fig. 6. Model of the Bridge of "Nikko Maru" Type

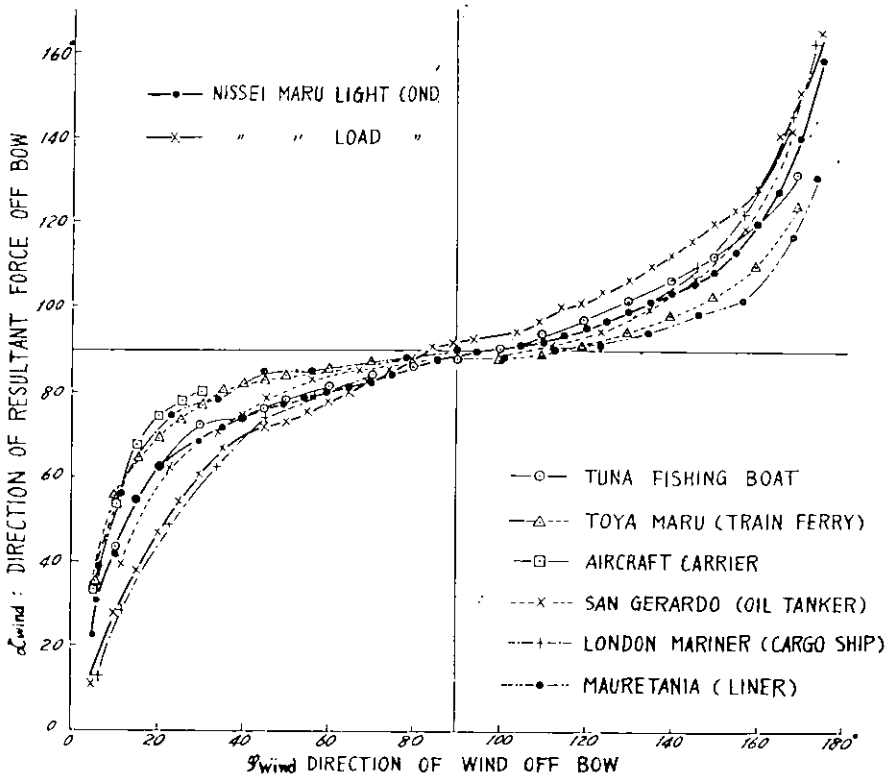

Fig. 8. Direction of Resultant Force

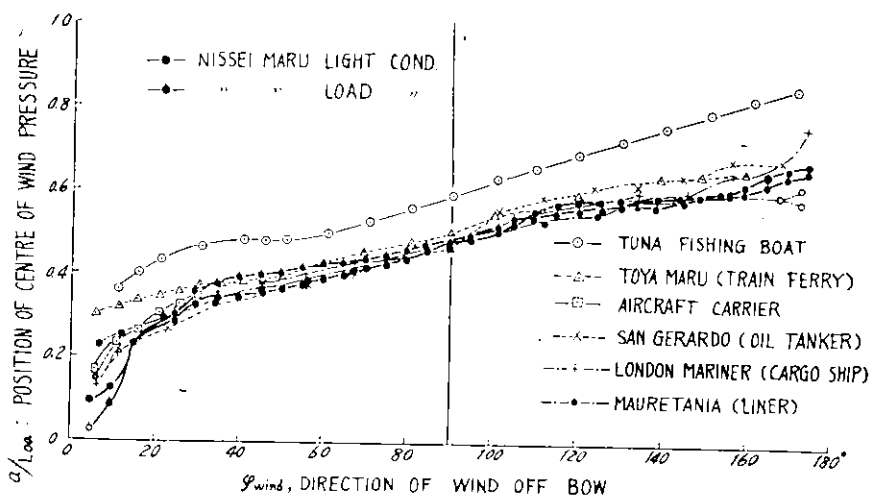

Fig. 9. Centre of Wind Pressure

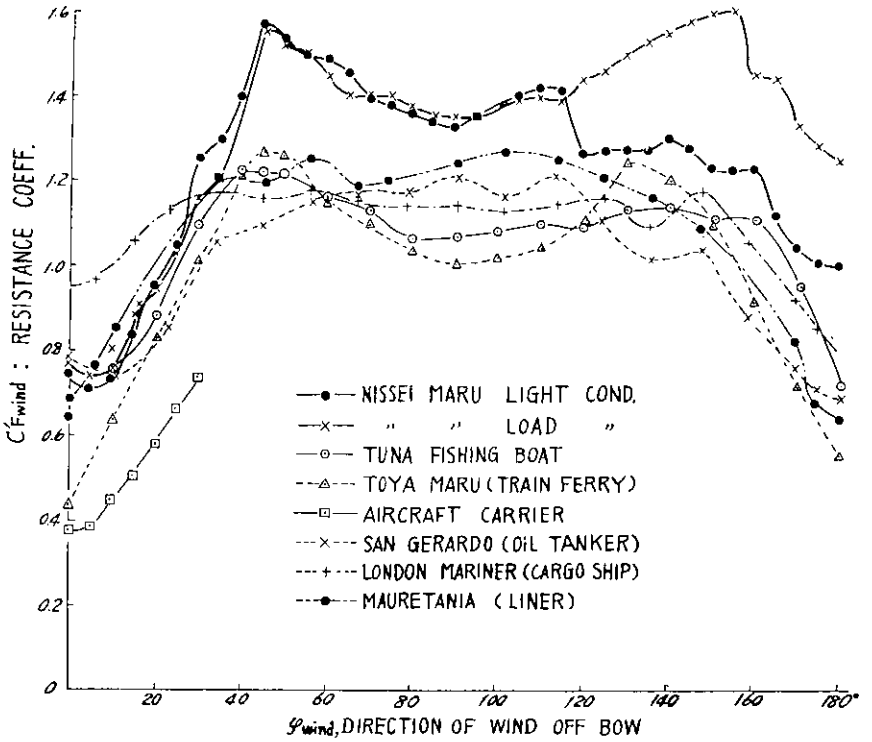

Fig. 10. Wind Resistance Coefficient

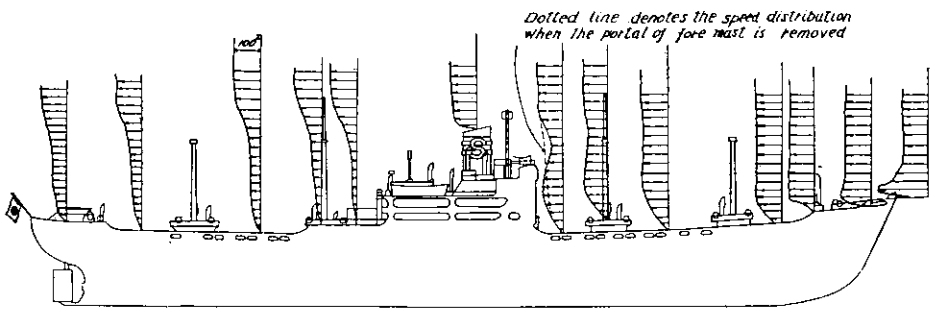

Fig. 16. Wind Speed Distribution on the Centre Line Plane

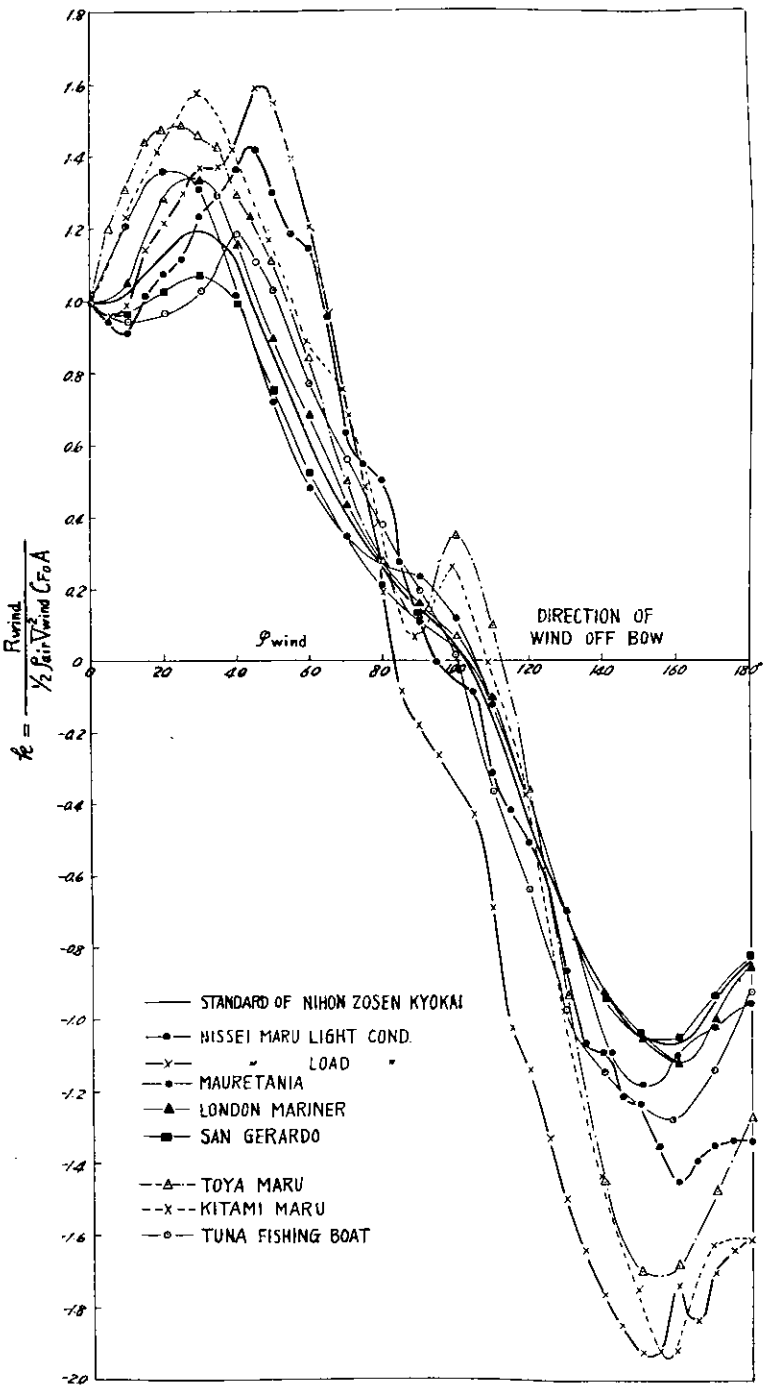

Fig. 11. Wind Direction Effect Coefficient

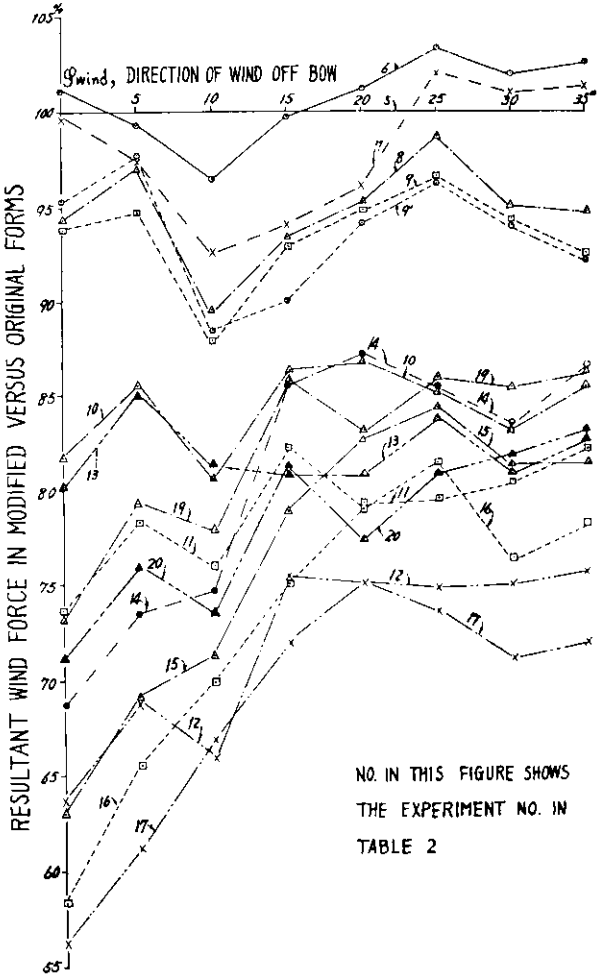

Fig. 13. Effect of Fitting, Bridge, and etc.

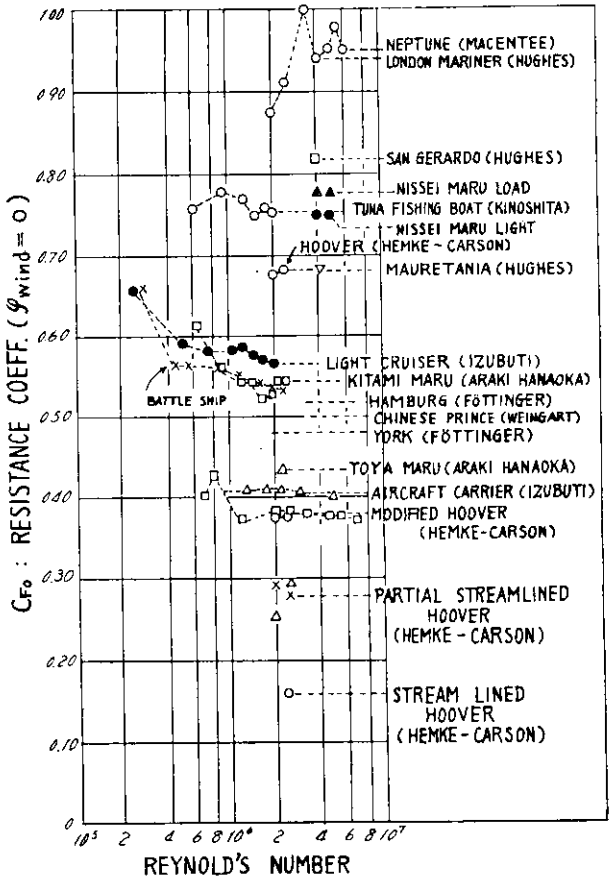

Fig. 12. Wind Resistance Coefficient, $\varphi_{wind}=0°$

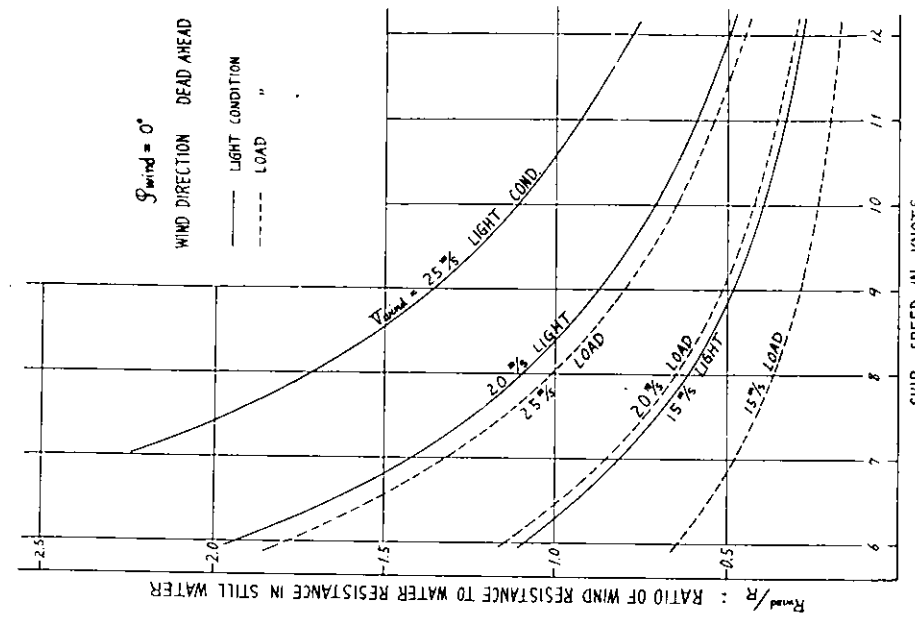

Fig. 14. Ratio of Wind Resistance to Water Resistance, $\varphi_{wind}=0°$

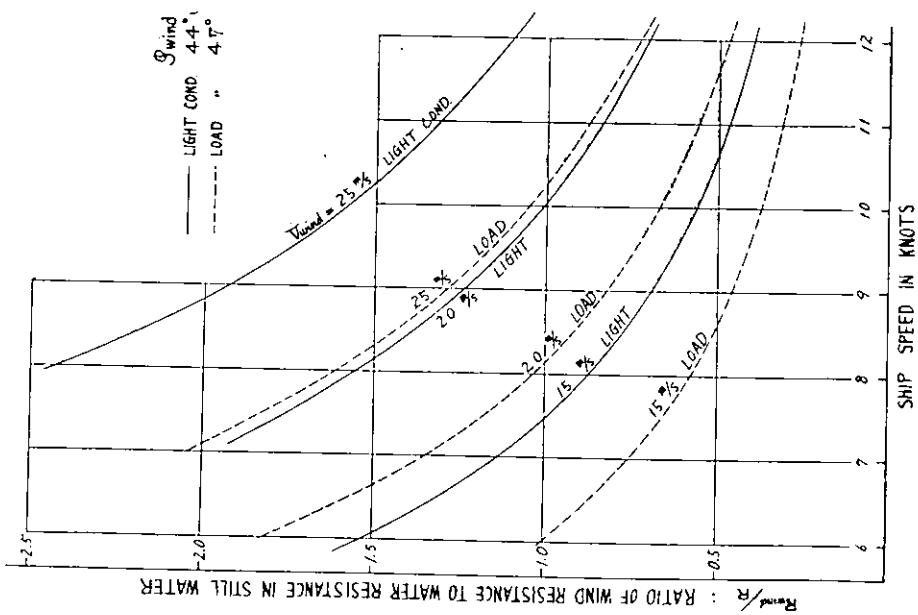

Fig. 15. Ratio of Wind Resistance to Water Resistance, φ_{wind} = angle at which k maximum

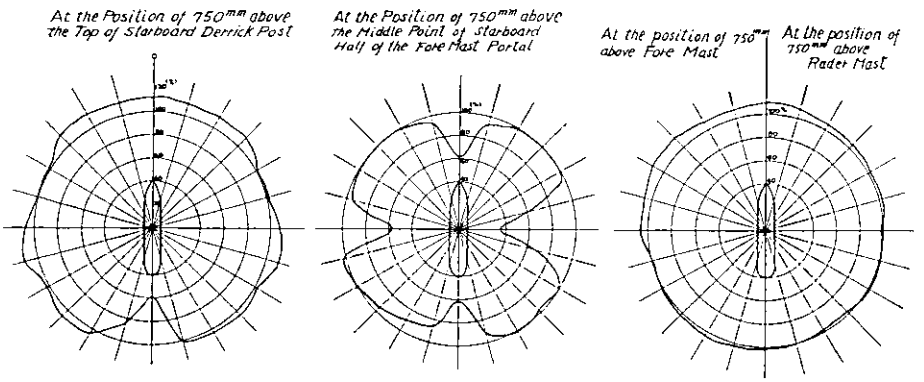

Fig. 17. Ratio of the Relative Wind Speed to the General Wind Speed

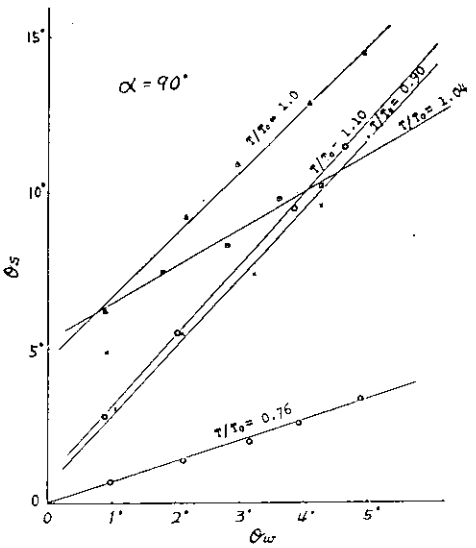

Fig. 19. An Example of Relation between the Wave Slope and the Rolling Angle

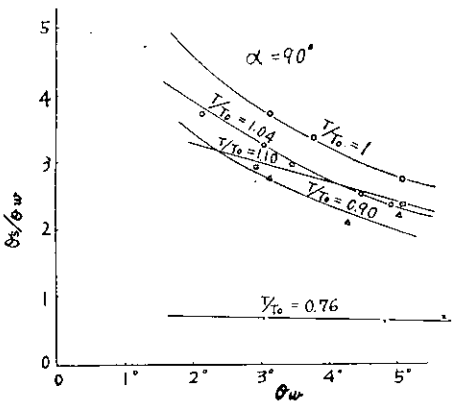

Fig. 20. An Example of Relation between the Wave Slope and the Ratio of the Rolling Angle to the Wave Slope

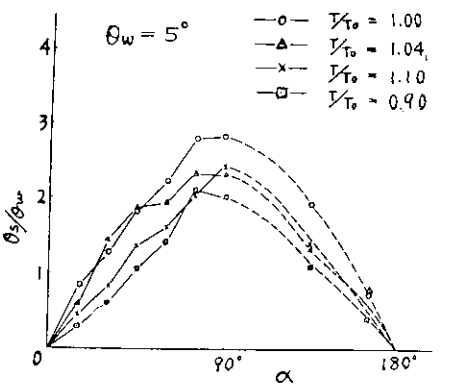

Fig. 21. Relation between the Angle of Encounter and the Ratio of the Rolling Angle to the Wave Slope

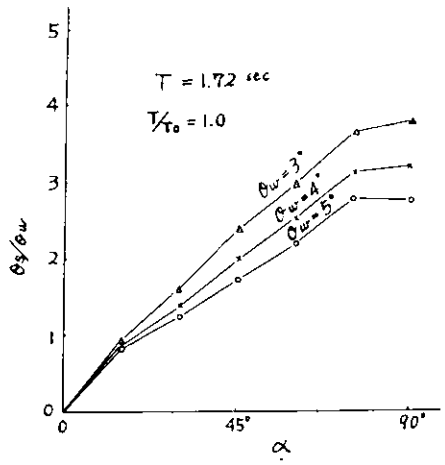

Fig. 22. An Example of Relation between the Angle of Encounter and the Ratio of the Wave Slope

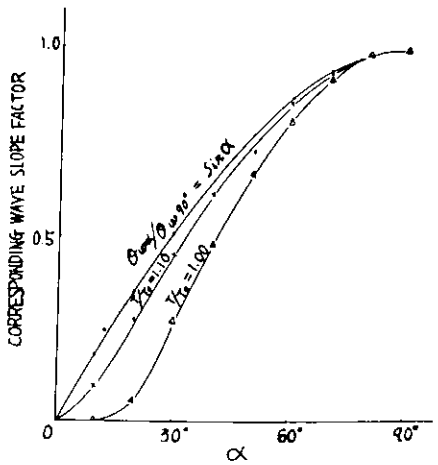

Fig. 23. Corresponding Wave Slope Factor

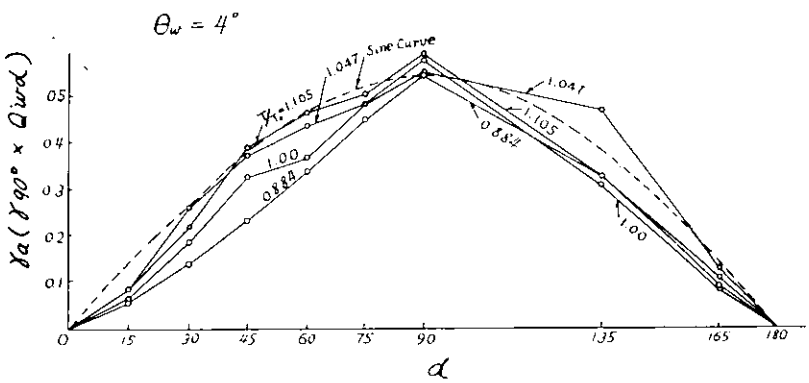

Fig. 25. The Measured Effective Wave Slop Factor

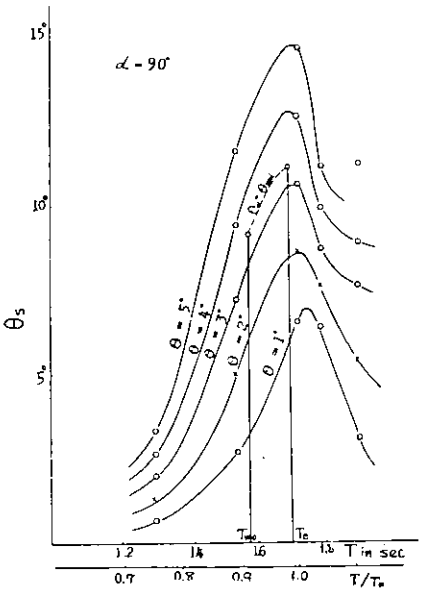

Fig. 27. The Resonance Curve for Rolling in Abeam Seas

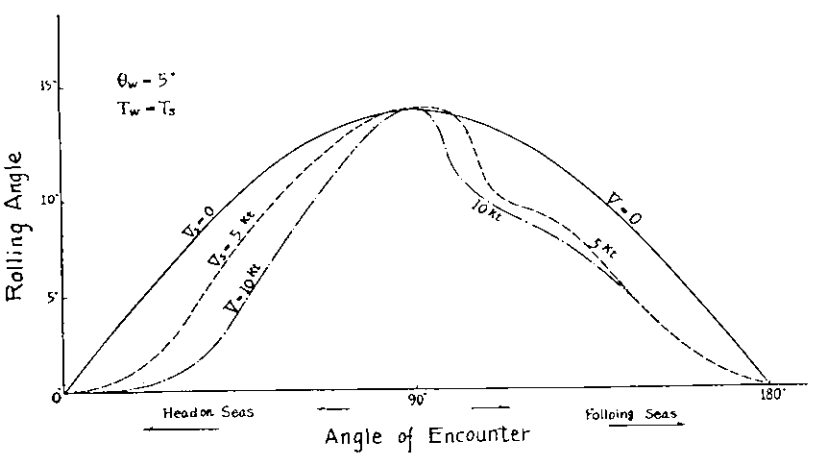

Fig. 28. Effect of the Ship's Speed on the Rolling Angle in Oblique Waves

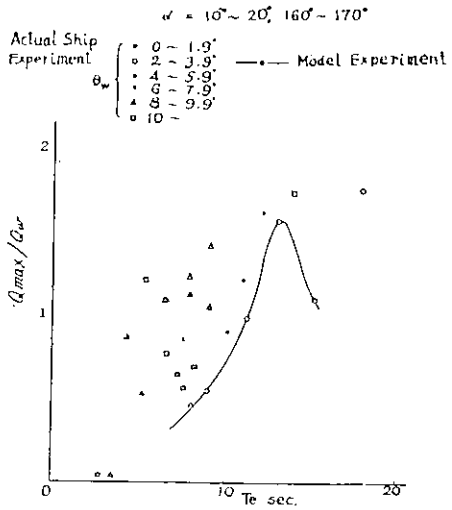

Fig. 30. Effect of the Irregularity of the Waves on the Ship's Rolling Angle

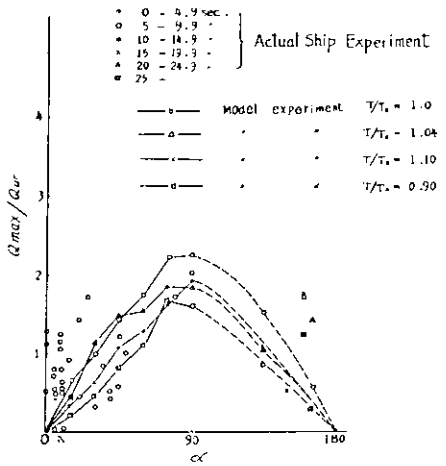

Fig. 31. Effect of the Irregularity of the Waves on the Ship's Rolling Angle

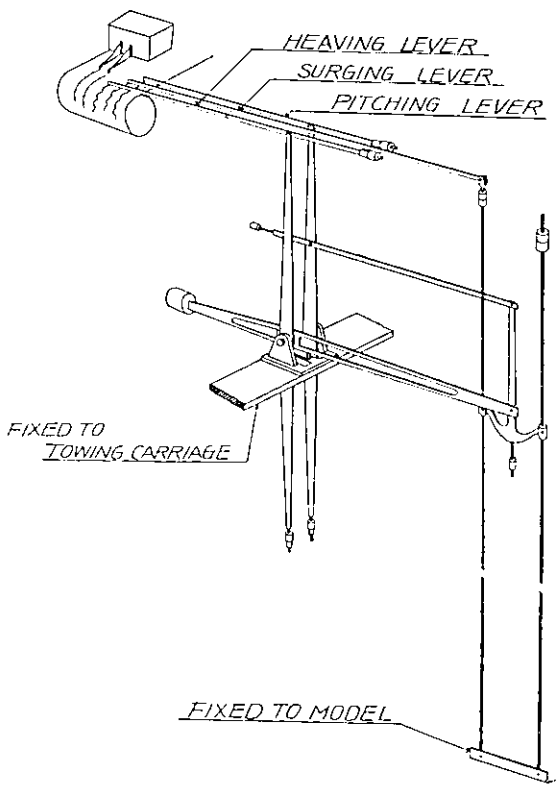

Fig. 32. Oscillation Recorder

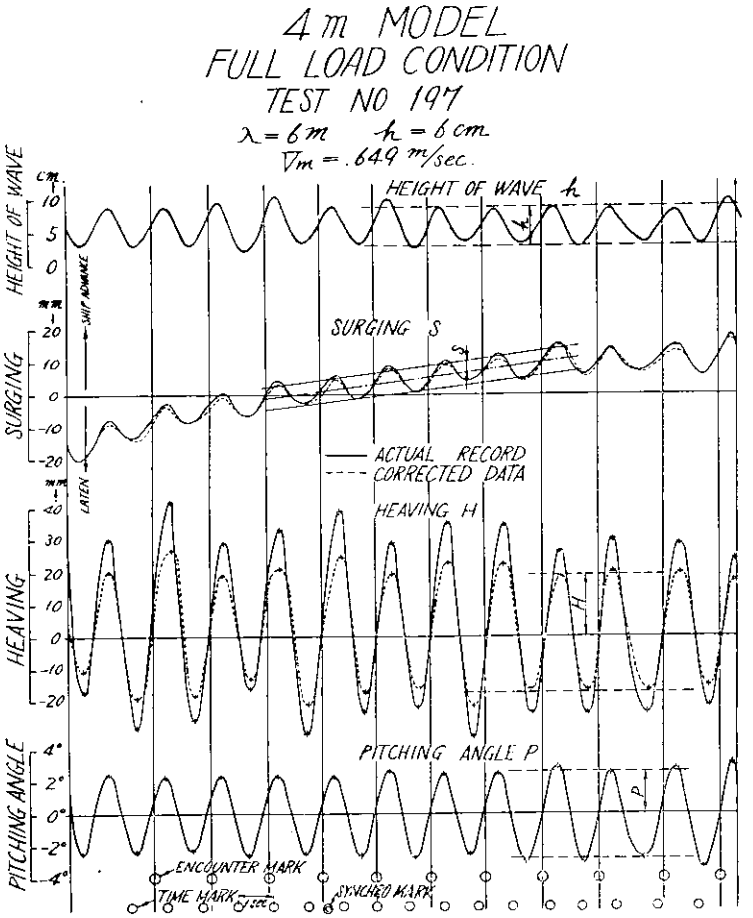

Fig. 33. An Example of Oscillation Record

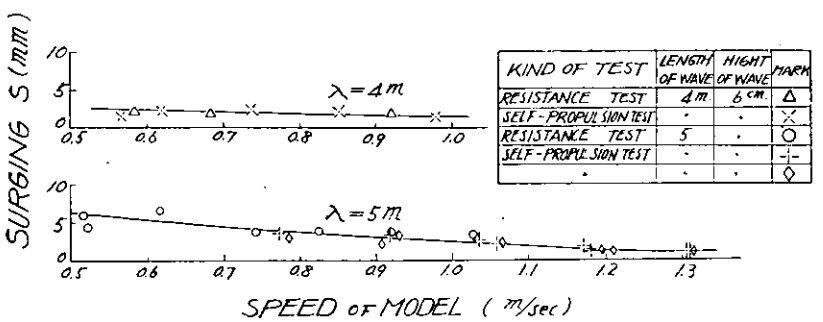

Fig. 35. Amount of Surging, 4 m Model

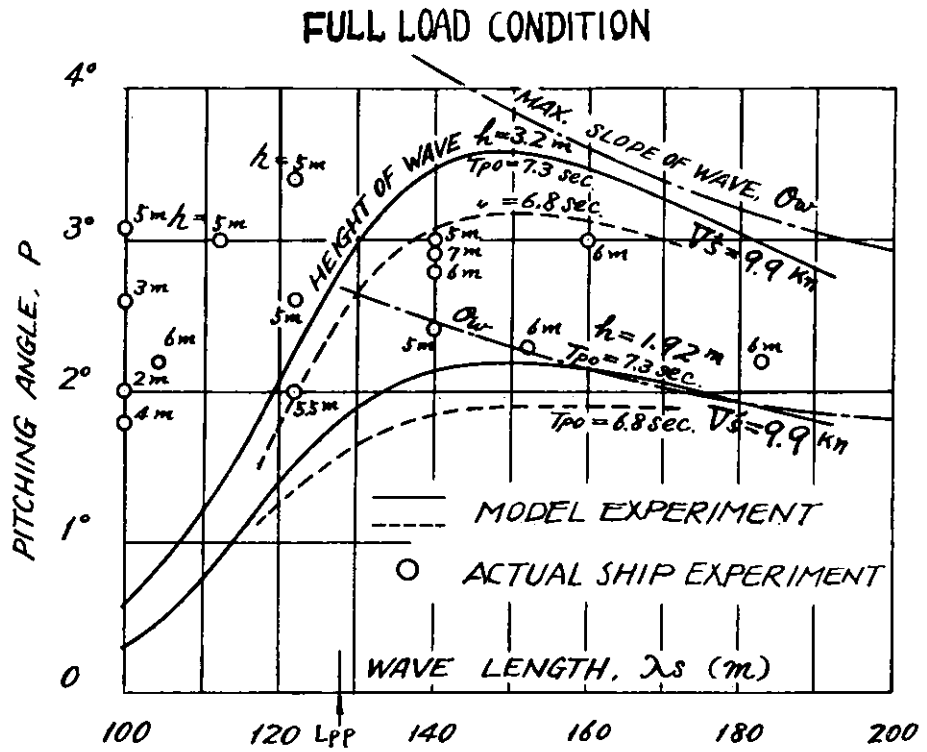

Fig. 34. Pitching Angle of Actual Ship and 4 m Model

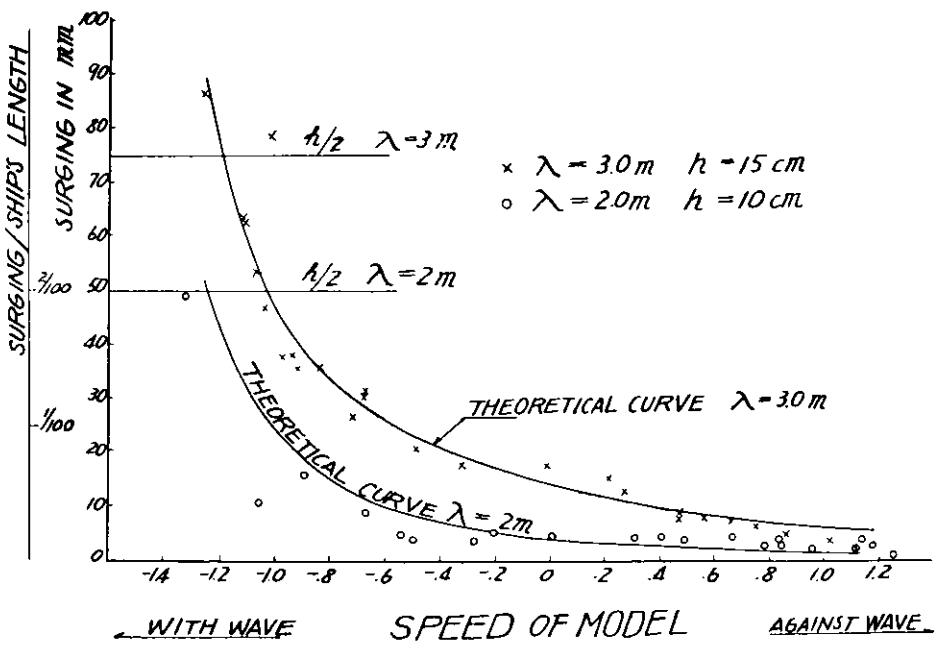

Fig. 36, Amount of Surging, 2.5 m Model

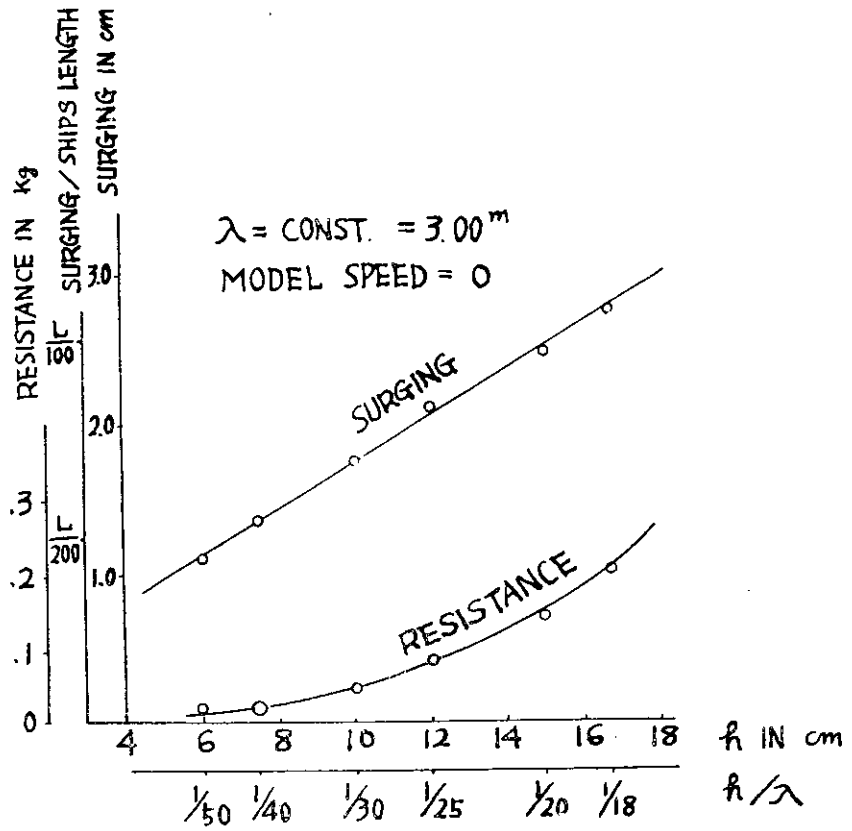

Fig. 37. Effect of the wave Height on the Surging Amplitude, when Ship is at Rest, 2.5 m Model

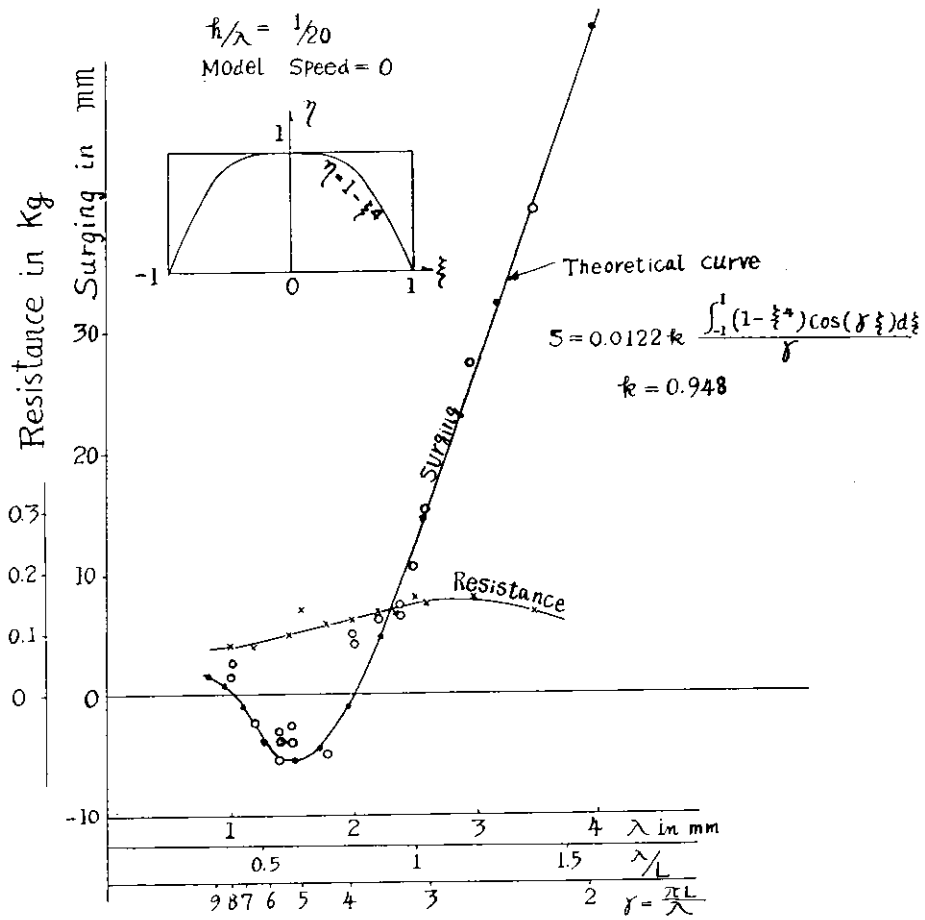

Fig. 38. Effect of the Wave Length on the Surging Amplitude, when Ship is at Rest, 2.5 m Model

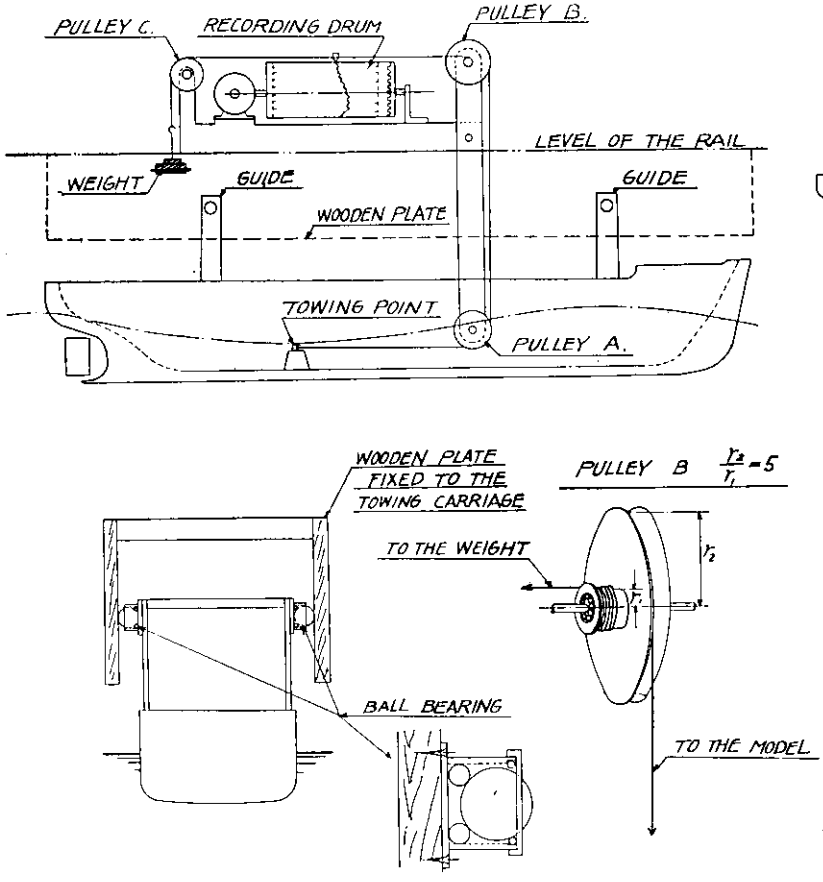

Fig. 40. Gravity Dynamometer used for 2.5 m Model

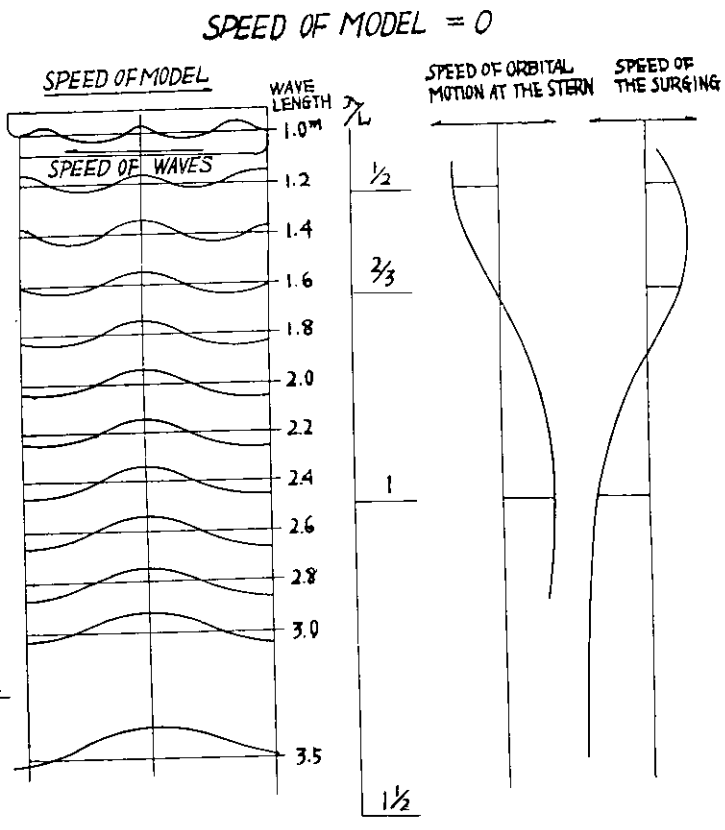

Fig. 39. Relation between Phase of the Surging and the Wave Length, when Ship is at Rest, 2.4 m Model

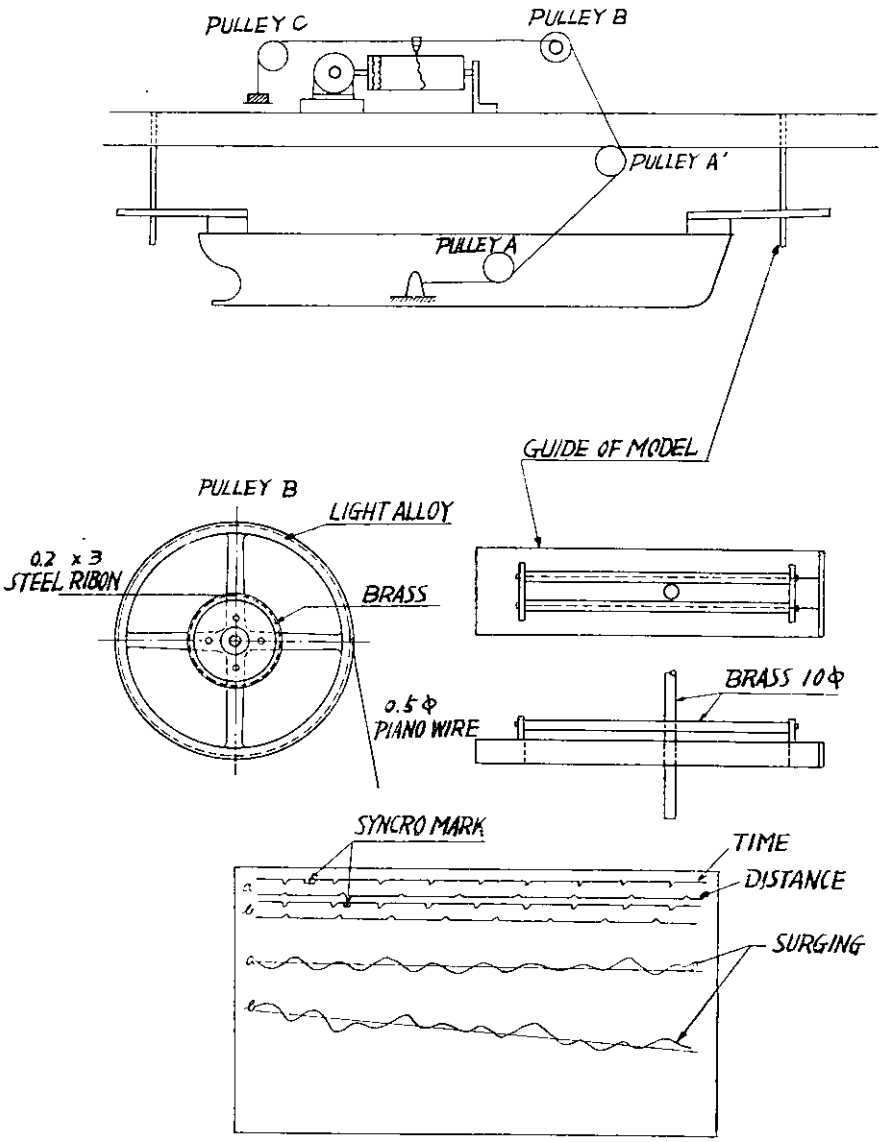

Fig. 41. Gravity Dynamometer used for 4.0 m Model

LENGTH OF MODEL (m)	CONDITION	DRAFT (m) ABOVE BOTTOM OF MODEL A.P.	M.S.	F.P.	DISPLACEMENT (kg)	WETTED SURFACE (m^2)	TEMP. OF WATER (°C)	APPENDAGE	MARK	DYNAMOMETER
4.00	FULL LOAD	.2637	.2509	.2381	400.5	3.394	8.0	BILGE KEEL & RUDDER	○——	GLEBERS TYPE
	LIGHT LOAD	.1852	.1314	.0776	191.8	2.389	〃			
	FULL LOAD	.2637	.2509	.2381	400.5	3.310	〃	BILGE KEEL	○— —	〃 〃
	LIGHT LOAD	.1852	.1314	.0776	191.8	2.307	〃			
6.00	FULL LOAD	.3956	.3764	.3572	1351.6	7.636	17.0	BILGE KEEL & RUDDER	△—·—	〃 〃
	LIGHT LOAD	.2778	.1971	.1164	647.3	5.376	〃			
4.00	FULL LOAD	.2637	.2509	.2381	400.5	3.394	21.0	〃	●———	GRAVITY TYPE
	LIGHT LOAD	.1852	.1314	.0776	191.8	2.389	〃			

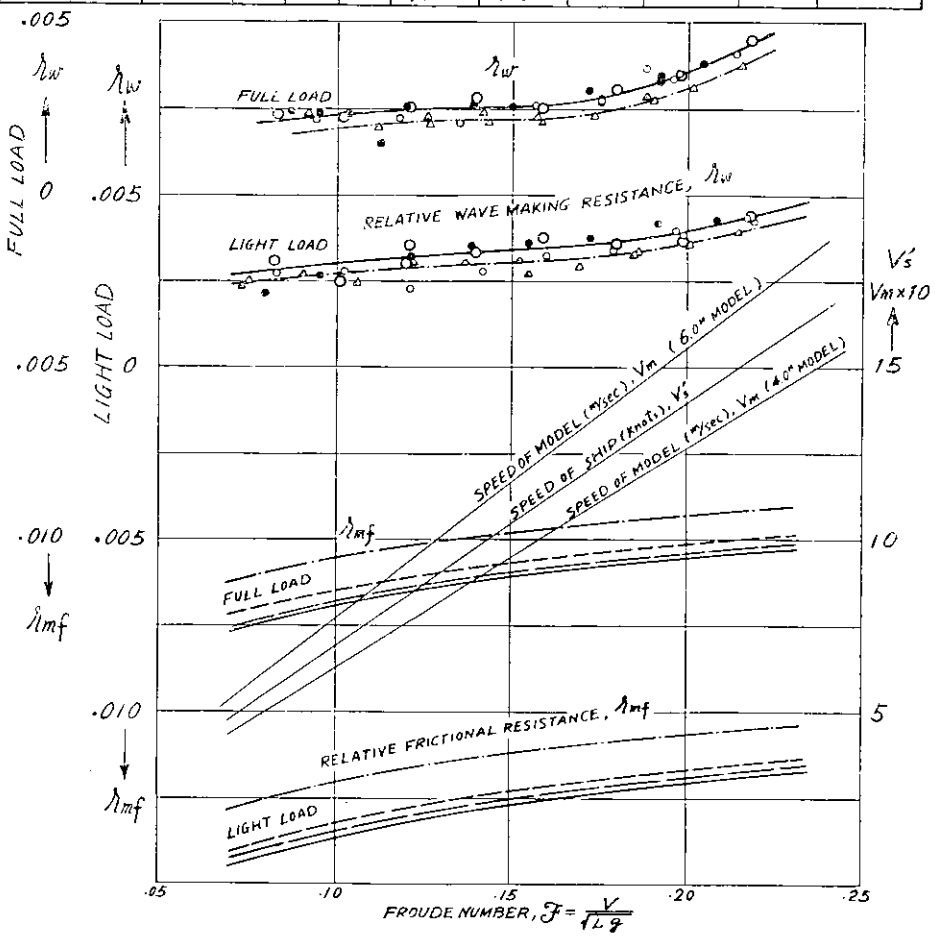

Fig. 42. Results of Resistance Tests in Still Water

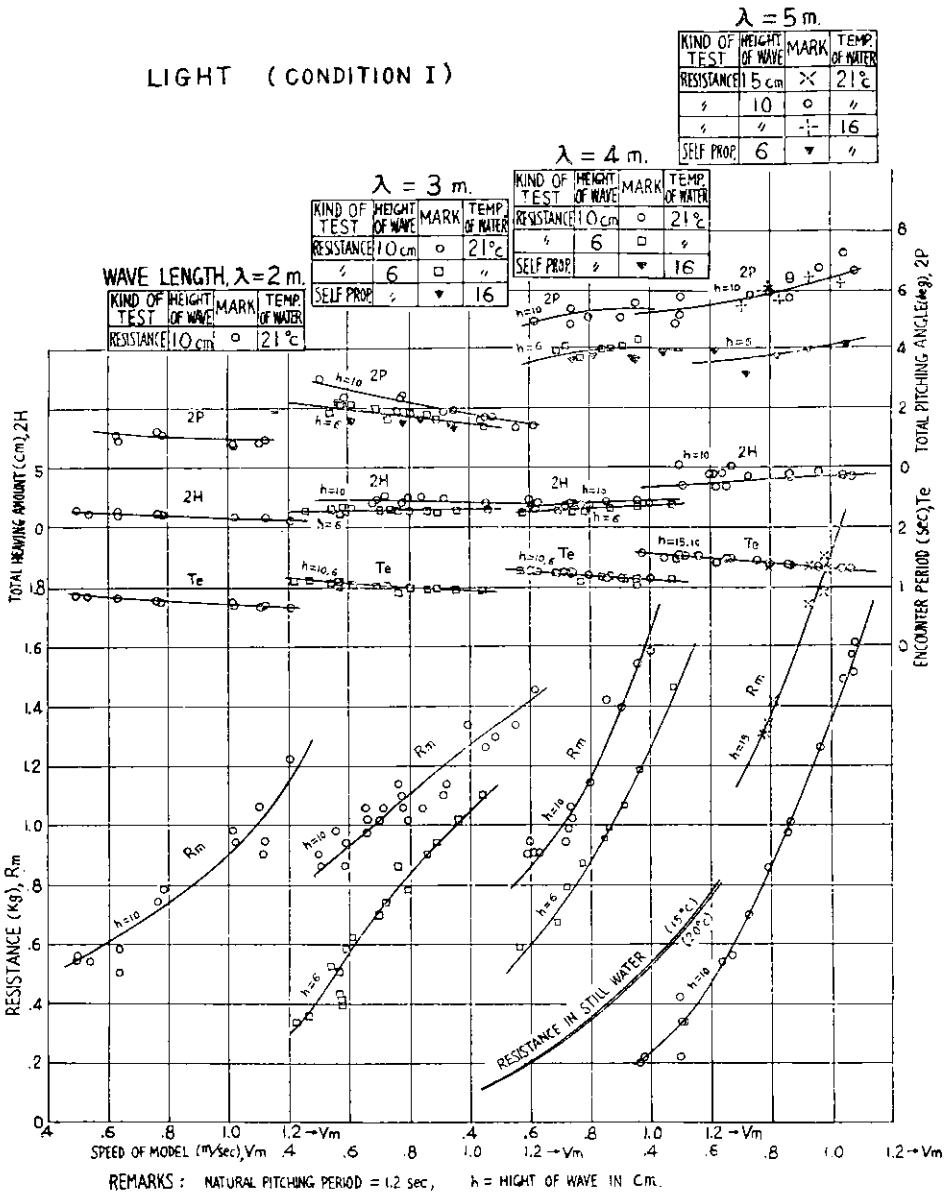

Fig. 43. Results of Resistance Tests in Rough Water, Light Cond., 4 m Model

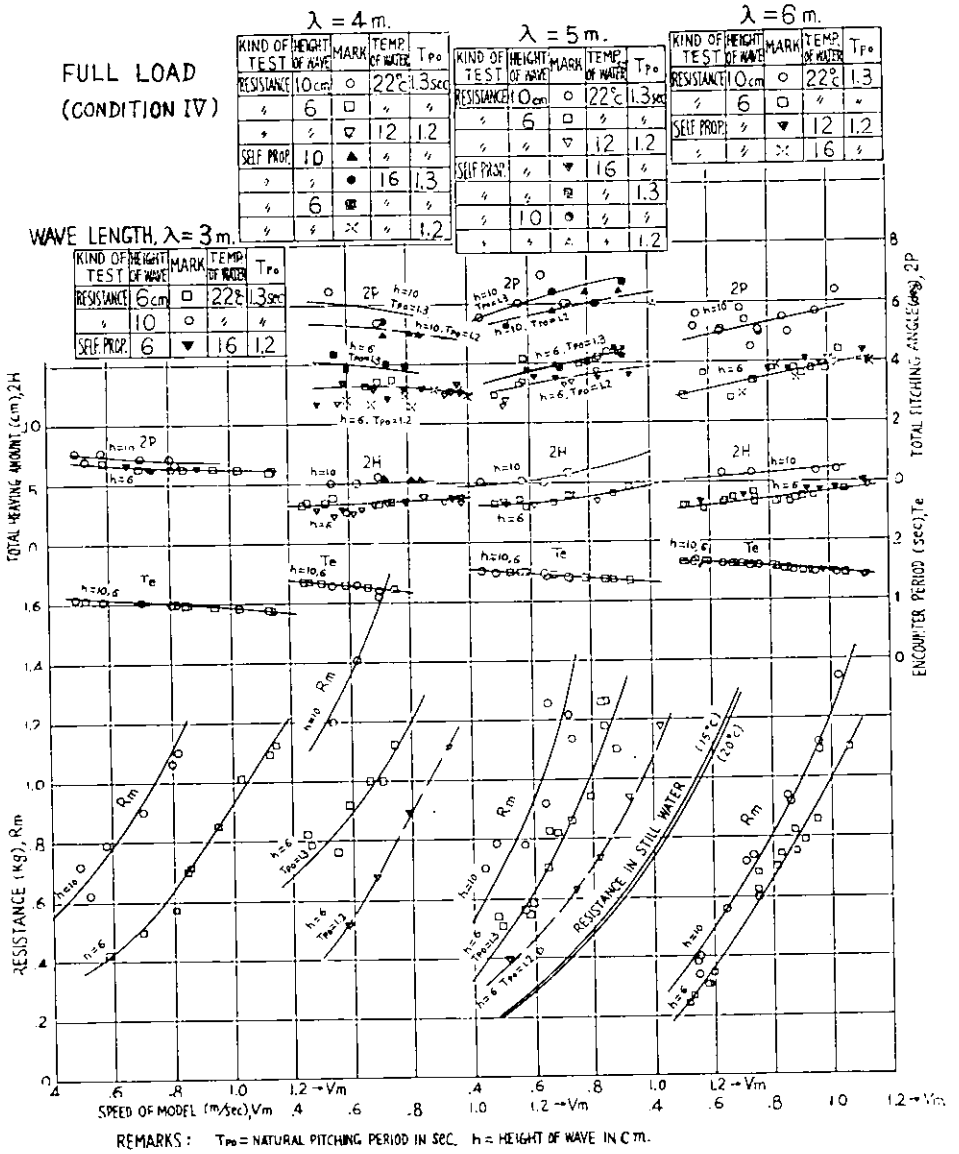

Fig. 44. Results of Resistance Tests in Rough Water, Full Load Cond., 4 m Model

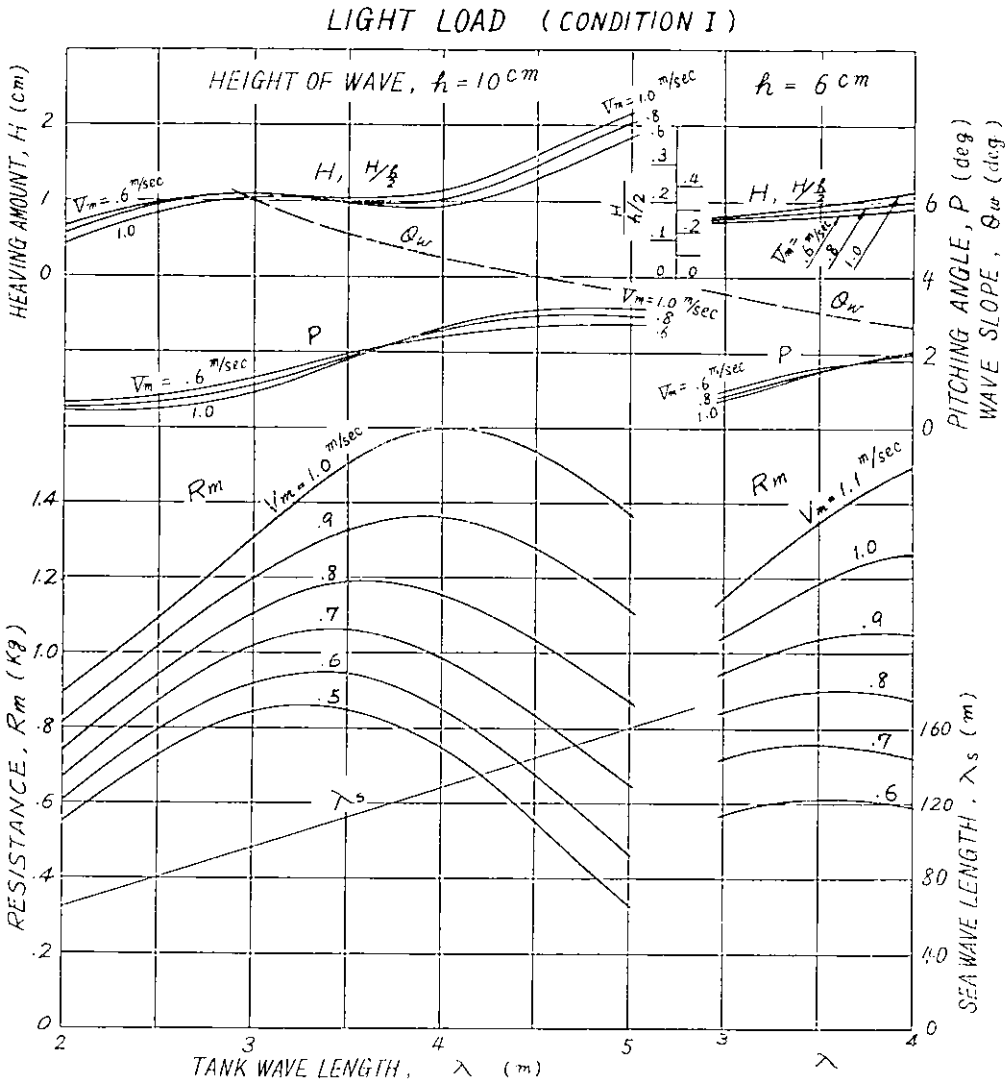

Fig. 45. Effect of the Wave Length, Light Cond., 4 m Model

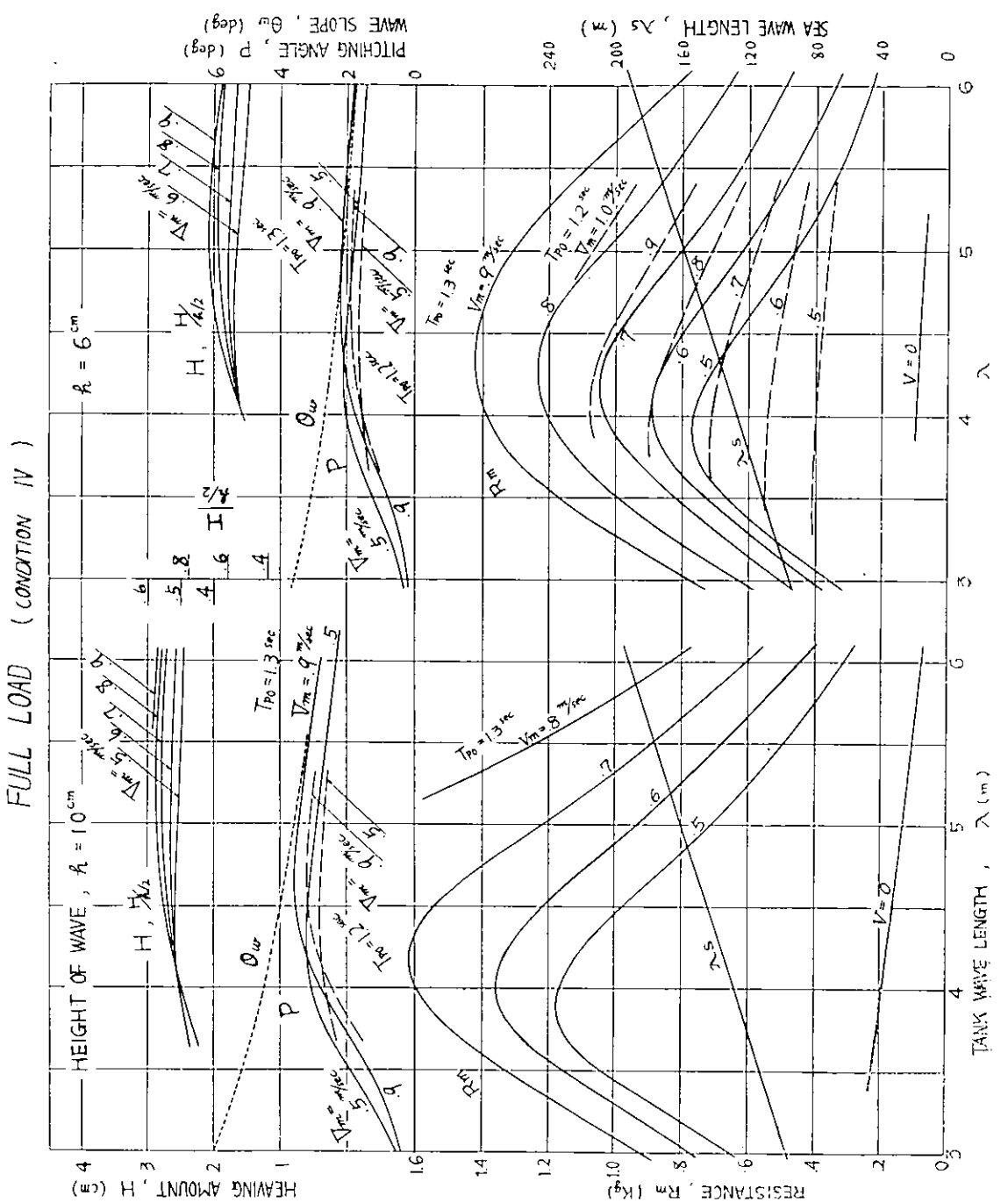

Fig. 46. Effect of the Wave Length, Full Load Cond., 4 m Model

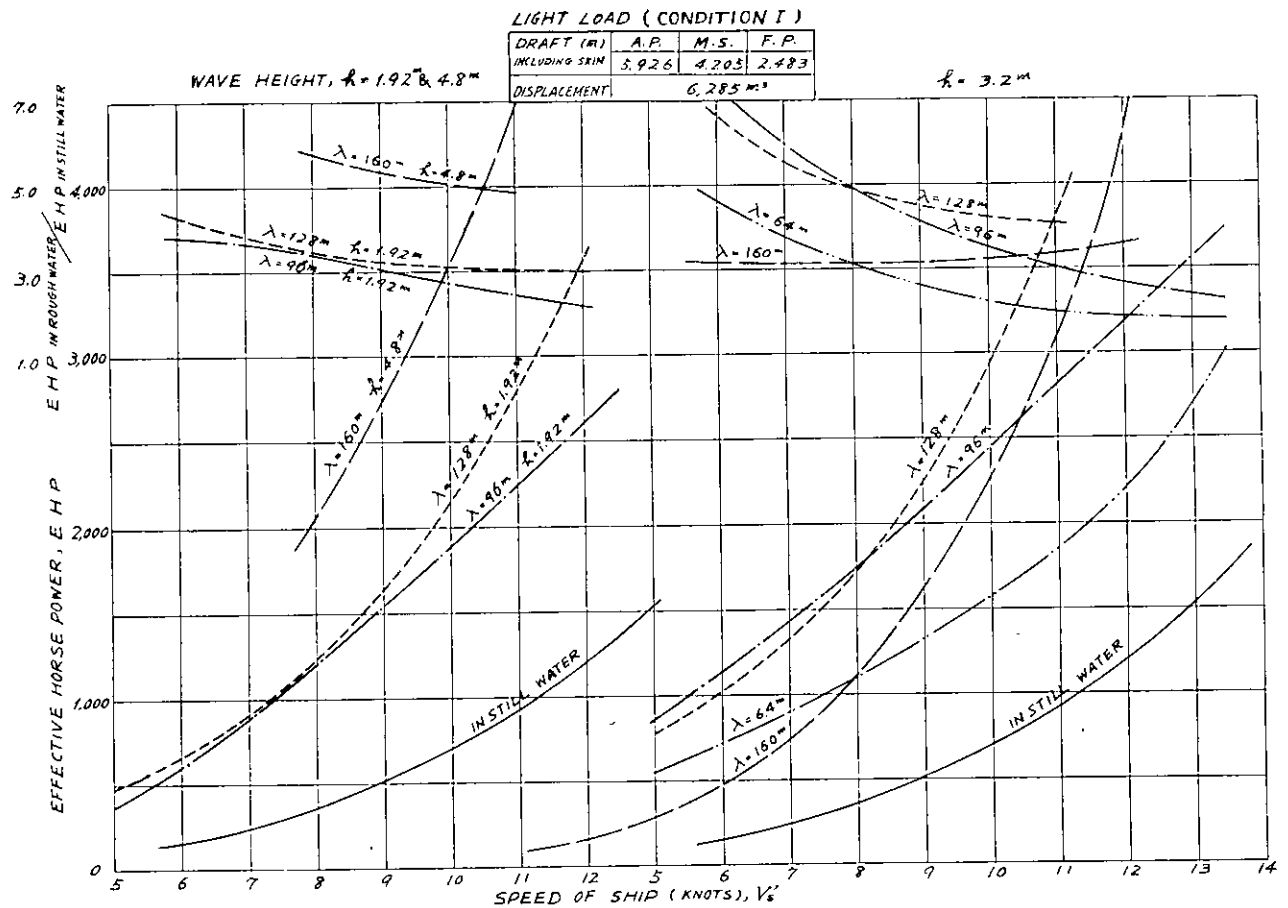

Fig. 47. EHP in Still and Rough Water, Light Cond. (Results of Tests on 4 m Model)

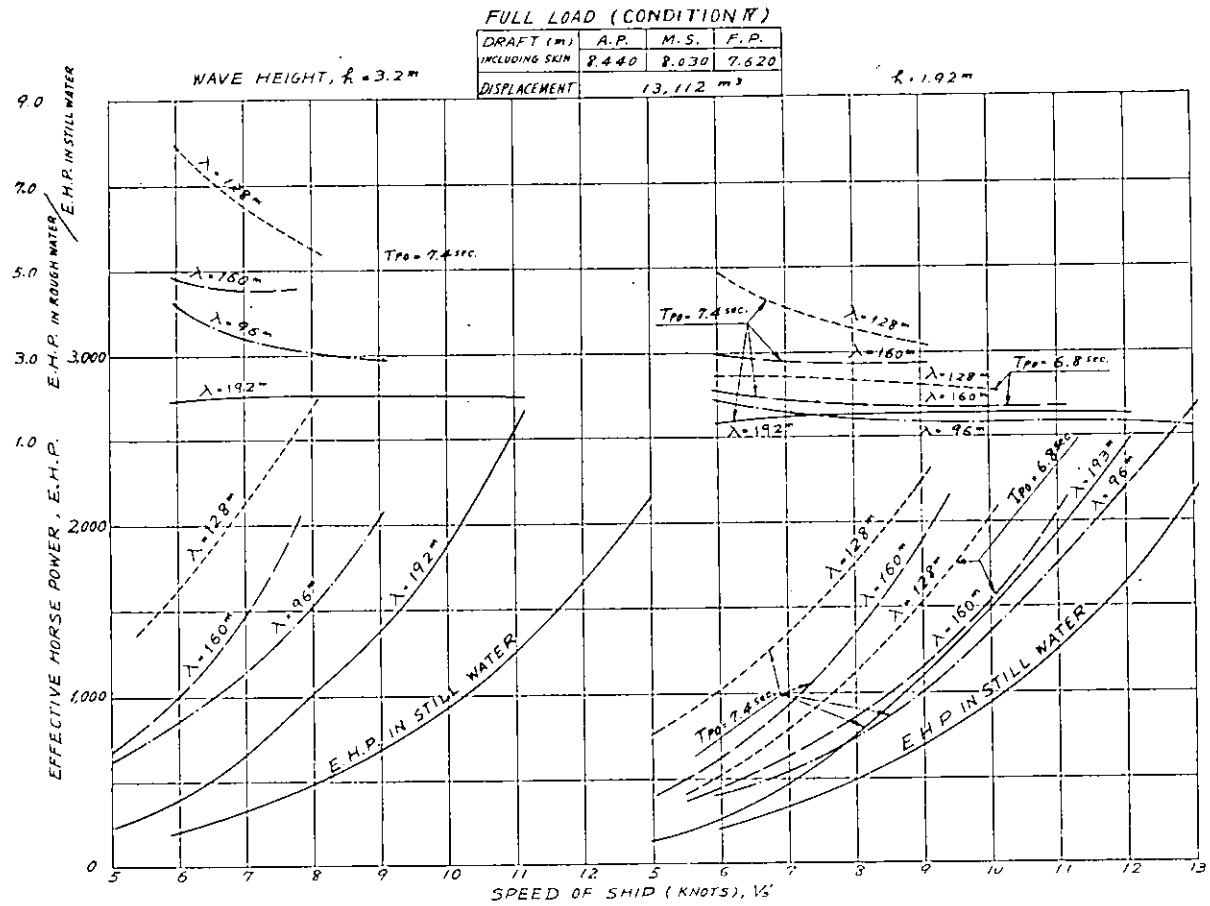

Fig. 48. EHP in Still and Rough Water, Full Load Cond., (Results of Tests on 4 m Model)

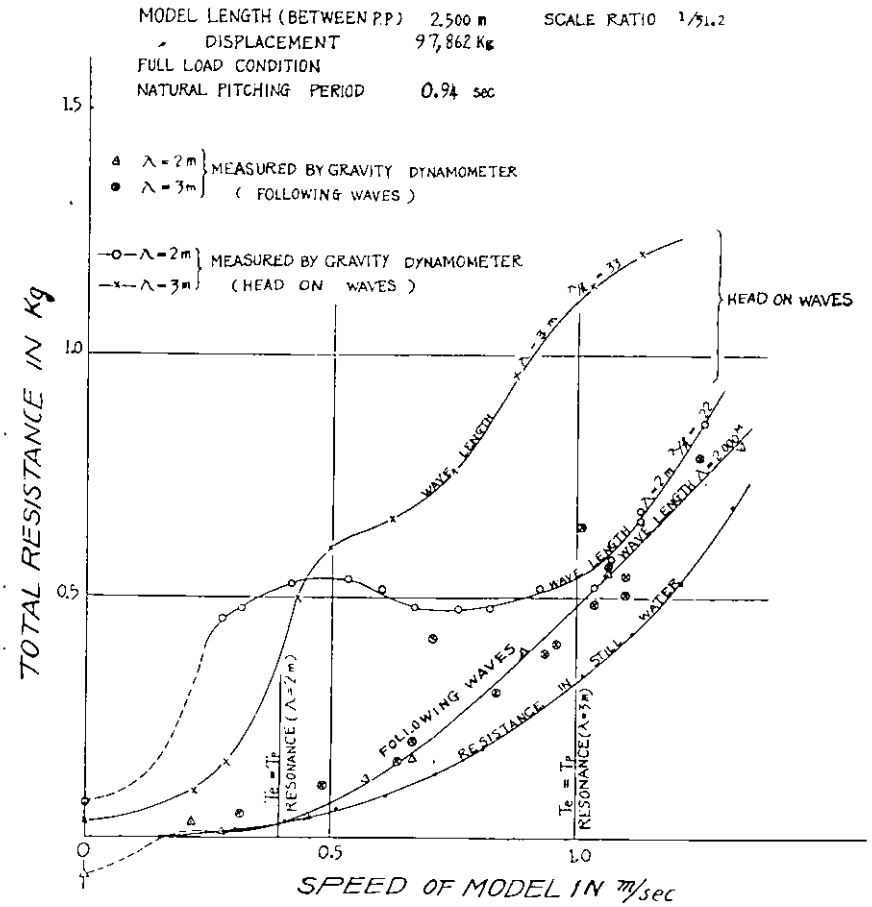

Fig. 49. Results of Resistance Tests in Still and Rough Water, 2.5 m Model

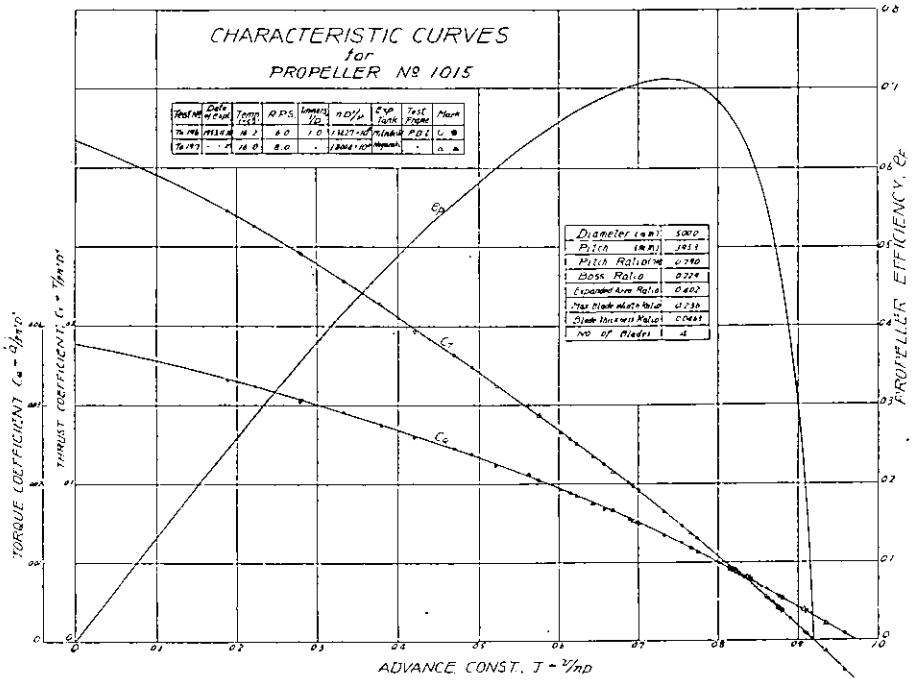

Fig. 50. Characteristic Curves of Propeller

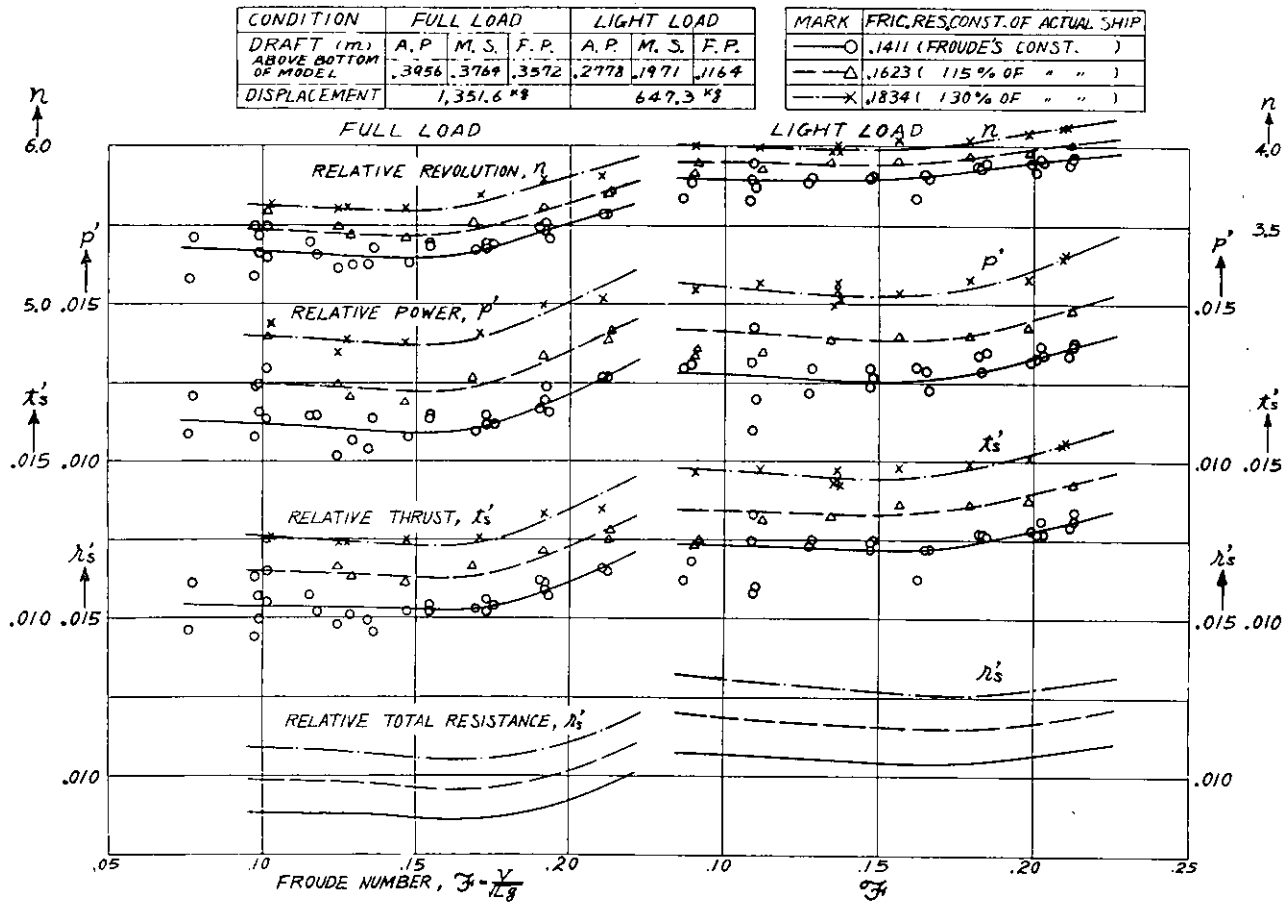

Fig. 51. Results of Self-Propulsion Tests in Still Water, 6 m Model

CONDITION	DISPLACEMENT (T)	MEAN DRAUGHT (M)	TRIM (AFT) (M)
FULL LOAD	13,440	8.030	0.820
LIGHT LOAD	6,442	4.205	3.443

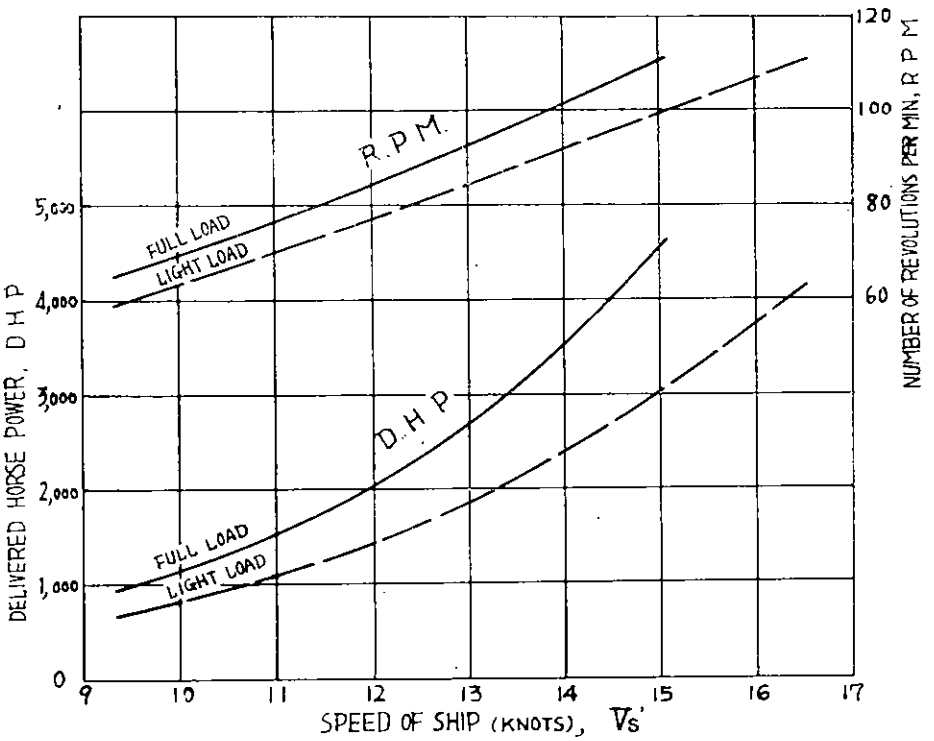

Fig. 52. DHP & RPM in Still Water (Results of Tests on 6 m Model)

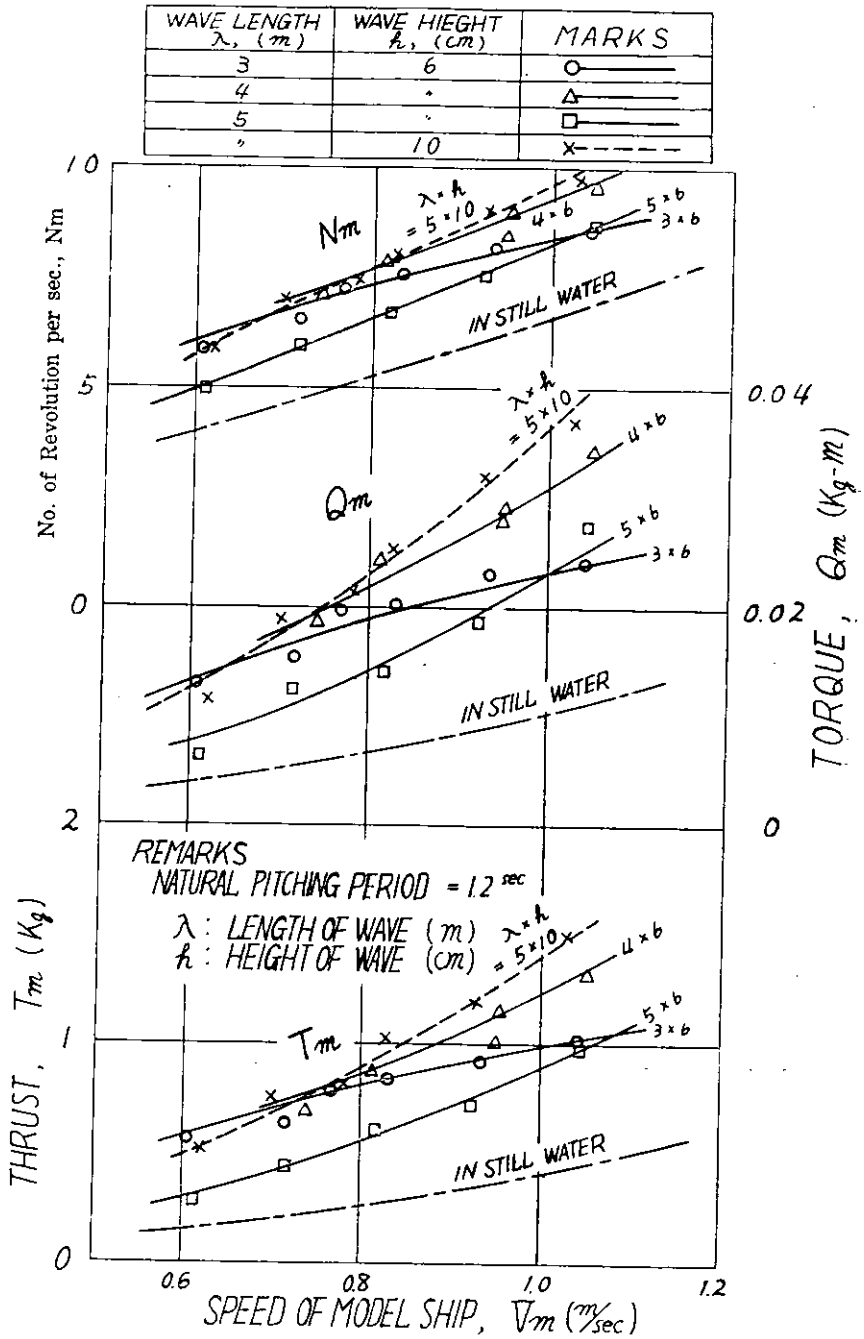

Fig. 53. Results of Self-Propulsion Tests in Rough Water, Light Cond., 4 m Model

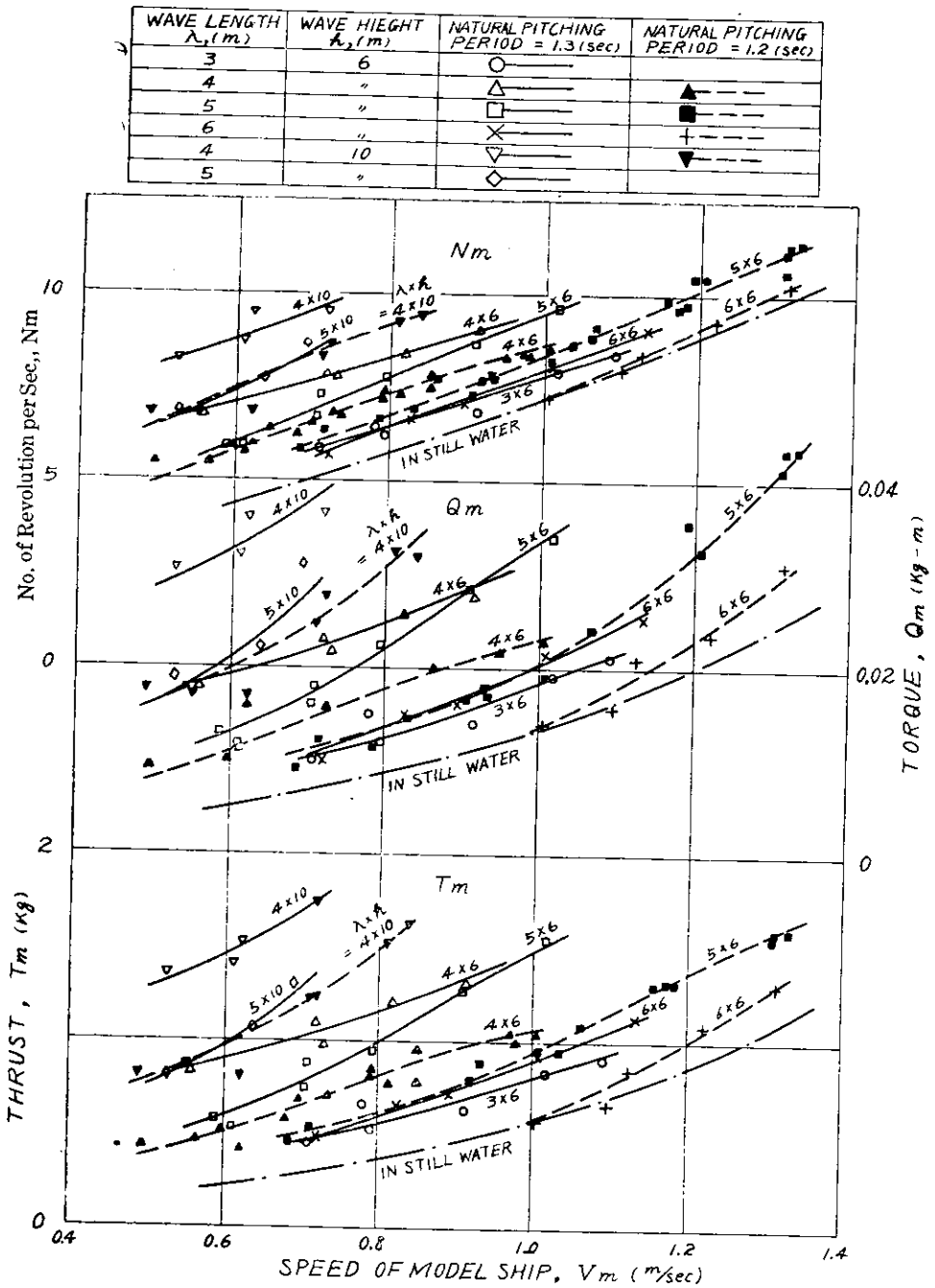

Fig. 54 Results of Self-propulsion Tests in Rough Water, Full Load Cond., 4 m Model

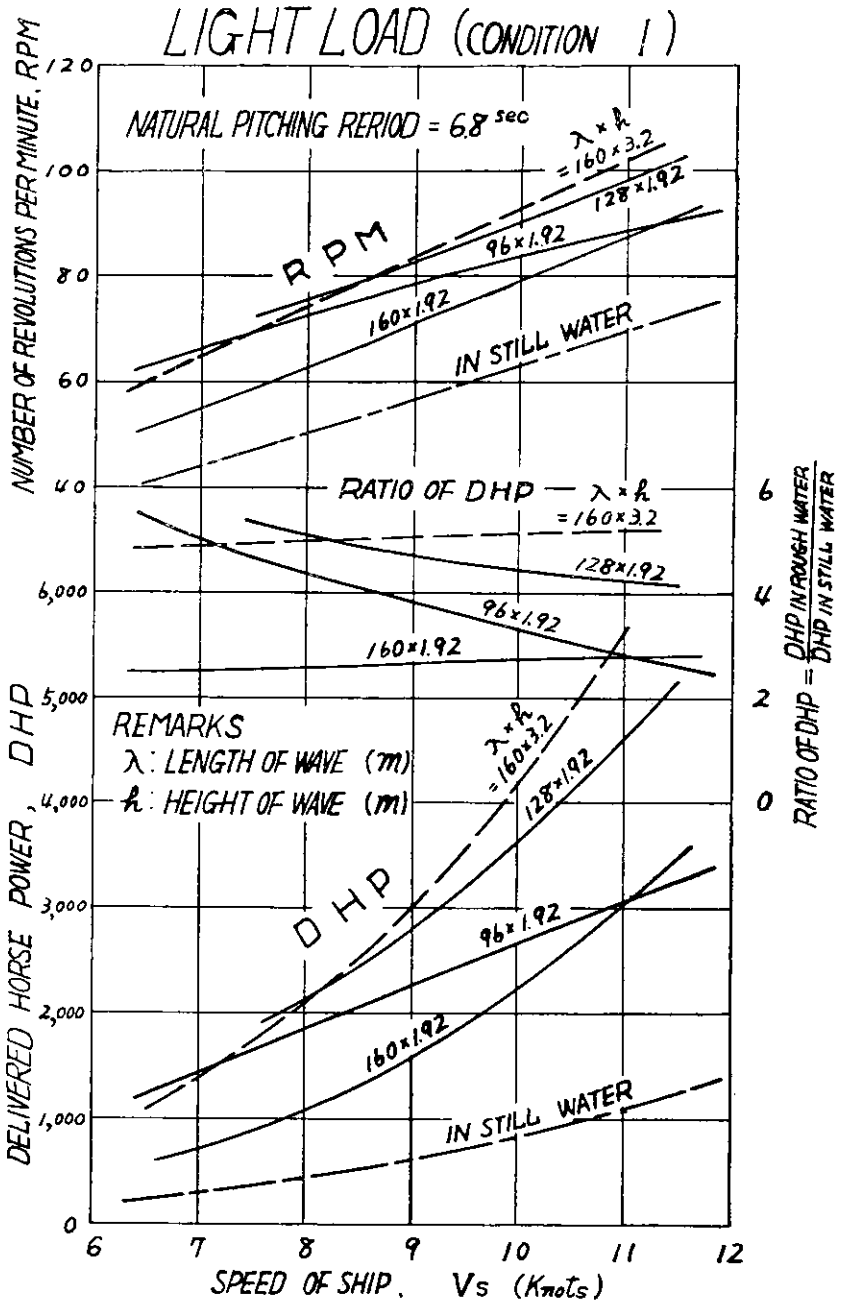

Fig. 55. DHP & RPM in Still and Rough Water, Light Cond., (Results of Tests on 4 m Model)

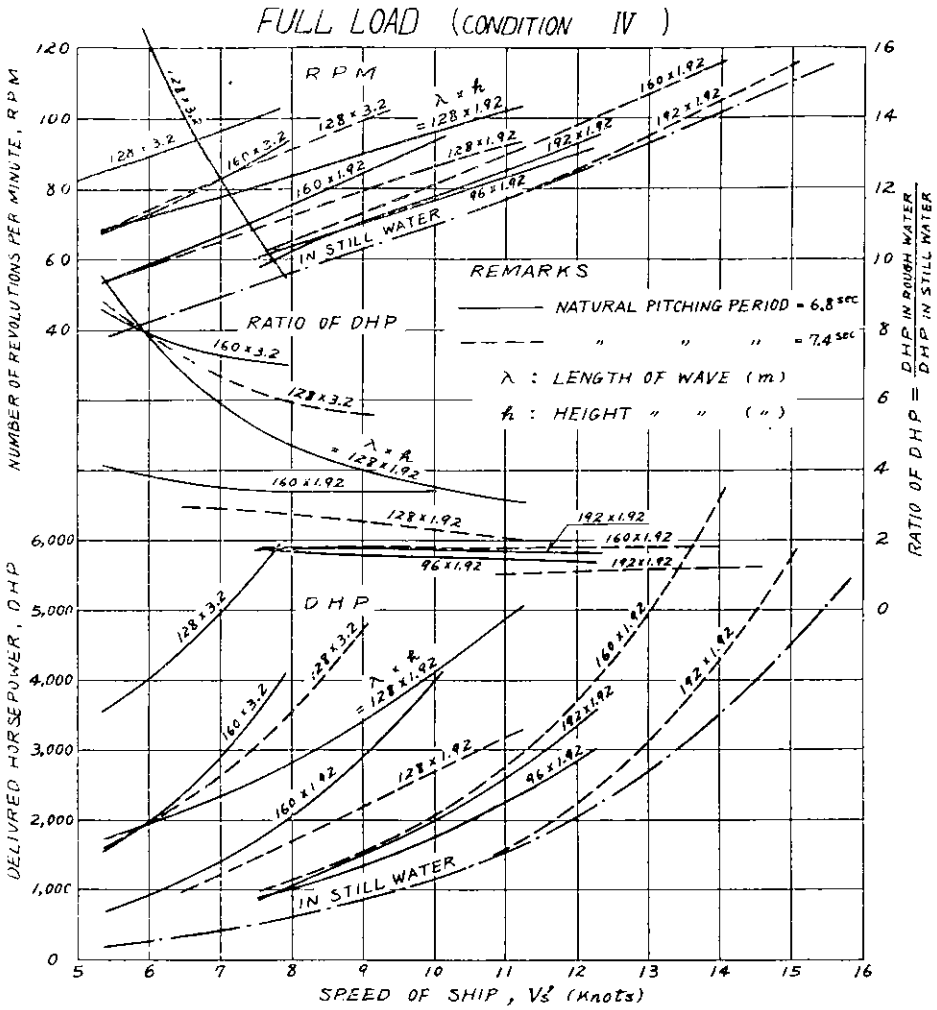

Fig. 56. DHP & RPM in Still and Rough Water, Full Load Cond., (Results of Tests on 4 m Model)

日本造船研究協会報告

昭和 29 年 8 月 1 日

編輯兼発行人　出　淵　巽

発行所　社団法人 日本造船研究協会
東京都中央区京橋一丁目二番地 セントラルビル五階

印刷所　笠井出版印刷社
東京都港区芝南佐久間町一丁目五十三番地